Holocene relative sea-level reconstruction for the central great barrier reef, Australia: a subtidal foraminiferal approach

Hardbattle, Michael Ian John

Holocene Relative Sea-Level Reconstruction for the Central Great Barrier Reef, Australia: A Subtidal Foraminiferal Approach

Michael Ian John Hardbattle

Thesis submitted for the degree of Master of Science

Department of Geography
University of Durham

September 2003

Declaration

This thesis is the result of my own work. Data from other authors that are referred to in the thesis are acknowledged at the appropriate point in the text.

Acknowledgements

I would sincerely like to thank all those people who have helped me along through the production of this thesis, and apologise in advance if I omit anyone from this list of thanks. Firstly I would like to thank Dr. Ben Horton for his inspiration, guidance, enthusiasm and time throughout the entire year, though particularly the last three months, in what has been a very busy time. I would also like to thank Drs. Piers Larcombe and Ingrid Ward for giving me such a valuable insight into the context of my study area, though particularly for putting up with me during my visit to Townsville in November. In addition, I would like to thank Dr. Glenn Milne for his guidance and input to the study, providing a forum through which I could attain different perspectives and valuable discussions.

In addition, I extend warm thanks to Sarah Woodroffe (Woody) for her unending patience and enthusiasm; Dr. John Whittaker for his excellent SEM photos; Dr. Damien Laidler for his help and guidance; Professor Bob Carter for his insightful preliminary discussion regarding this thesis; and Matt Brain for his endless coffee-time chats and 'good' jokes. I also wish to thank members of the geography department, specifically Derek Coates, Frank Davies, Neil Tunstall and Brian Priestley for their help and assistance in the laboratory; Terry Harrison and Jody Welch for being there when another computer blew up! Without the Durham Geography Golfers, this year would have been much less enjoyable and so I thank (in no particular order) Matt Wright, James Smith, Drs. Dave Roberts, Toru Higuchi, Gordon MacLeod, Jerry Lloyd and Mike Bentley.

Finally I thank my Mum - Sue, Dad - John and Sister - Charlotte for their constant support and love, without which none of this would be possible.

Abstract

Holocene Relative Sea-Level Reconstruction for the Central Great Barrier Reef, Australia: A Subtidal Foraminiferal Approach

Michael Ian John Hardbattle

Contemporary subtidal foraminiferal samples and associated environmental information were collected from two embayments along the central Great Barrier Reef coastline, Australia, to comprehend the relationship of benthic foraminiferal assemblages with respect elevation and their environment. Subtidal foraminifera from Bowling Green Bay illustrate a strong relationship with elevation (-6.7m to -48.0m AHD), whereas samples from Cleveland Bay display an arbitrary relationship to elevation (-4.2m to - 9.8m AHD). The datasets were combined to generate a regional training set for the first foraminifera-based subtidal transfer function, subsequently applied to 13 fossil vibracore samples, reconstructing former sea levels. The results show a comparable trend with regional geophysical models, depicting a rapid transgression across the shallow continental shelf to a constrained mid-Holocene highstand and a subsequent late Holocene fall. Analysis of the results reveals that benthic foraminifera can be related to subtidal elevation. Furthermore, the subtidal foraminiferal transfer function can be used to reinterpret subtidal samples to generate more accurate and precise reconstructions. This is the first foraminifera-based subtidal transfer function for environmental interpretations and thus may benefit existing semi-quantitative subtidal reconstructions through reinterpretation with a fully quantitative technique. In addition, combination with an inter-tidal foraminifera-based transfer function may help widen the window of our understanding of contemporary benthic foraminiferal distributions and assemblages, and hence prove a more valuable tool for palaeoenvironmental reconstruction.

List of Contents

List of Figures

Chapter 3 **Page**

Chapter 4

List of Tables

Chapter 1

Introduction

1.1 Background

Relative sea-level (RSL) is the study of the position of the sea relative to the land with distinct changes in RSL occurring over differing timescales and magnitudes. Specific study of Holocene (10,000 years to present) sea-level change is important, spanning the post-glacial meltwater phase of the last glacial maximum (LGM), generating data inputs for geophysical modellers to test ideas of meltwater timings and sources (Nakada et al., 2000; Tarasov and Peltier, 2003). The study of RSL is also vital for the present, as the impacts of changing sea levels on the human population are considerable. These scenarios include inundation of low-lying areas, erosion of beaches and bluffs, salt intrusion into aquifers and surface waters, higher water tables, and increased flooding and storm damage. Furthermore, analysis of the physical impacts of a sea-level rise are made more complex by the dense human occupation of many coastal areas, by their often high economic value and by the continuous interaction between human activities and natural processes (Pirazzoli, 1996). However, in a wider context, attempts are made to link sea-level changes to extremes of climate (Baker, 1993; Oerlemans, 2003; McGregor and Gagan, 2003), and in this day-and-age of increased speculation over 'global-warming' studies seek to use sea-level change as a proxy for climatic changes (Meehl *et al.*, 2000; Chase *et al.*, 2003).

The recent transition of the earth system from a glacial to interglacial state produced a dramatic global sea-level response. Regions distant from the major glaciation centres (far-field sites) are characterized by a sea-level rise of ~120 m since the LGM due, largely, to the influx of glacial meltwater to the oceans (Fairbanks, 1989; Chappell and Polach, 1991; Bard *et al.*, 1996). In contrast, sea

levels have dropped by many hundreds of metres in regions once covered by the major ice sheets (near- and intermediate-field sites) as a consequence of the isostatic 'rebound' of the solid Earth (Shennan *et al.,* 2000b; Long *et al.,* 2003). The study area, the Great Barrier Reef (GBR) coastline, Australia, is a tectonically stable far-field site where glacio-eustatic changes in sea level are considerably greater than glacio-isostatic and hydro-isostatic effects (Lambeck, 2002). The importance of the region for valuable Holocene RSL reconstructions is emphasised by the purity of the eustatic sea level signal, accessibility and relative tectonic stability. Studies within the region (Horton *et al.,* 2003) using foraminifera have shown promise for quantifying contemporary intertidal environments as a reconstruction tool for former sea levels.

The use of foraminifera as both chemical and biological proxies for palaeoenvironmental reconstructions are well documented (Phelger and Walton, 1950; Walton, 1952; Phelger, 1970; Murray, 2001). Planktonic foraminifera provide insights into palaeoceanography, giving proxy records of former sea-surface temperatures (Funnell and Swallow, 1997) and bio-productivity (Loubere, 2003). Benthic foraminifera, amongst other applications, offer the ability to reconstruct quantitative former sea-levels via proxy, with inter-tidal studies well documented throughout Europe (Horton et al., 1999a; b; Edwards and Horton, 2000) and the USA (Phelger and Walton, 1950; Walton, 1952; Scott and Medioli, 1978; 1980; Gehrels, 1994; 2000; Gehrels et al., 2001; Van de Plassche et al., 2002). Studies reconstructing former sea-levels using subtidal benthic foraminifera are scarce (Yokoyama et al., 2000) and semi-quantitative at best. Studies from the GBR region (Larcombe et al., 1995) show a majority (>60%) of existing sea-level indicators to be subtidal in nature, reflecting the narrow confines of the intertidal sediment window within the wider scope of the marine expanse.

1.2 Aims and Objectives

1.2.1 Aims

1. To develop the first subtidal foraminiferal-based transfer function as a tool to quantify contemporary foraminiferal relationships to their environment.

2. To apply this transfer function to fossil samples in order to generate a new generation of accurate and precise former sea-levels.

1.2.2 Objectives

1. Summarise RSL observations from near-, intermediate- and far-field sites, understanding the wider context for this study.

2. Identify differing RSL reconstruction techniques employed in order to better understand the nature of the Holocene RSL changes.

3. Systematically document the benthic foraminiferal assemblages in subtidal environments of the GBR lagoon.

4. Understand the relationship between subtidal foraminifera and their environment, testing the hypothesis that subtidal foraminifera are controlled by depth.

5. Develop the first subtidal foraminiferal-based transfer function.

6. Apply this transfer function to fossil samples to produce a new generation of accurate and precise RSL reconstructions based on subtidal sediments.

7. Compare these findings with the wider literature for the GBR, Australia and far-field sites.

1.3 Thesis Structure

This thesis presents the results of a study of two embayments along the GBR coastline (Bowling Green Bay and Cleveland Bay), the development of quantitative techniques to reconstruct former sea-levels using subtidal foraminifera, and the application of these techniques to generate a range of new sea-level index points.

Chapter 2 introduces the concept of Holocene sea-level change across all regions of the globe using the work of Clark *et al.* (1978) as a stimulus. Sea-level data is presented for near- and intermediate-field sites (Greenland and Northwest Scotland respectively) and discussed within the context of regional trends. The focus is drawn upon far-field sites with a detailed analysis of sea-level reconstruction techniques, including corals, lithostratigraphic and biostratigraphic approaches. Finally the emphasis is placed on Australia, specifically the GBR as an area of palaeoenvironmental and sea-level reconstructions, with analysis of established data.

Chapter 3 introduces foraminifera and their shows their applicability for use as proxy records of sea-level change, with specific focus on the GBR lagoon, Australia. The necessary laboratory and statistical methodologies are outlined to attain contemporary benthic foraminiferal assemblage data along with their contemporary environmental settings for Bowling Green and Cleveland Bay. The foraminifera-environment relationships are then discussed for each embayment before conclusions are drawn.

Chapter 4 introduces the concept of the transfer function highlighting past applications of the technique. The study area is outlined along with methodological approaches and the development of a transfer function. The transfer function is then applied to a series of fossil samples and a reinterpretation of existing sea-level index points is undertaken. Limitations of the technique as a whole, and specifically, are discussed with future applications being considered before conclusions are deduced.

Chapter 5 concludes the thesis by considering to what extent the initial aims and objectives (Section 1.2) have been met before finally proposing future research recommendations.

Chapter 2

Holocene Relative Sea-Level Change from Far Field Locations

2.1 Introduction

The changes in relative sea level (RSL) throughout the Holocene (last 10k. BP) refer to a vertical playoff between the land and the sea. There are, however, many factors that control the RSL at any given time and place, summarised in the following schematic equation.

$$\Delta\xi_{rsl}(\tau,\varphi) = \Delta\xi_{eus}(\tau) + \Delta\xi_{iso}(\tau,\varphi) + \Delta\xi_{tect}(\tau,\varphi) + \Delta\xi_{local}(\tau,\varphi)$$

$\Delta\xi_{rsl}(\tau,\varphi)$ = the time and space dependant RSL function.

$\Delta\xi_{eus}(\tau)$ = the time dependant eustatic function.

$\Delta\xi_{iso}(\tau,\varphi)$ = the time and space dependant total isostatic effect of glacial rebound.

$\Delta\xi_{tect}(\tau,\varphi)$ = the time and space dependant total effect of tectonic activity.

$\Delta\xi_{local}(\tau,\varphi)$ = the time and space dependant total effect of local processes within the lagoonal environment, such as changes in tidal regime and sediment consolidation since deposition.

RSL changes are very complex and the result of interplay between eustatic (changes in the volume of water in the oceans), isostatic (the Archemedian forces to equilibrate loading, such as sediment, ice or water), tectonic influences (sporadic and gradual crustal movements) and local factors (such as sediment consolidation and changes in tidal regime). Most sea-level studies are concentrated in near-field (Greenland, Norway) (Long *et al.*, 2003) and intermediate-field sites (North America, Northwest Scotland) (Scott *et al.*, 1995; Plater *et al.*, 2000; Shennan *et al.*, 2000b), with increasing importance being placed on far-field sites in the last 20 years. This change in emphasis echoes a desire to discern a eustatically

dominated sea-level signal, driven by geophysical modellers trying to establish last glacial maximum (LGM) (19-22k calendar yr BP) ice volumes, melting rates and meltwater sources.

The ability to model sea level data across the globe has undergone research since the late 1970s, attempting to understand the deformation of the earth's surface and its geoid by changing ice and water loads. As Clark *et al.* (1978) illustrate, the sea-level response to even a very simple glacial history (such as a single melting event at a given time) can be quite complex. Thus, the use of far field locations is ideal for Holocene sea-level reconstructions because of their displacement from former ice masses and subsequent eustatic signal purity. Far field locations take their name from their position relative to former glacial ice masses, in addition to near-field, ice margin sites and intermediate-field sites. These sites correspond to those zones proposed by Clark *et al.* (1978); near-field being equivalent to zone 1, ice margin sites to the transition zone (1-2), intermediate-field sites to zone 2 and far field sites to all other zones (Fig. 2.1).

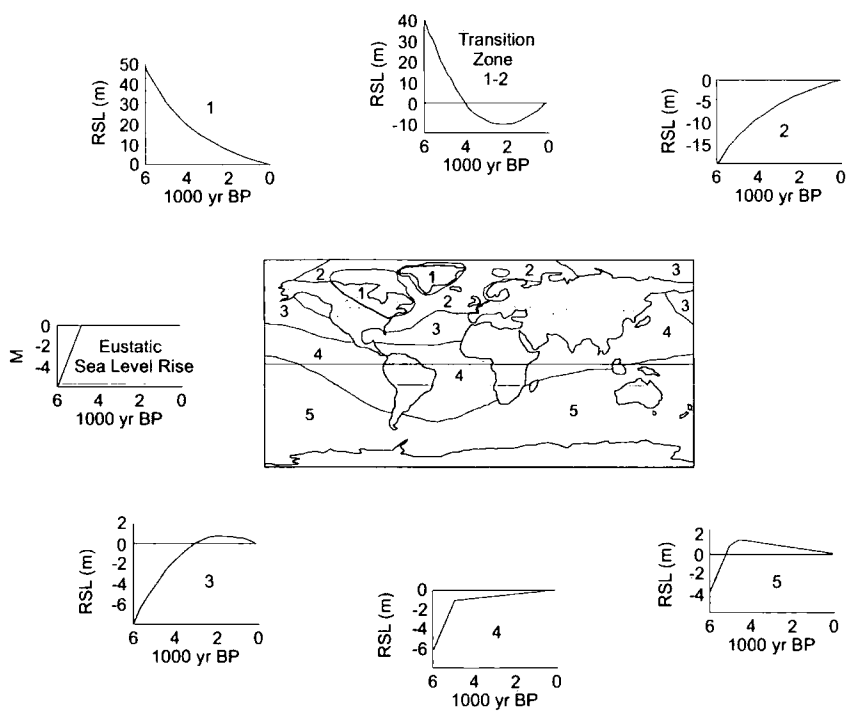

Fig. 2.1 Sea-level zones and typical RSL curves deduced for each zone by Clark *et al.* (1978) under the assumption that no eustatic change has occurred since 5,000 yr BP.

Relict shoreline features of Holocene age well below present sea-level strongly support the belief that, following ice sheet retreat, meltwater increased the volume of the oceans. However, attempts to reconstruct sea levels since the LGM are prone to difficulty in differing locations. Clark *et al.* (1978) in their seminal paper attempted to model the global response to a uniform instantaneous ice melting, where 1000m of ice melted at 18,000 BP from all glaciated regions. These results (Fig. 2.1) demonstrate that there are no 'stable' regions from which eustatic sea level can be measured, as deglaciation and the addition of water to the ocean basins deform the Earth and change the observer's point of reference (Clark *et al.*, 1978).

Evolution from this seminal work by Clark *et al.* (1978) leads to a series of further models being produced allowing RSL to be reconstructed for any place on Earth. However, there has been some debate within the modelling community (Long, 2001) as to the nature of the deglaciation, and subsequent sea-level histories during the Holocene. Modellers agree that since the LGM there has been a sea-level rise, though it is the nature of this rise and mantle viscosities that is at issue. Long (2001) notes that recent interest has focussed on the eustatic minimum at the LGM and on identifying periods of rapid sea-level rise, with rather less interest in the timing and magnitude of the mid-Holocene slow-down. Peltier (1998b) argues that all meltwater release terminates between 8,000-5,000 cal. yr BP, a view not supported by Fleming *et al.* (1998) and Nakada *et al.* (2000) who date a slow-down to between 7,400-6,800 cal. yr BP. Fleming *et al.* (1998) and Nakada *et al.* (2000) in addition to Lambeck (1999) and Shennan *et al.* (2000a) all support the contrasting view that a continued gradual release of meltwater occurred through the mid and late Holocene, amounting to between 3-5m of sea-level rise.

To address these and previous issues, it is essential to test the geophysical models with field observations from a wide range of sea-level indicators and spatial locations, increasing the accuracy and precision of the models as better tools of prediction. Within the context of some of the issues raised here, the aims of this chapter are:

- To summarise RSL observations from Near, Intermediate and Far-field locations.
- To identify sea-level reconstruction techniques in the study area (Great Barrier Reef (GBR) coastline, Australia) and other far-field locations to better understand the nature of Holocene RSL change.

2.2 Relative Sea-Level Records form Near, Intermediate and Far field locations

2.2.1 Near-field sites

Near-field sites (e.g. Greenland, Norway and Canada) are defined as showing a more complex pattern of RSL as the dominant glacio-isostatic signal interacts with eustatic changes in a spatially and temporally complex manner (Long, 2001). They are characterised by an almost exponential fall in RSL throughout the early and mid Holocene (glacio-isostatic uplift), with a rise to present as a result of glacio-isostatic submergence (ca. 5.8 ± 1.0 mm yr^{-1} at Kellyville (South Greenland)) (Long *et al.*, 2003). Fig. 2.2 shows an example of sea-level reconstructions from Disko Bugt, Greenland, and illustrates a similar trend to proposed models for the area (Clark *et al.*, 1978; Peltier, 1998b; Shennan *et al.*, 2000b).

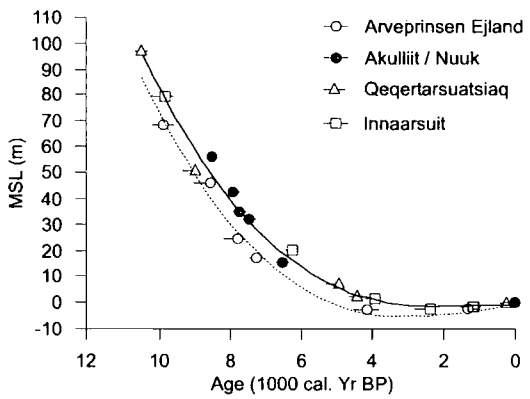

Fig. 2.2 RSL depicting MSL. The trend lines summarizing the data from Arveprinsen Ejland (Alluttoq), and the combined Innarsuit and Qeqertarsuatsiaq data, are third-order polynomials. Other data are from Long and Roberts (2003) (Qeqertarsuatsiaq), Long and Roberts (2002) (Akulliit/Nuuk), and Long *et al.* (1999) (Arveprinsen Ejland (Alluttoq)).

Ice margin sites, such as Northwest Scotland (Fig. 2.3), illustrate an initial phase of early Holocene land emergence (RSL fall) with the rate decreasing to a stage where eustatic sea-level rise is equalled by isostatic land uplift (Phase 1). Contemporary rates of land uplift/subsidence for context in the British Isles are shown by Shennan (1989), ranging from +2mm in northwest Scotland through to -2mm in southeast England. The rate of land uplift then decreases further resulting in RSL rising before being equalled by land uplift rates as a result of decreased eustatic sea-level rise (Phase 2).

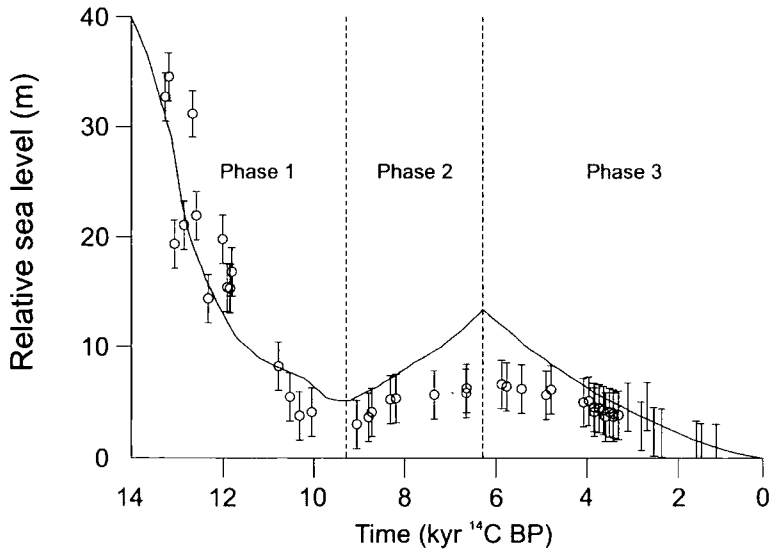

Fig. 2.3 Raised tidal marshes and isolation basin data for Kentra – Airsaig region, Northwest Scotland, compared against predictions. The predictions are based on earth model E-0, ice model BR-D, with a nominal eustatic sea-level function in which all melting had ceased by 6000 BP (Shennan *et al.*, 2000b).

Finally RSL decreases to present as a result of a falling rate of eustatic sea-level rise coupled with a stable rate of isostatic land uplift (1.98 mm yr^{-1}) (Shennan and Horton, 2002) (Phase 3).

2.2.2 Intermediate-field sites

Intermediate field sites (e.g. Nova Scotia, Great Britain and Eastern USA) correspond to the peripheral bulge around the former ice margin, lying within 2000 km or so of the former ice sheet margins (Long, 2001). The peripheral bulge subsides in late glacial times and as a result the RSL continues to rise to present

values at a decreasing rate (Fig. 2.4). The glacio-isostatic signal is dominant here and is usually negative because of crustal subsidence caused by the flow of mantle material towards the deglaciated areas (Long, 2001). This data shows a comparable trend when compared to the models of Peltier (1998b) and Shennan *et al.* (2000b).

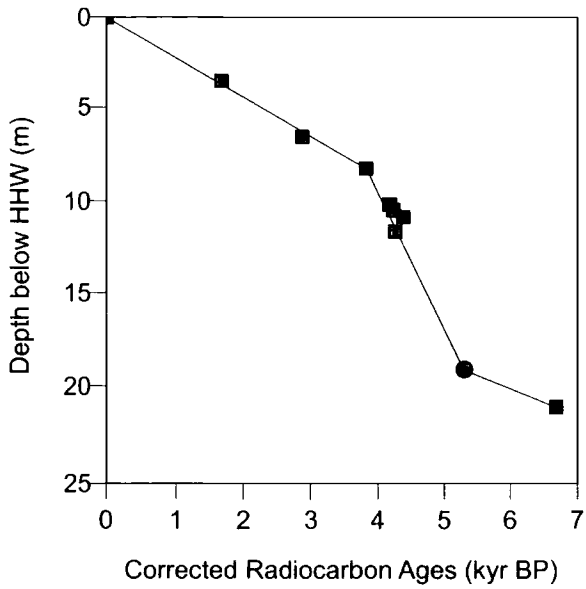

Fig. 2.4 RSL data from Chezzetcook, Nova Scotia (Scott *et al.*, 1995).

2.2.3 Far-field sites

Far field sites are defined as areas at distance from the ice sheets and predominantly show glacio-eustatic changes in sea level that are considerably greater than glacio-isostatic and hydro-isostatic contributions (Pirazzoli, 1996). As a result of the combined isostatic effects being low, RSL curves from these sites provide a reasonable approximation of eustatic changes (Long, 2001). Further, the RSL rise only predominates during the deglaciation period, often followed by a slight RSL fall during the late Holocene (Pirazzoli, 1996; Long, 2001). As a result of this eustatically dominated signal, far field sites are proving to be at the forefront of Holocene sea level research.

2.3 Far-field Sea-Level Reconstruction Techniques

There are an increasing number of far field studies (Fairbanks, 1989; Chappell and Polach, 1991; Bard *et al.*, 1996; Nunn, 2001) focussing on Holocene sea-level change to better understand the eustatic signal. The majority of these studies use coral as a sea-level indicator. However, assorted reconstruction techniques are used, including lithological (encompassing raised/submerged shorelines and stratigraphic sediments) and biological methods (fixed biological indicators (FBIs), microfossils and sea grasses).

2.3.1 Corals as a Proxy for Sea-Level Reconstruction

Subtidal and intertidal corals provide an insight into former sea levels throughout the Holocene. Coral microatolls, for example, are discoid intertidal corals that are limited in their upward growth by sub-aerial exposure during low tides, thus preserving a filtered record of changes in the height of living coral and by proxy a record of former constraining water levels (Smithers and Woodroffe, 2001). However, the precision of individual species of coral is varied and thus care needs to be taken in comparisons between studies.

Fairbanks (1989) drilled coral reefs offshore Barbados to provide the first continuous and detailed record of sea-level change during the last glaciation. His reconstruction which utilised the Caribbean reef-crest coral *Acropora palmata* (Fig. 2.5) shows that RSL was 60 ± 5 m lower in the early Holocene. This species of coral carries many advantages for its use in such a reconstruction as it is fast growing, abundant, large in stature, and has a generally pristine aragonite skeleton, allowing for easy ^{14}C or ^{230}Th / ^{234}U dating. However, *A. palmata* has relatively large altitudinal ranges (± 2.5m), when compared to other biological indicators. When dealing with small-scale Holocene RSL changes, such as the Mid-Holocene High Stand (MHHS), it is important to recognise that the best altimetric indications for the reconstruction of former sea-level are obtained from those species with the narrowest vertical zonation (Pirazzoli, 1996). Further errors are associated with the absence of selective dissolution of the calibrated dates, a

step that was introduced later by Edwards *et al.* (1993) to reduce contamination of the sample. Nevertheless, the pioneering research by Fairbanks (1989) illustrated that Caribbean coral growth rates could keep pace with the Holocene sea-level rise, posing the question of whether other far field locations could do the same.

Chappell and Polach (1991) also used corals as a sea-level indicator on the Huon Peninsula, Papua New Guinea. Their results show that the dominant taxa were able to keep pace with sea level as it rose by over 50m from 11,000-7,000 ^{14}C yr BP. This is confirmed by Woodroffe *et al.* (2000) who reveal that reefs have grown very rapidly in the Torres Strait, catching up with the MHHS. Chappell and Polach (1991) compare their data (after correction for uplift; 1.9m kyr^{-1}) to Fairbanks (1989) to conclude that sea-level rise was similar at both locations.

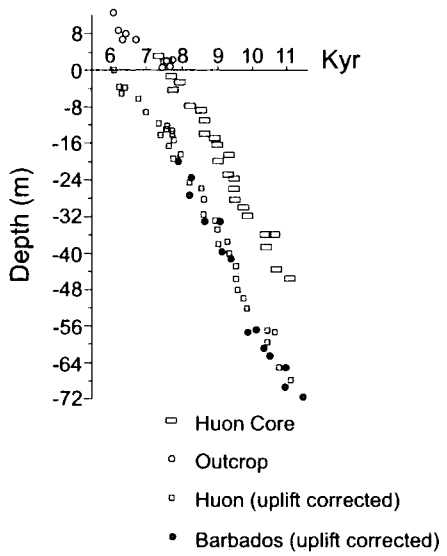

Fig. 2.5 Summary core log and age-depth plots of radiocarbon SLIPs (Chappell and Polach, 1991). The upper age-depth series is for samples uncorrected for uplift; lower series is corrected for uplift and is compared with Barbados (Fairbanks, 1989).

The synchronous tracking of both records, uplift corrected, implies that both reefs are recording the same signal, that of a eustatic post-glacial sea-level rise (Chappell and Polach, 1991). Similar errors are presented within this reconstruction regarding the constraint of corals as the biological indicator and thus the sea-level reconstruction. Bard *et al.* (1996) comment that tectonic movements are large and often discontinuous in these areas, so that the apparent RSL records may be contaminated by a complex tectonic component. However, it may not be

appropriate to assume a consistent uplift rate in the past, as contemporary tectonic activity ranges from the consistent to the sporadic. Detailed errors are shown for this reconstruction (<±100 years) and all are corrected for the marine reservoir effect (Chappell and Polach, 1991).

Bard *et al.* (1996) carry out a similar study of the coral reefs surrounding Tahiti, placing particular influence on the timing of the global meltwater discharge. Their 120m core contains a range of different coral species, in addition to detailed studies of other organisms. Through analogy to the modern biotic reef zonation and ecology, these assemblages are diagnostic of a high energy reef front or upper reef zone, at depths less than 6m below mean sea level (MSL) (Bard *et al.*, 1996). This sea-level indicator is coupled with the ^{230}Thorium / ^{234}Uranium assays that reduce the errors down to approximately 30 years, whilst maintaining a relatively high altitudinal error (±3m). Holocene sea-level data from Tahiti (Fig. 2.6) place it 40m below present day levels at 10,000 cal. yrs BP, depicting a linear rise to 7,000 cal. yrs BP (10m below present) before a sharp change in rate of sea-level rise to present for the last 6,000 cal. yr BP.

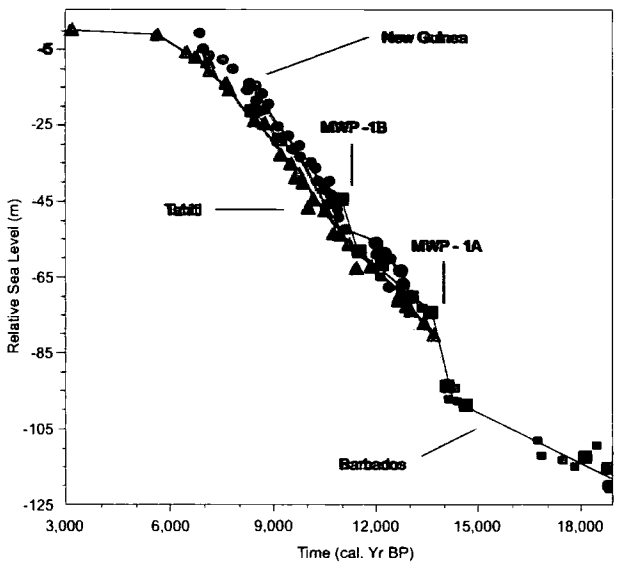

Fig. 2.6 Sea-level history reconstructed for long drill cores from Tahiti (Bard *et al.* (1996)) (triangles), Barbados (Fairbanks (1989)) (squares) and Papua New Guinea (Chappell and Polach (1991)) (dots). All radiocarbon dates have been corrected to calendar years and all data points have been appropriately corrected for uplift/subsidence.

Significantly the sea-level data presented by Fairbanks (1989) and Chappell and Polach (1991) is consistently between 5-10 m shallower than Bard *et al.*, (1996), with account being made for the subsidence rate of 0.2 mm yr^{-1} for Tahiti. However, the general form of the rise is similar for all three locations within the period, further supporting the suggestion that the coral records are tracking the same eustatic signal across the globe.

A similar offset in observations was noted by Edwards *et al.* (1993) in their work on coral sequences for the Huon Peninsula, Papua New Guinea. They observed that paired ^{14}C and ^{230}Th ages were abruptly offset and proposed that the atmospheric $^{14}C/^{12}C$ ratio dropped by 15% during the latter part of the Younger Dryas. When compared to Fairbanks (1989), the ^{14}C dates are still offset but when the ^{230}Th dates are used, the Huon Peninsula data is brought more into line with those from Barbados. This drop in the ratio coincides with a prominent reduction in the rate of sea-level rise. They conclude that reduction of melting because of cooler conditions during the Younger Dryas may have caused an increase in the rate of ocean ventilation, leading to a fall in the atmospheric ratio of $^{14}C/^{12}C$. As a result, their sea-level curve exhibits a very similar shape to that produced by Fairbanks (1989) and the application of paired ^{14}C and ^{230}Th converted dates may have a bearing on other far field sea-level studies utilising coral sequences to avoid the overestimation of depth resulting from a drop in the atmospheric $^{14}C/^{12}C$ ratio (Edwards *et al.*, 1993).

The three seminal records of Fairbanks (1989), Chappell and Polach (1991) and Bard *et al.* (1996) can be considered a benchmark for sea-level reconstructions from far field locations throughout the Holocene and have paved the way for a wide range of sea-level studies since. Recent reconstructions from corals show a characteristic RSL plot, consisting of a transgression up to the MHHS followed by a regression from then to present. Nunn (2001) documents Fijian corals that show a MHHS of 1.6m (Fig. 2.7) and a hiatus at around 4,200 cal. yr BP. A suite of index points at a lower level are separated by approximately 1m from two higher index points. Nunn (2001) states that the two higher dates represent the maximum level achieved by the sea during the Holocene. He

continues that the lower dates must represent a reef that did not reach this sea-level, noting that the tectonic component for this site is negligible. Three offers of explanation are given. Firstly the lower family of corals may represent a reef which did not grow up to the contemporary sea surface, a consideration that must be made for all coral reconstructions, suggesting potential changes in ecological tolerances. Secondly the higher dates come from microatolls that were growing in moated pools, an equally important consideration in identifying a fossil coral, was it recording actual sea level?

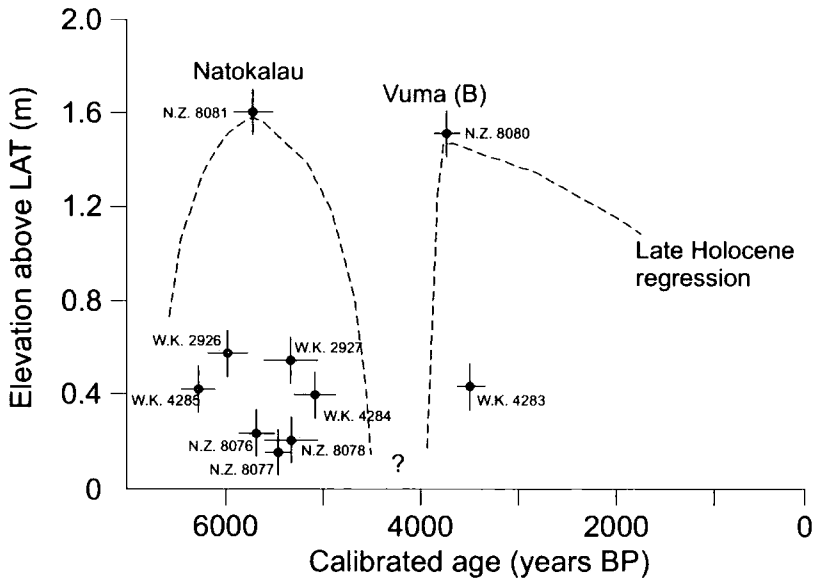

Fig. 2.7 Plot of emergence magnitude against calibrated age for fossil Holocene corals around Ovalau (Nunn, 2001).

Finally the higher dates represent short lived rapid transgressions and regressions from the sea-level depicted by the lower points, again an important factor that must be considered, supported by the Bard *et al.* (1996) demonstration of potential meltwater pulses causing sea level to rise 20m in 750 years (Fig. 2.6). Nunn (2001) concludes that sea-level for the Holocene did peak above present levels, characteristic of the region, and remains cautious about the cause of the hiatus. He notes that potentially this could be a rapid sea-level fall, thus killing off corals, secondly an influx of cool water through El Nino, though he concedes that this is unlikely, and thirdly a rapid increase in terrestrial sediment influx.

In summary, evidence utilising corals from far field locations can be used to generate useful reconstructions of the glacio-eustatic sea-level throughout the Holocene. Studies from Barbados, Papua New Guinea, Tahiti and Fiji all show the benefits of using corals as a sea-level indicator in addition to highlighting some of the limitations. Data from Brazil and Belize show the applicability of a stratigraphic approach to sea-level reconstructions as an attempt to counter some of the limitations of using corals. As with all techniques however, there are inherent errors which have a direct bearing on the data input for models and the precision of their generated predictions.

2.3.2 Lithostratigraphic Techniques

Bezerra *et al.* (2003) presents sea level data from Brazil using a range of sedimentary sea-level indicators throughout the Holocene, including raised deposits, shorelines and tidal flats. These results (Fig. 2.8) show evidence for a double highstand during the Holocene, the first being ca. 5,000 cal. yr BP and the second ca. 2,000 cal. yr BP, both peaking at approximately 3.5m above present. The data envelope generally agrees with the model predictions of Peltier (1998a), with the exception of the second highstand, also having a broad correlation with the Central Brazilian coast data (after Bittencourt *et al.*, 1979; Suguio *et al.*, 1985).

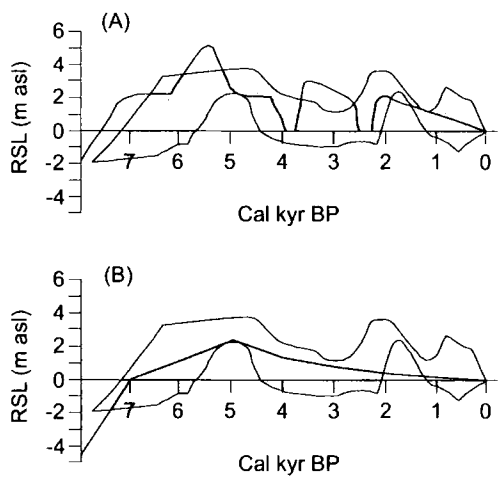

Fig. 2.8 Final sea-level curve for the study area (gray) against (A) the RSL curve for the Central Brazilian coast (solid line) of Bittencourt *et al.* (1979) and Suguio *et al.* (1985) and (B) the glacio-isostatic prediction of Peltier (1998a) (solid line) (Bezerra *et al.*, 2003).

Bezerra *et al.* (2003) conclude that such oscillations have been found elsewhere (Miller *et al.*, 1993; Baxter and Meadows, 1999) and can be explained by minor climate changes or tectonics. However they indicate that in northeast Brazil the local sea level record may have been disturbed by tectonics or wind-wave patterns, and they stress that local events have an important role in the history of coastal progradation and retreat. As highlighted, there are possible explanations for these fluctuations that are inherent to all sea-level reconstructions, though when using lithostratigraphic indicators it is essential to consider the elements of changing sedimentation rates and the effect of sediment compaction, having the potential to under or over estimate rates of change of former sea levels.

Gischler (2003) present data using peat, soils and carbonate sediments from a lagoon platform, Belize. These data show a broad rise of sea-level to present levels, a general western Atlantic sea-level trend after Lighty *et al.*, (1982) (Fig. 2.9) being superimposed. There is no distinct discrepancy between the indicators despite their specific and communal limitations. As a consequence of sediment compaction, one might expect to find these sea-level index points to be considerably lower that those coral indicators. However, this is not the case.

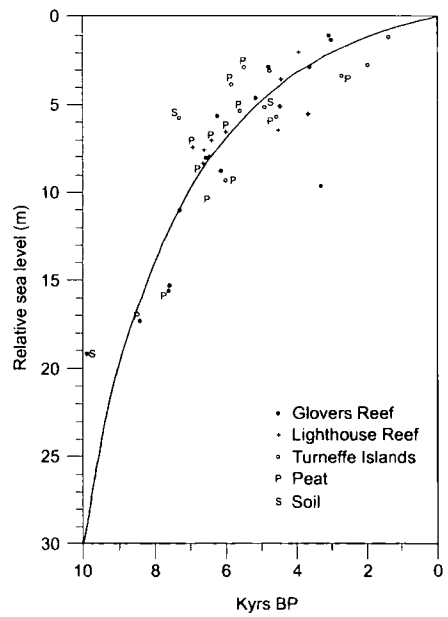

Fig. 2.9 Belize atoll sea-level data from rotary cores and vibracores plotted on Holocene sea-level curve of western Atlantic (Lighty *et al.*, 1982). Data points not indexed by P (= peat) or S (= soil) are from corals or carbonate sediment (Gischler, 2003).

An explanation may be the use of basal soils and peat above Pleistocene limestone bedrock, preferential to intercalated sediments that are prone to compaction (Shennan and Horton, 2002).

Carter *et al.* (1986) present data from New Zealand and indicate that the post-glacial transgression in the SW Pacific was episodic, comprising major stillstands punctuated by rapid rises in sea level (Fig. 2.10).

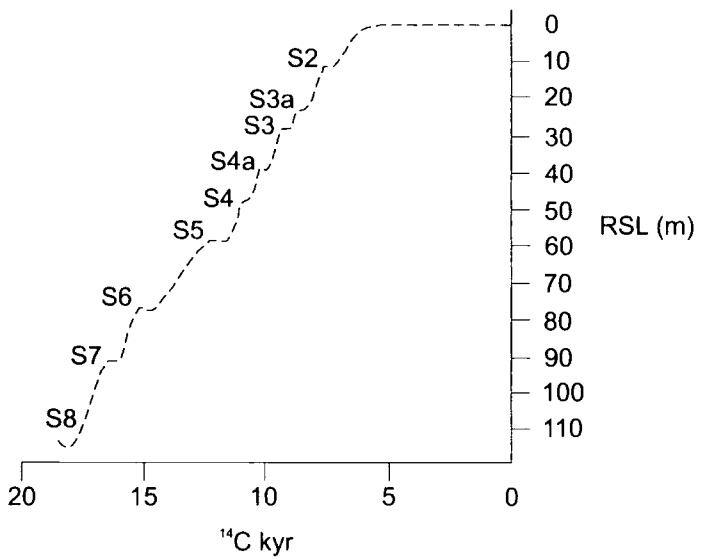

Fig. 2.10 Summary regional sea-level curve, with probable shoreline pauses, based on the model of episodic transgression (Carter *et al.*, 1986).

They describe 8 submerged shorelines, with the use of seismic profiling and radiocarbon dates, encompassing the Holocene transgression to a MHHS. These data support the oscillating movement through the transgression as discussed by Baker *et al.* (2001a) and Baker *et al.* (2001b) for the SE coast of Australia. These shorelines are large sediment wedges, the size and presence of which imply that sea level stabilised at some shorelines for a considerable period of time (up to 1-2,000 years) with the intervening sea-level rises being too rapid to allow the reworking of the wedges into a transgressive sediment sheet (Carter *et al.*, 1986). Such large-scale geomorphic features lend themselves to an equally large scale causal factor and thus have the potential to be important data points within the sea-level record.

2.3.3 Biostratigraphic Techniques

Baker *et al.* (2001a) have studied a wide range of sites along the New South Wales coastline using predominantly tubeworms, oysters and barnacles as FBIs.

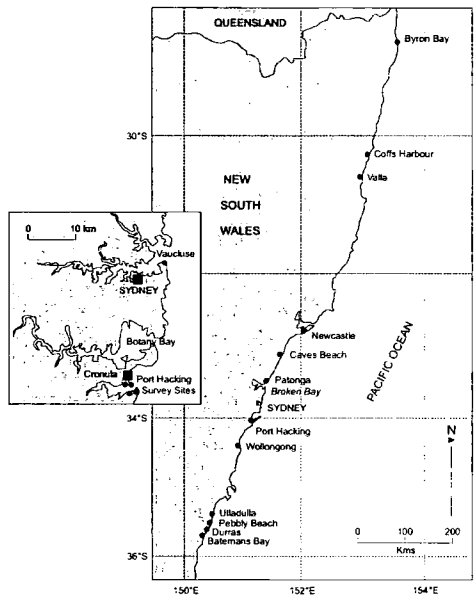

Fig. 2.11 Location map for the sites currently being investigated by Baker *et al.* (2001a) and referred to in the text.

To the north of their study area, they demonstrate evidence from Valla Cave (Fig. 2.11) using the tubeworm *G. caespitosa*. Cave evidence shows a MHHS of around 1.7m ± 0.1m above present at 3810 cal. years BP (Table 1).

Site	Height (m) above MSL (± error)	Calibrated years BP	Species and its location
Northern NSW			
Valla Cave	1.7 ± 0.1	3810	*G. caespitosa* – sheltered sea cave
Valla Cave	1.0 ± 0.1	3810	*G. caespitosa* – sheltered sea cave
Central NSW			
Port Hacking	1.7 ± 0.2	3930	*G. caespitosa* – sheltered estuary entrance
Port Hacking	0.8 ± 0.25	1350	*G. caespitosa* – ~1m platform under rock fall
Southern NSW			
Wasp Head	3.0 ± 0.5	2960	*G. caespitosa* – under visor
Dark Beach	1.3 ± 0.25	4990	*L. australis* – within barnacle at base of shellcrust

Table 2.1 Selected sea-level reconstruction points for all sites investigated by Baker *et al.*, (2001a).

Furthermore, at the same location they record evidence of a shoreline at 1.0m ± 0.1 m for the same calibrated date. This highlights some potential errors in addition to those quoted within the confines of the tidal cave. Further south in central NSW, Baker *et al.* (2001a) show evidence for a maximum high stand of 1.7 ± 0.2 m, again taken from tubeworms found in a sheltered estuarine location (Port Hacking). These data, along with others, provide detailed evidence for fluctuations in sea-level at similar dates to other sites in the transect (~3400 cal. yr BP) (Baker *et al.*, 2001a).

Sites in southern NSW, specifically Wasp Head and Dark Beach, show sea-level to be even higher than those to the north, conflicting with the model predictions of Nakada and Lambeck (1990). Wasp Head is a site with a mid Holocene shoreline at 3m ± 0.5 m above present sea level. This is coupled with a late date for such a high sea level in the context of other studies in the area. Similar levels are achieved for adjacent Dark Beach, though the dates appear more realistic within the regional picture of Holocene sea-level. Baker *et al.* (2001a) reject as invalid this 3m height, given the extreme exposure to ocean swell as a result of being located on the lee side of a highly exposed headland. However they accept that there is no doubt that this and another anomalously high site at Clear Point reflect markedly higher sea-level than today. They state that Dark Beach is a more protected environment and yet displays no evidence of a ~3m RSL where it would have certainly been preserved in quiet conditions (Baker *et al.*, 2001a). Evidence presented from work on Rottnest Island, Western Australia, illustrates that sea-level changes were at a substantial rate, evidence not easily found elsewhere in Australia, with an elevation of ~2 m above present (Baker *et al.*, 2001a). The preservation of abandoned wave cut notches, particularly in soft and easily erodable limestone coastlines, is a likely indicator of rapid change. However the strongest indicator of rapid change is the preservation of fragile shell remains in great abundance on the surface of these notches (Laborel, 1986) which are prevalent at Rottnest Island (Baker *et al.*, 2001a). This evidence for higher Holocene sea-level at Rottnest Island proposed by Fairbridge (1961) has long been explained by possible tectonic displacement. However, the identification of two distinct bands of different ages, with a 1m gap in the notch wall in between,

makes the interpretation problematic (Baker *et al.*, 2001a). This can be resolved if one postulates two distinct major tectonic uplifts within a few thousand years, an unlikely scenario given the tectonically stable context of Australia.

Evidence from the southwest Australian coast provides an interesting comparison and support to the east Australian data, suggesting a degree of consistency of sea-level change over a wide longitudinal, as well as latitudinal span (Baker *et al.*, 2001a) (Fig. 2.12).

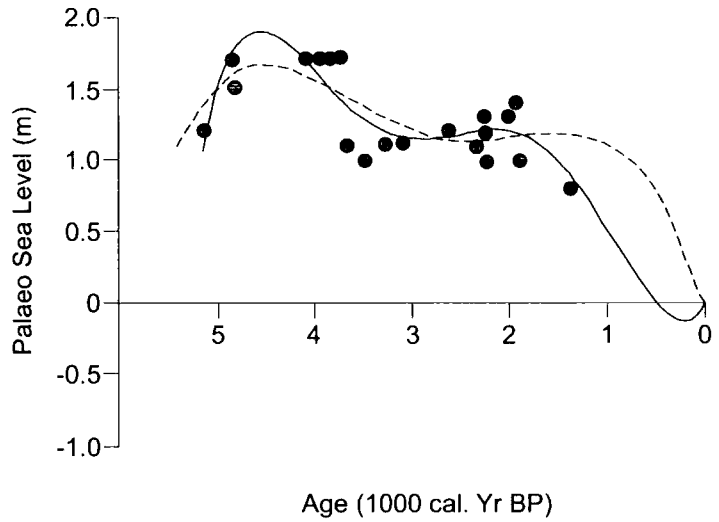

Fig. 2.12 The linear oscillating regression model (5th order polynomial) of Australian data for the past 5000 years for calibrated dates. No regional or southern hemisphere corrections are made with the calibrated dates (Baker *et al.*, 2001a).

The curve of Baker *et al.*, (2001a) depicts a series of index points with associated statistical regressions. Simple analysis of the points reveals a complex signal of sea-level change. Models for southern Australian coasts (Lambeck, 2002) depict a 'smooth decline' hypothesis that does not match the complex distributions of past and present marine species in Queensland, NSW, South Australia and Western Australia (Baker *et al.*, 2001a). They conclude that an oscillating model best fits the data (Fig. 2.12) and a rethink of the processes that underpin these changes is necessary. However, the 5th order polynomial regressions seem hard to justify within the context of the data, given the large gaps between data points and the scatter present. This scatter may be the result of the spatial differences between sea-level index points, reflecting differential crustal

responses to deglaciation. However, this scatter may also be indicative of a double highstand as found by Bezerra *et al.* (2003) in Brazil, though is very difficult to infer without the presence of vertical and horizontal error bars. It is also very hard to interpret the regression from 1,500 cal. yr BP to present, interpolated by the curves, with the absence of any index points to support this trend.

Further work by Baker *et al.* (2001b) draws comparisons between their Port Hacking sea-level reconstructions from NSW and similar reconstructions from the Laguna-Imbituba region of Southern Brazil (Fig. 2.13), highlighting again the potential for a spatially separate, yet temporally synchronous, double highstand.

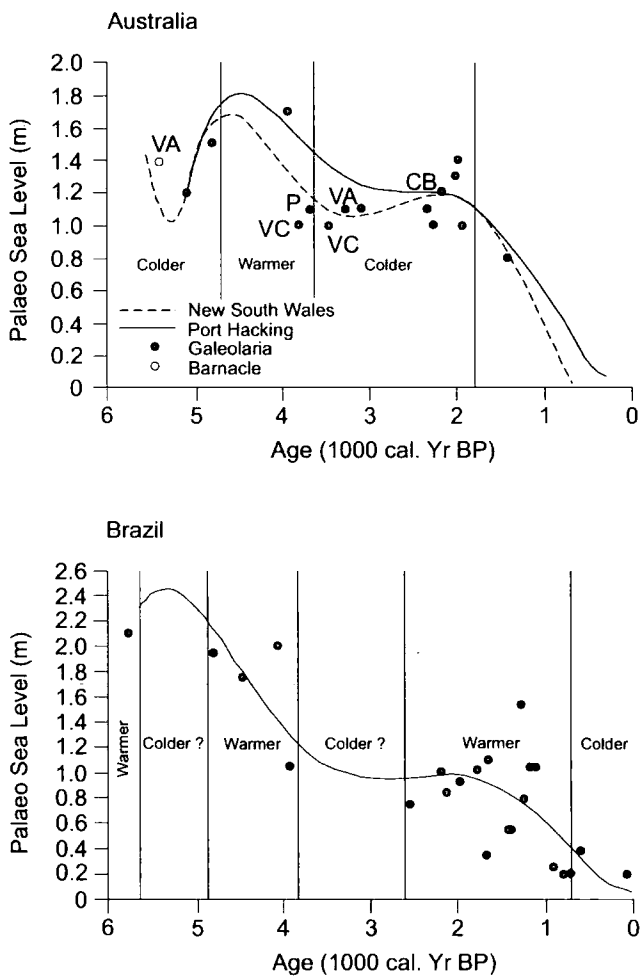

Fig. 2.13 The quintic polynomial regression models and histogram distribution of points. The vertical lines are event horizons of palaeoenvironmental change (Baker *et al.*, 2001b).

The evidence suggests that colder relative oceanic temperature prevailed from ~5200 to ~4500 cal. yr BP, and the onset after ~4500 cal. yr BP of a warmer than present phase is accompanied by a possible rapid sea-level rise to at least ~1.7 m above present (Baker *et al.,* 2001b). Baker *et al.* (2001b) conclude with a further check on the $\delta^{18}O$ content, there appears to be a striking coincidence between two colder and one warmer-than-present phase. Similar late Holocene oscillating sea-level curves for the South Australian and Brazilian coastlines, imply they are both tracking the same forcing factor. Additional evidence (Baker *et al.,* 2001b) demonstrates that the oscillating model for Port Hacking (Fig. 2.12) and for several other case studies in the southern hemisphere (Baker *et al.*, 2001a) were as statistically valid as the 'smooth' sea-level fall model, predicted by the models (Lambeck 2002). However, hemispheric synchronicity after ~2400 cal. yr BP breaks down between the two records, suggesting that there may be regional variations and lag effects in differential ocean warming. This may be related to the dynamics of ocean circulation and the relative strength of global forcing effects pitched against local influences. However, these data prove difficult to interpret as they are open to similar problems as lithostratigraphic reconstruction techniques, such as sediment compaction, in addition to the absence of error bars and presence of hiatuses in both records.

In addition to the work by Baker *et al.*, (2001a) and Lambeck (2002) there are other research areas that have produced sea-level reconstructions for Australia. Cann *et al.* (2000) have used Holocene foraminifera as indicators of sea-level change from the Murray River, South Australia, highlighting a maximum oceanic influence (MHHS) at 5255 ± 60 cal. yrs BP and estuarine influence at 3605 ± 70 cal. yrs BP. This evidence, coupled with an attributed sea-level fall around this period, has been implicated in the onset of climatic aridity locally. Wang and Chappell (2001) use foraminifera as Holocene environmental indicators in the South Alligator River, Northern Australia, an infrequently used FBI for the Australian region. They show that, as with North American (Gehrels, 1994; 2000, Gehrels *et al.*, 2001) and European studies (Horton *et al.,* 1999; 2000), foraminifers in intertidal sediments have distinctly different assemblages in the uppermost tidal, mid-tidal (mangrove), lower tidal and sub-tidal zones. They conclude that

foraminifers provide new information about Holocene palaeoenvironments not available from sedimentology or pollen analysis, though it must be stressed that the technique is bound by the limitations of seasonality and post mortem bioturbation. Detailed limitations of this technique are discussed in Chapter 3.

Evidence from southern Australia presented by Belperio *et al.* (2002) does not support the view of a stagnated transgression during the Holocene. The data are an amalgamation of a range of sea-level indicators, such as seagrasses, mangroves and sand flats, taken along a 1000km stretch of the South Australia coastline and conform to the general shape of sea-level curves for the region. The data show evidence for a rapid transgression in the early Holocene to a highstand at a maximum of 4m above present, using a combination of 233 supratidal, intertidal and subtidal indicators. This number of points shows a considerable degree of scatter as a result of errors associated with each reconstruction technique in addition to crustal disparities over the region. It is important to consider this factor when analysing such a volume of data as misleading interpretations, such as exaggerated crustal warping, can be drawn from plots encompassing a range of techniques and spatial localities.

In summary, from the results presented by numerous studies for Australia, evidence abounds for a MHHS shoreline around the entirety of the land mass utilising a range of biological indicators and geological features. A sporadic sea-level rise to the MHHS is suggested (Carter *et al.*, 1986) that does not get reflected by the geophysical models (Lambeck, 2002). However, the consensus is that the evidence conforms to the model of Lambeck (2002) depicting a MHHS for Australia. The nature of the subsequent regression from evidence shows a more fluctuating pattern of sea-level fall across Australia, with geophysical modelling indicating that spatial and temporal variability in the sea-level record can be expected to be the norm rather than the exception (Belperio *et al.*, 2002).

2.4 Environmental Change and Sea Level Reconstructions for the Great Barrier Reef (GBR)

Evidence abounds for the MHHS as the terminus for a rising limb of the early Holocene RSL change (Carter *et al.*, 1986; Cann *et al.*, 2000; Baker *et al.*, 2001a; b; Wang and Chappell, 2001; Belperio *et al.*, 2002). Being both tectonically stable and far from formerly glaciated regions, continental Australia is particularly well suited for the study of sea level evolution since the LGM and the late glacial stage (Yokoyama *et al.*, 2001). Methodologies adopt a slightly different guise here, though there is still the use of FBIs (Cann *et al.*, 2000; Wang and Chappell, 2001) in addition to coral studies (Woodroffe *et al.*, 2000) and geological based techniques (Belperio *et al.*, 2002). Examples illustrating spatially synchronous late Holocene sea-level fluctuations have been shown from 3000 km of north-south coastline along eastern Australia (Baker *et al.*, 2001a) in addition to studies from Tasmania, Western Australia and the Northern Territory. Within Australia the calcareous tubeworm *Galeolaria caespitosa* fits the condition of tightly constrained vertical zonation necessary to obtain good altimetric indications (Pirazzoli, 1996) and is widely used in reconstructions as a result. Sea-level models (Nakada and Lambeck, 1990) accept that the Queensland and New South Wales (NSW) data show a MHHS sea-level of approximately 1m above present, though they argue that the central and southern NSW coasts would contain no evidence much above present. However, studies presented show there to be a plethora of evidence suggesting sea levels in excess of 3m ± 0.5m at the highest sites, even towards the south of the eastern transect (Baker *et al.*, 2001a). Lambeck (2002) presents a model that predicts a smooth decrease in sea-level since the mid-Holocene for Australia, though the nature of the regression and transgression are cause for debate.

The GBR continental margin is an important region for sea-level studies, both for its tectonic stability and its evidence of RSL from fossil coral reefs (Larcombe *et al.*, 1995). Fortunately for reconstructions, the tidal ranges along the central GBR shelf are relatively small, increasing the constraints on indicators. As highlighted by Carter *et al.* (1986) the identification of relict Holocene shorelines is

possible throughout the SW Pacific. Indeed, Carter and Johnson (1986) document that they have recognised the 8 shorelines in the GBR referred to by Carter *et al.* (1986) with the addition of further sub shorelines confined to the GBR. This implies that a similar signal of sea-level rise in the early Holocene was being tracked by both systems. This is particularly striking as the sea-level changes are being documented by two different proxies, that of subtidal sediment wedges in New Zealand and drowned *in situ* coral growth from the GBR.

Further studies (Carter *et al.*, 1993; Beaman *et al.*, 1994; Larcombe *et al.*, 1995; Larcombe and Carter, 1998) have been completed on islands within the GBR, such as Magnetic Island (Fig. 2.14), as the result of accessibility, favourable tidal ranges, minimal tectonic activity and excellent stratigraphic preservation.

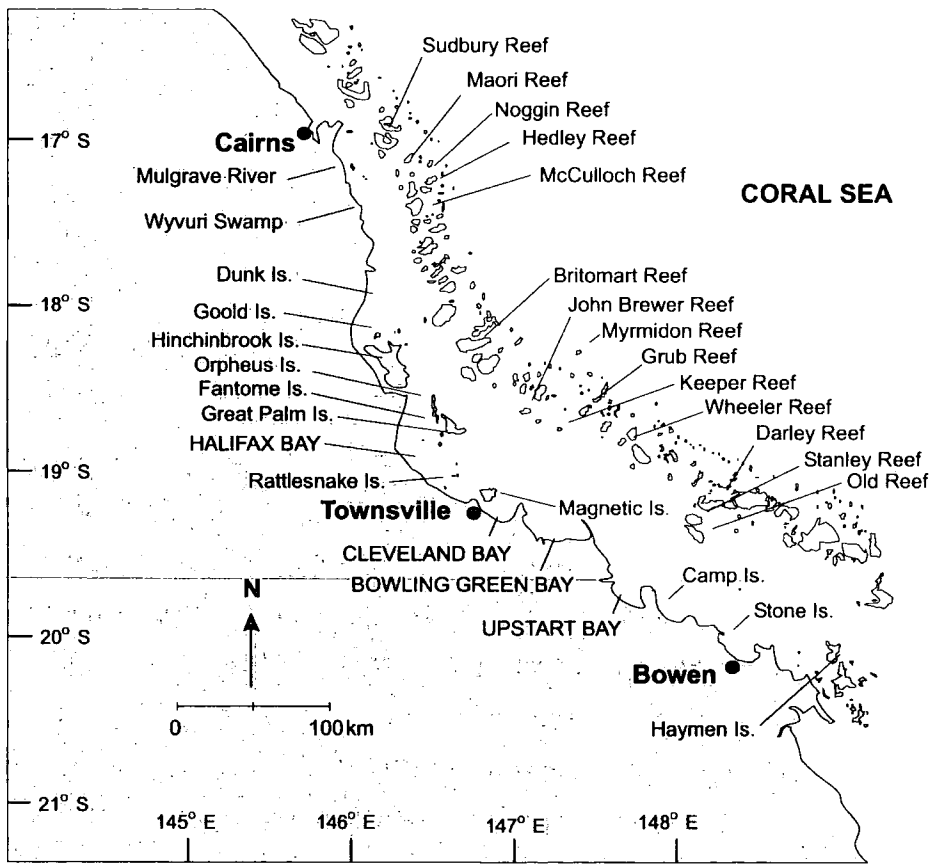

Fig. 2.14 Locality map of the central GBR shelf off Townsville (Larcombe *et al.*, 1995).

Carter *et al.* (1993) focus on Cleveland Bay and apply the sea-level data derived from the shoreline reconstruction technique (Carter *et al.*, 1986; Carter and Johnson, 1986) to assess the evolution of the embayment. This shows successive stages in the development of Cleveland Bay palaeogeography (Fig. 2.15).

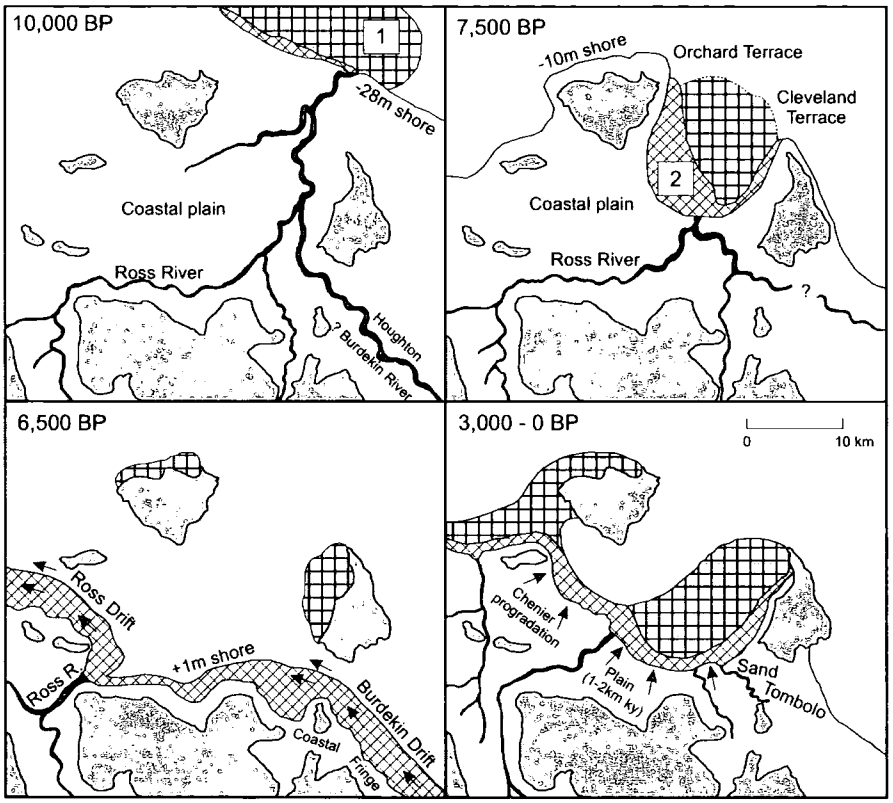

Fig. 2.15 Successive stages in the development of Cleveland Bay Palaeogeography, at 10, 7.5, 6.5 and 3-0 ka BP. Sediments shown use the following key: 1 = Bay fill sediment, 2 = Sand. The grey shading indicates mountainous high-ground (Carter *et al.*, 1993).

The model of Carter *et al.* (1993) helps to explain the presence of the sediment facies discussed by Larcombe *et al.* (1995) and Larcombe and Carter (1998) the result of interplay between the terrigenous sediment sources, such as the Ross, Burdekin and Houghton Rivers, and the sea. This provides a valuable context for the study area used in this project. Beaman *et al.* (1994) present data for fossil *in situ* oyster beds of intertidal origin on Magnetic Island (Fig. 2.14), supporting the general trend for a MHHS in the region. Their data suggest that the highstand was attained no later that 5660 ± 50 cal. yr BP at a level of 1.6-1.7m above modern levels and remained there for ca. 1600 yr. This compares to a

MHHS predicted at ca. 6,500 cal. yr BP suggested by Carter *et al.* (1993) and highlights a discrepancy perhaps caused by differing reconstruction techniques. These data plot 1-5m above terrigenous derived mangrove records of Holocene RSL change from northern Queensland, potentially indicative of underlining errors associated with sediment compaction in tropical mangrove deposits.

Larcombe and Carter (1998) present further Holocene RSL data (Fig. 2.16) using supra-, inter-, and subtidal indicators.

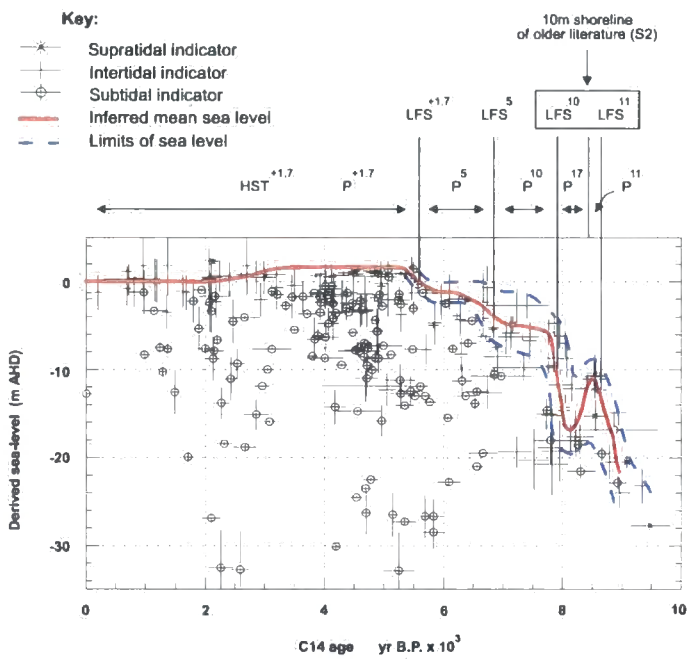

Fig. 2.16 Holocene RSL curve for the central GBR shoreline – inner shelf (Larcombe *et al.*, 1995).

The data show a wide scatter of sea-level index points and therefore they cautiously adopt a sea-level envelope to better understand the Holocene sea-level changes (Fig. 2.16). As a result, the MHHS is very difficult to interpret from the data (Larcombe and Carter, 1998) as errors in dating combined with altitudinal errors make them difficult to resolve in both absolute, and rate of sea-level change (Larcombe *et al.*, 1995). The data presented show that sea levels rose through its present level at 5,800-5,600 ^{14}C yrs BP towards the MHHS. In addition, this graph shows considerable scatter. However, similar scatter is present in the work of Belperio (2003) and can be attributed here, in part, to the range of spatial locations

(spanning an area 700kms by 150kms) used in the final plot undergoing differential crustal movements (Milne, *pers. comm.,* 2003). As a result, it may be difficult to accurately interpret a regression and transgression shown as a 'blip' between 8,500-8,000 ^{14}C yr BP (Larcombe *et al.*, 1995).

Larcombe *et al.* (1995) compare their data to the work of Chappell and Polach (1991) in the Huon Peninsula, Papua New Guinea. It is noted that there is an offset. This is explained by a differing geographical stetting (after correction for uplift) in addition to temporal changes in the rates of Huon coral growth unrelated to sea-level change, and/or by a variable rate of tectonic uplift, not uncommon in this area (Larcombe *et al.*, 1995). This is informative as it attempts to establish whether two differing records of sea-level change are spatially and temporally synchronous, mirroring work done by Carter *et al.* (1986) for New Zealand and the GBR. It is concluded that the data show supratidal and subtidal indicators providing upper and lower boundaries to the sea-level envelope (Fig. 2.16). As the quantity and resolution of the data improves there is increasing evidence for episodic and abrupt changes to sea level adding support to the conclusions of Baker *et al.* (2001a) with their oscillating sea-level models (Larcombe *et al.*, 1995).

2.5 Conclusions

The volume of data presented here occupies a wide range of locations and trends, all indicative of the interplay between the eustatic, isostatic, tectonic and local factors. Evidence from near-field and ice margin sites demonstrates a rapid fall in RSL from the early Holocene to present values, with ice margin sites displaying a brief rise at ca. 6,000 cal. yr BP before falling to present. Intermediate field sites display a rise in RSL at an ever-decreasing rate to present values, never straying above present day MSL. Far field sites show a rapid transgression to a MHHS followed by a fall in RSL to present values, with broad agreement in the character of RSL curves. This does not however withstand the fact that RSL data towards the end of the Holocene are ambiguous, mainly due to the relatively low precision of sea-level indicators (Larcombe *et al.,* 1995), in addition to the timing and amplitude of the MHHS.

This chapter has highlighted a wide range of sea-level indicators used in sea-level reconstructions, all of which are prone to both individual and communal limitations inherent to that specific technique. The use of corals produces excellent data, though the technique is prone to numerous pitfalls, including a lack of tightly constrained depth species and the inability of certain species' growth rates to keep up with rapid rates of RSL rise. Other biological proxies suffer from similar limitations, though are also open to post-depositional changes, such as carbonate dissolution, and *ex situ* contamination, such as inwash. Lithological proxies can produce a range of features, from the large through to small-scale laminations, most bearing a relationship to changes in RSL. However, in turn these features have vertical errors that can be proportional to the proxy feature. Lithostratigraphical techniques demonstrate that although a good resolution could be drawn, the chronology itself may be questionable due to differing rates of sedimentation. Underestimation of RSL is also a big issue in lithostratigraphic techniques as a result of post-depositional sediment compaction, lowering the elevation of the index points. It is therefore essential to consider the spatial extent of data, in addition to these inherent errors during interpretation to ensure that changes identified are actual and not manufactured.

As shown through studies using the intertidal transfer function technique for quantitative environmental reconstruction in Europe (Horton *et al.*, 1999a; Edwards and Horton, 2000; Gehrels, 2000; Gehrels *et al.*, 2001; Horton *et al.*, 2000; Edwards, 2001) and Australia (Horton *et al.*, 2003), this technique allows relatively precise reconstruction of former sea levels using a statistically based relationship among contemporary foraminiferal assemblages, their measured association to sea level and their fossil counterparts. This increased accuracy and precision will facilitate a meaningful definition of the transgression across the GBR shelf to the MHHS, and further the fall in RSL to present, having the potential to reinterpret the sea-level 'blip' referred to by Larcombe *et al.* (1995). In addition further understanding of the deglacial history, such as meltwater sources and timings may be possible, through generating a continuous record extending through the early, mid and late Holocene that may provide valuable inputs to geophysical models.

Chapter 3

Contemporary Sub-tidal Foraminifera Distribution, Great Barrier Reef Lagoon, Australia

3.1 Introduction

Foraminifera form part of a group of testate rhizopods belonging to the same family as thecamoebians and allogromiids. These one-celled organisms form a shell (test), occupying a generation time of between 3 and 4 months (Murray 2000). Foraminifera occupy every marine habitat from the highest high-water level to the deepest parts of the world's oceans, often with abundances greater than 1,000 individuals per 10cc of sediment (Scott *et al.,* 2001). Therefore, although much remains to be learned about the ecology of benthic foraminifera and the taphonomic processes that affect their preservation in the fossil record, they are nevertheless the best meiofaunal group for giving a proxy record of past marine and marginal marine environments (Murray 2000). Foraminifera are well-suited proxies for reconstructing sea levels, and subsequent palaeoenvironments (Phelger and Walton, 1950; Walton, 1952; Culver, 1990; Culver and Snedden, 1996), as studies from modern European and USA salt marshes (Scott and Medioli, 1978; Gehrels, 1994; de Rijk, 1995; Horton *et al.,* 1999a; 1999b; 2000; Gehrels *et al.,* 2001) have demonstrated distinct relationships between elevation and the tidal frame, that may be used to calibrate down core and temporal sequences (Haslett *et al.* 2001). Pilot studies in the Great Barrier Reef (GBR) (Woodroffe, 2002; Horton *et al.* 2003) have shown there is promise for the transfer function technique in the mangrove-dominated tidal areas found in tropical and sub-tropical regions, demonstrating a foraminiferal relationship with respect to elevation within the tidal frame.

In summary, foraminifera prove to be the most suitable proxy for this study because of their tolerance of environmental variables in contemporary habitats, ease of collection in time and cost, statistically significant populations, speed of data production and preservation within the fossil record. The sedimentary environment of the inner shelf of the GBR lagoon facilitates sub-tidal sampling of the mid-late Holocene record as a result of stratigraphic evidence presented by Larcombe *et al.,* (1995) and Larcombe and Carter (1998) in addition to the quiet water depositional environments already studied for inter-tidal sampling within the region (Horton *et al.* 2003; Woodroffe, 2002). However subtidal foraminiferal studies are few in number, demonstrating a semi-quantitative relationship with marine influence (Yokoyama *et al.,* 2000) and environments (M^{c}Intyre, 1996). Furthermore, fully-quantitative palaeoenvironmental reconstructions exhibiting a foraminiferal relationship to subtidal depth are non existent. Therefore, in consideration of some of these issues, the aims of this chapter are:

- To identify benthic foraminiferal species distributions living in subtidal environments of the Central GBR lagoon.

- To understand the relationship between foraminiferal species and their environment, thus testing the hypothesis that subtidal foraminifera are related to depth.

3.2 Study Area

The two tropical embayments I used in this study are Bowling Green Bay (19°20' S, 147°15' E) and Cleveland Bay (19°13' S, 146°55' E), part of the central GBR lagoon region, Queensland, Australia (Fig. 3.1). Fringing the entirety of the Queensland coast, the Great Dividing Range of mountains dominates a largely flat region. The study area is situated in the dry tropics with a wet season (November till March) accounting for 90% of the annual rainfall (M^{c}Intyre, 1996).

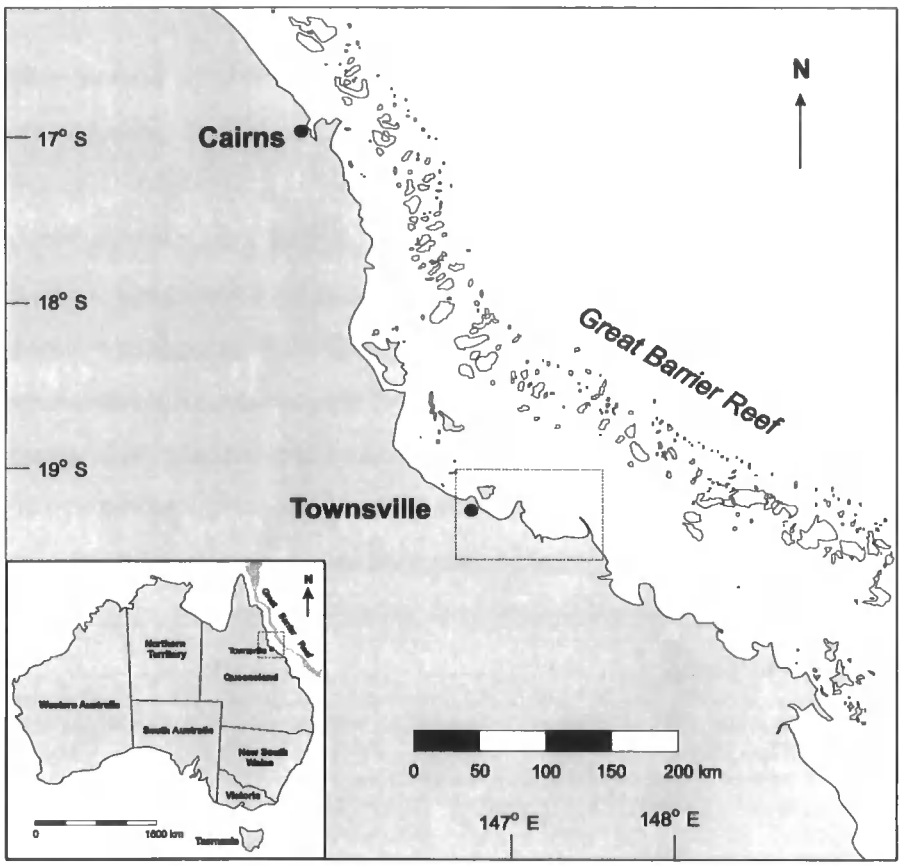

Fig. 3.1 Regional overview of the Central GBR Shelf, with an insert of study area

The embayments to a certain extent are protected by headlands (Cape Bowling Green and Cape Cleveland respectively) though lie open to northerly and north-easterly weather, and the effects of occasional tropical cyclones (M^{c}Intyre, 1996). Oliver (1978) notes that twenty-two cyclones passed within 167 km of Townsville, Cleveland Bay, in the 30 year period of 1940-1969, giving some idea of the frequency of storm inundation. As an offshore feature, the GBR lies some 60-80 km offshore, ranging from beyond Cape York in the north to some 600 km south of the two embayments, a total of over 2,000kms. The GBR shelf is some 100km wide in the central region with water depths reaching 80m (Orpin, 1999). Belperio (1983) recognises three zones that are important for defining sediment characteristics of the central GBR shelf; terrigenous (inner shelf), palimpsest (middle shelf) and reefal (outer shelf). For this study area, these zones correspond respectively to: 0-25m, containing a shore connected wedge of post-glacial terrigenous sediment that fill coastal embayments such as Cleveland Bay; 25-40m,

from the shore connected wedge to the inner edge of the reef tract; and 40-80m, encompassing the reef tract and areas beyond the shelf break (Larcombe and Carter, 1998).

Bowling Green Bay is the larger of the two embayments (Fig. 3.2) and is located some 30 km further south east along the coast from Cleveland Bay.

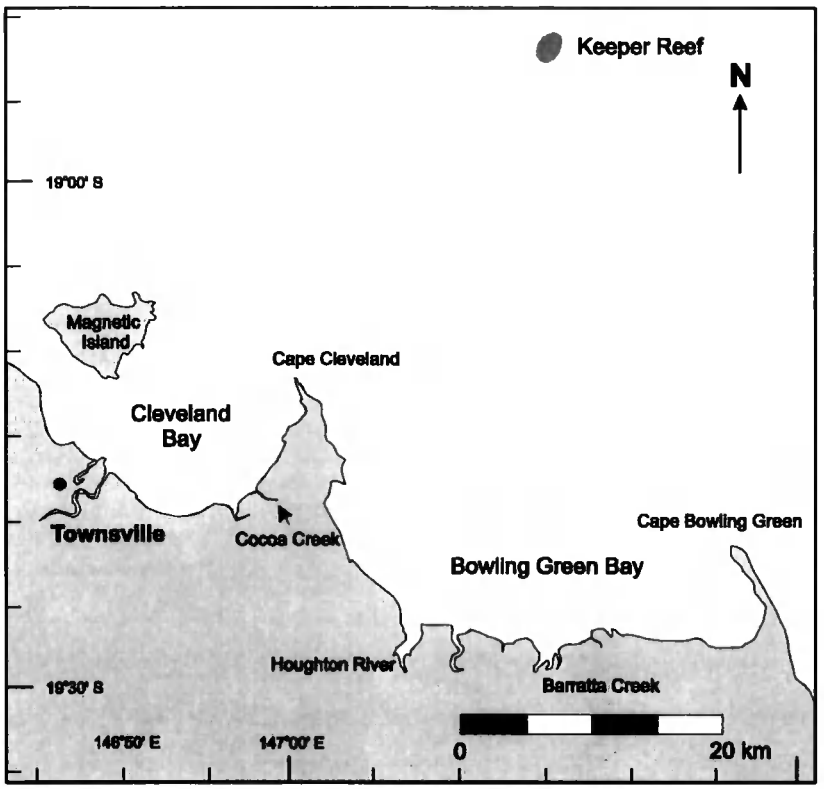

Fig. 3.2 Local overview of Cleveland and Bowling Green Bay

Cape Bowling Green is a sand spit and protects the easterly side of the bay from the dominant waves and currents from the south-east, and the Houghton River and Barratta Creek flow into the bay as a source of terrigenous sediment. Cleveland Bay is protected by Cape Cleveland, a granitic outcrop, with the Ross River discharging into it. Magnetic Island is an offshore granitic outcrop and is located to the north-west of the embayment.

3.3 Methodology

I collected contemporary foraminiferal samples from sub-tidal locations along transects in Bowling Green Bay and Cleveland Bay (Fig. 3.2). I used more than one transect in order to provide a ready opportunity for comparison between the two in addition to being able to create a regional database of subtidal benthic foraminiferal distributions. I used specific elevational ranges to investigate both the detailed distributions within a very constrained elevational range (Cleveland Bay) and further macro-scale distribution patterns (Bowling Green Bay).

3.3.1 Sampling Strategy

Contemporary samples have been selected to provide modern analogues for fossil cores in order to reconstruct RSL during the Holocene. I have selected two neighbouring embayments with contrasting physiographic conditions in order to encompass as many modern analogues as possible within the fossil cores. Samples were collected at semi-regular intervals in Bowling Green Bay and Cleveland Bay across the entirety of the transect.

3.3.2 Bowling Green Bay

This transect extends from a depth of -6.7m AHD through the inner, mid and outer shelves of the GBR lagoon to a depth of -48.0m AHD (Fig. 3.3) and contains 25 samples all of which were surface grabs. The surface samples were taken using an Ekman grab, producing $10cm^3$ of sediment of which a $5cm^3$ sub-sample was used. The sample size of $10cm^3$ has been used for over 50yrs and reflects a convention that was started at the Scripps Institution of Oceanography by F. B. Phelger, one of the pioneers of living foraminiferal distribution studies (Scott *et al.*, 2001).

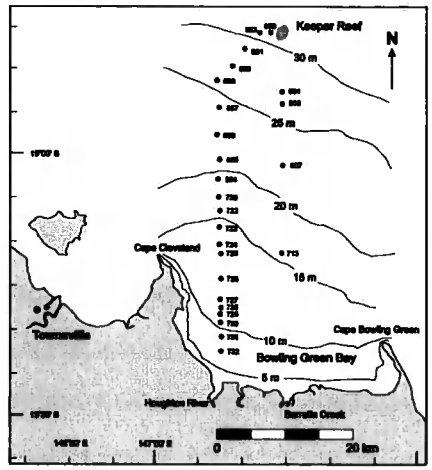

Fig. 3.3 Bowling Green Bay transect

3.3.3 Cleveland Bay

This transect is a composite of two smaller transects (Fig. 3.4), commencing at a depth of -4.2m AHD through to -9.8m AHD.

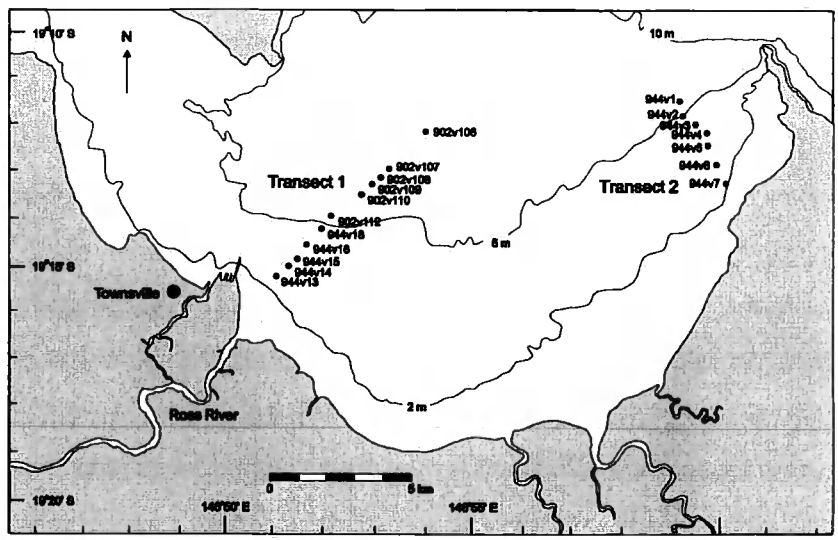

Fig. 3.4 Cleveland Bay transect (after M^{c}Intyre, 1996)

A total of 18 samples constitute Transect 1 (11) and Transect 2 (7). These were either surface grab samples, using the Ekman grab, or surface sampled vibracores, using the top 1cm providing 10cm^3 of sediment.

3.4 Laboratory Analysis

3.4.1 Foraminiferal Preparation

Samples of $5cm^3$ were passed through a $63\mu m$ sieve with organics being separated from the substrate by a process of decantation and wet splitting to eight parts (Appendix 1). Each eighth of a sample is then placed into a counting tray with successive eighths being added till the statistically significant total of 200 specimens is acquired (after Patterson and Fishbein, 1989). The assemblages used in this study are based upon total assemblages and all species are benthonic. Murray (2000) notes that the dead assemblage of lagoons and microtidal estuaries closely resemble the living except in those areas subject to powerful tides, and having identified the low tidal range for this site (a maximum of 4.01m between LAT and HAT), this suggests that the total assemblages will be of applicable use in this study. Furthermore, Scott *et al.* (2001) note that the use of total assemblages is the most accurate for use in contemporary and palaeoenvironmental reconstructions. Taxonomy follows Bronniman and Whittaker (1993), Wynn-Jones (1994), Loeblich and Tappan (1994), Yassini and Jones (1995), Hayward *et al.* (1999), Woodroffe *pers. com.* (2003) and Whittaker *pers. com.* (2003). Scanning Electron Microscope (SEM) illustrations of major species (those >2% of the distribution) can be seen in Appendix 2 (*pers. comm.* Whittaker, 2003).

3.4.2 Environmental Variables

Three environmental variables were collected for each sample along all transects. These include depth, loss-on-ignition and particle size analysis. Depth was recorded from the ship's depth sounder and calibrated with the tidal curve to give a depth in metres AHD for each sample.

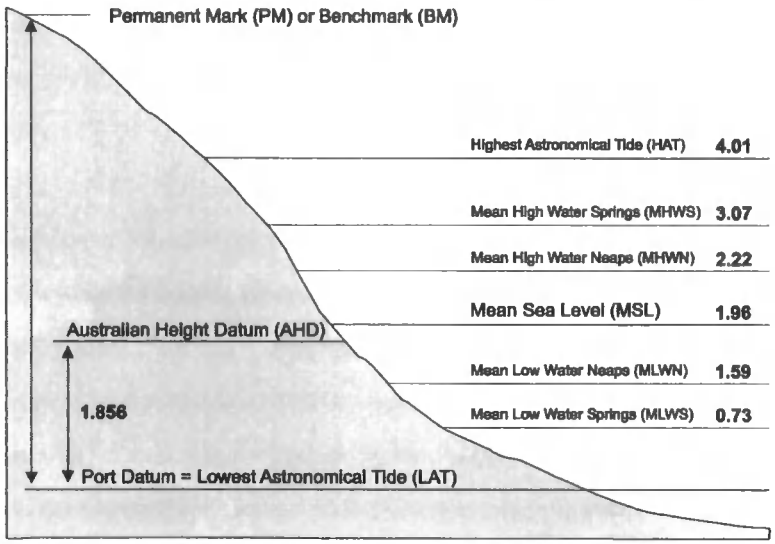

Fig. 3.5 Tidal levels for Townsville Port (1999). All elevations are given in metres above Port Datum = LAT (after Queensland Department of Transport, 1999).

This was achieved using knowledge of a series of benchmark elevations relative to the tidal curve at a given time and place, converting these to the national datum (AHD – Australian Height Datum) (Fig. 3.5). The error assigned to this calculation ranges from 0.3-0.5m dependant upon the vessel used in sample collection. Loss on ignition is used as a proxy for organic content within the substrate and followed the methods of Ball (1964) (Appendix 3). Data produced are expressed as a percentage of the total dry mass. Grains size analysis was carried out using a Coulter Laser Particle Granulometer (Appendix 4).

3.4.3 Statistical Techniques

Cluster analysis is a method that allows ecologists to classify sites, species or variables. There are several types of cluster analysis based on differing ideas about the clustering concept. The technique has been employed within this study to group sites with similar foraminiferal assemblage characteristics from all transects. The form of cluster analysis used here is unconstrained based on unweighted Euclidean Distance (no transformation or standardisation of the data) to classify contemporary samples into homogenous clusters using the CONISS statistical program. All figures pertaining to foraminifera are quoted as a percentage of the total assemblage maximum value within the specific sites for that

zone, having removed those species with a less than 2% count score (Horton *et al.*, 2003; Shennan *et al.*, 2000a). Detrended Correspondence Analysis (DCA) is an alternative technique that generates evidence for ecological zones, and when used in conjunction with cluster analysis provides an independent test for derived zones. The dataset is plotted on one diagram allowing comparisons to be drawn, plotting similar samples together and dissimilar apart.

Canonical Correspondence Analysis (CCA) is an ordination technique that has become widely used in ecological studies since it was first developed (ter Braak, 1986; 1987). CCA is a refined technique stemming from Correspondence Analysis (CA), a method of Ordination. The aim of ordination is to arrange species and site data such that those closer together correspond to sites that are similar in species composition, and points that are far apart correspond to sites that are dissimilar in species composition (Jongman *et al.*, 1995). CA seeks to construct a variable that best explains the species data, through generating an environmental gradient, and terms this the first ordination axis (Jongman *et al.*, 1995), and thus can be applied without the presence of environmental data. The second axis also explains the species data, but is not subject to the constraint of being uncorrelated with previous CA axes. In practice we ignore the higher numbered CA axes that explain only a small proportion of variance in the species data (Jongman *et al.*, 1995). However, in this study environmental data is present and therefore a canonical version of the technique is employed, CCA.

3.5 Subtidal characteristics of Great Barrier Reef embayments

3.5.1 Foraminiferal Distributions of Bowling Green Bay

I have identified 30 species from 25 sampling stations within Bowling Green Bay. Eight species are identified as dominant in abundance (Fig. 3.6) (Appendix 5) and these include *Discorbinella complanata, Triloculina oblonga, Cribrononion sydneyensis, Dendritina striata, Amphistegina lessonii, Operculina complanata, Quinqueloculina pseudoreticulata and Quinqueloculina vernusta.* For the statistical analysis we remove species groups that contribute less than 2% of

any assemblage (Patterson and Fishbein, 1989; Fatela and Taborda, 2002). *T. oblonga, C. sydneyensis* and *D. complanata* dominate the inner shelf region, with *D. striata* and *A. lessonii* increasing rapidly their dominance within the mid shelf. Individually *A. lessonii* dominates the outer shelf region, with *T. oblonga, C. sydneyensis* and *D. striata* having only a small relative abundance. Total counts of specimens achieved show a general increase from 563 individuals in the lowest of the inner shelf region to 4,420 individuals in the outer shelf region.

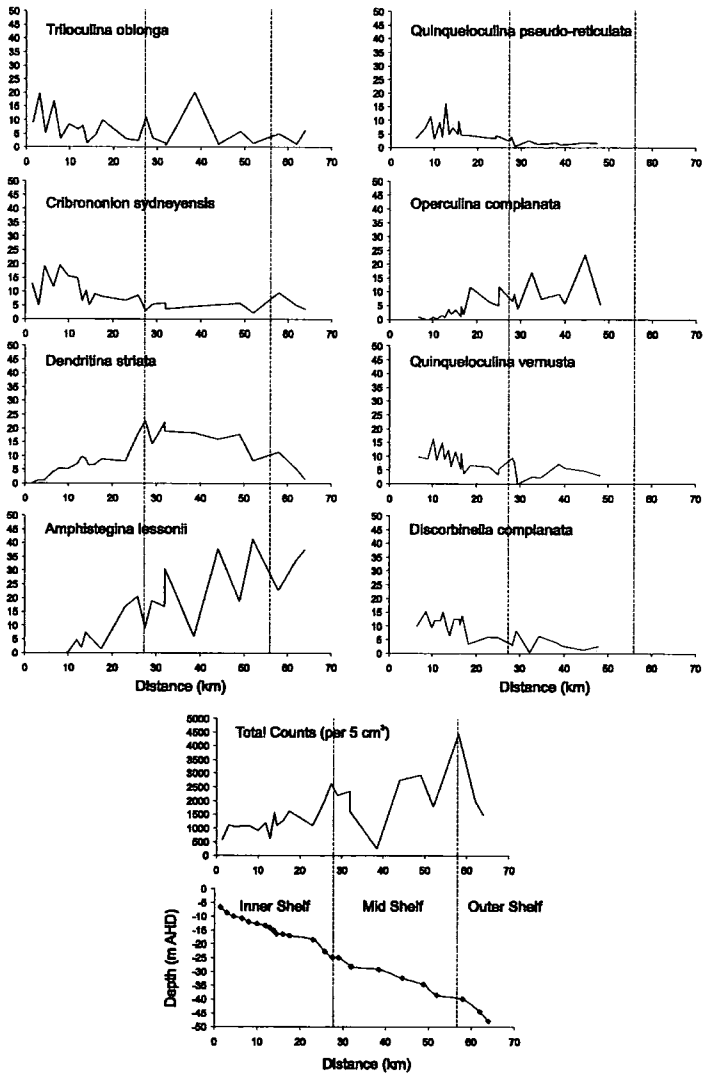

Fig. 3.6 Species plots with respect to distance offshore. Total counts are per 5cm^3 of sediment and extrapolated using the wet splitter. The inner, mid and outer shelf categories as defined by Belperio (1983).

3.5.2 Cluster Analysis, Detrended Correspondence Analysis and Zonal Elevation of Bowling Green Bay

This transect demonstrates 2 clusters (Fig. 3.9) that are supported by DCA analysis (Fig. 3.7). Zone 1 comprises 12 sites and is dominated by *Quinqueloculina venusta*, *C. sydneyensis* and *D. complanata*. Zone 2 encompasses 13 sites with *O. complanata*, *D. striata* and *A. lessonii* being dominant. Zone 2 differs from Zone 1 by having the highest percentages of *A. lessonii*: the relative percentages exceed 20% in 7 of the 13 samples. Additionally, *D. striata* and *O. complanata* have pronounced increases in distribution in Zone 2, with *D. striata* exceeding 20% of the relative abundance in 7 of the 13 samples.

Zone 1 displays a depth range of -6.7 to -17.0m AHD, separately defined from Zone 2, showing a range of -18.5 to -48.0m AHD.

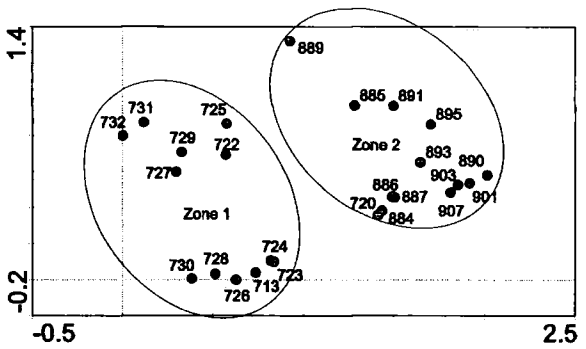

Fig. 3.7 Bowling Green Bay DCA results.

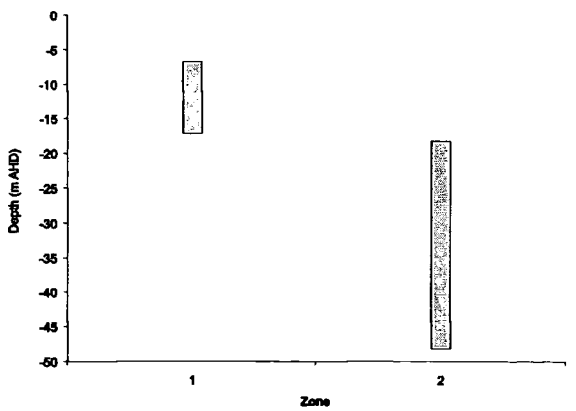

Fig. 3.8a Zone elevations and ranges derived from cluster and DCA analysis for Bowling Green Bay

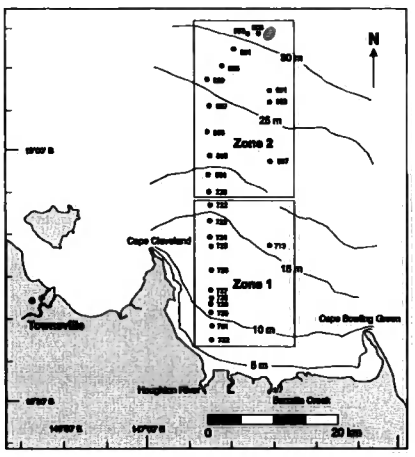

Fig. 3.8b Bowling Green Bay illustrating the geographical distribution of Zone 1 and 2 as identified in Fig. 3.8a

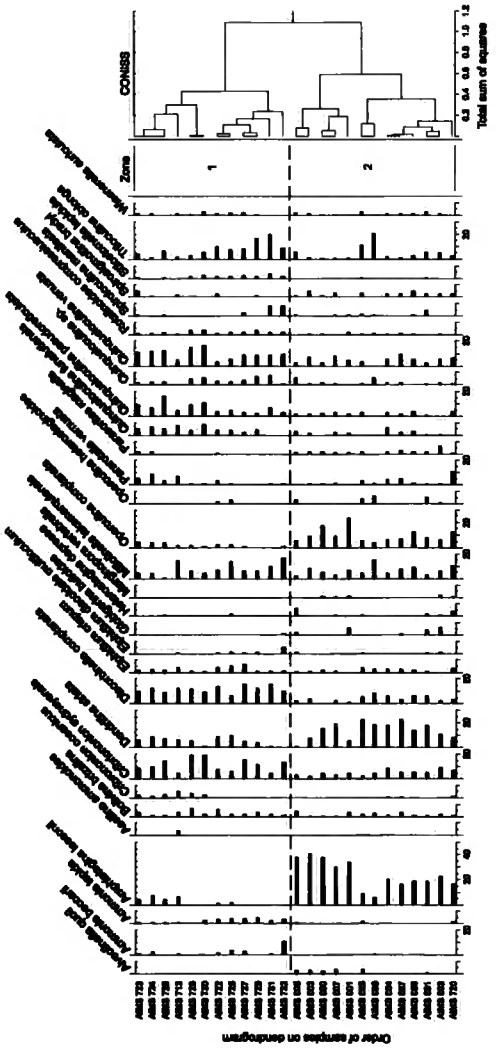

Fig. 3.9 Bowling Green Bay foraminiferal distributions (noting that *Globigerina bulloides* is a planktonic species)

3.5.3 Environmental Variables for Bowling Green Bay

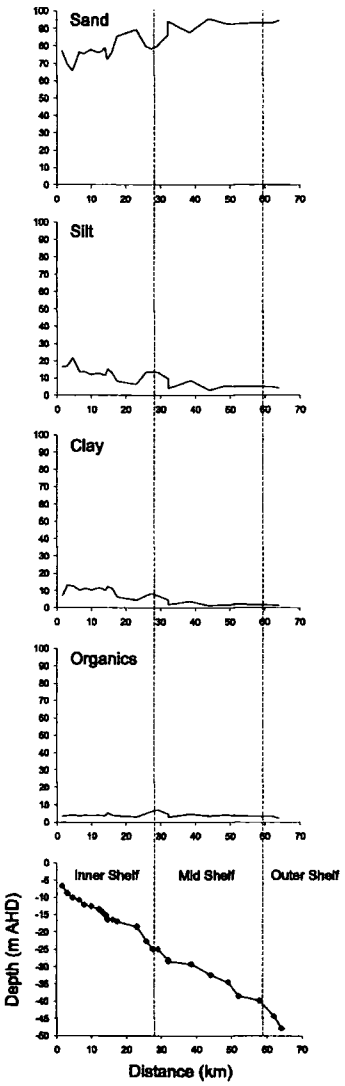

Fig. 3.10 Environmental variables with respect to distance for Bowling Green Bay. The inner, mid and outer shelf categories as defined by Belperio (1983).

At all stages the sand fraction is dominant and ranges from a minimum value of 65.8% (Site 730) to a maximum of 95.6% (Site 890) (Fig. 3.10). The silt fraction is considerably lower than the sand fraction and ranges from a maximum value of 21.6% (Site 730) to a minimum of 3.1% (Site 890). As a consequence of the high sand fraction and moderate silt content, the clay fraction is low throughout, ranging from a maximum of 13.2% (Site 731) and a minimum of 1.4% (Site 890 and 895). The organic content fluctuates very little along a consistent trend, with a maximum value of 7.2% (Site 886) and a minimum of 2.9% (Site 720).

Bowling Green Bay exhibits strong intercorrelations between sand, silt, clay and depth, all exceeding the critical value at the 99.9% confidence value (Table 3.1).

	Sand	Silt	Clay	Organics	Depth
Sand	1.0000				
Silt	-0.9750	1.0000			
Clay	-0.9669	0.8859	1.0000		
Organics	*-0.3604*	*0.4056*	*0.2869*	1.0000	
Depth	-0.8542	0.8025	0.8606	*0.1467*	1.0000

Table 3.1 Intercorrelations between environmental variables for Bowling Green Bay. Italics denotes poor organic content correlations.

Organic content shows a less statistically significant correlation with the remaining variables, though exceeding the critical value at the 90% confidence value for organics, sand and clay.

3.5.4 Relationship between Foraminifera and the subtidal environments of Bowling Green Bay (CCA)

As explained in the methodological section, CCA axis one and two are synthetic environmental variables that best explain the species data. Therefore correlations of the environmental variables with axis one and two show the strength of the variable in explaining the species data, a modern technique used to verify relationships already outlined. The length of the environmental arrow works in conjunction with the direction, and this depicts the rate of change in that direction. The location of a plotted species is a function of the contribution of environmental variables.

Axes	**1**	**2**	**3**	**4**	**Total inertia**
Eigenvalues	0.286	0.057	0.038	0.026	0.888
Species-environment correlations	0.952	0.818	0.689	0.777	
Cumulative percentage variance					
of species data	32.2	38.6	42.9	45.8	
of species-environment relation	68.4	82.2	91.2	97.4	
Sum of all eigenvalues					0.888
Sum of all canonical eigenvalues					0.417

Table 3.2 CCA summary statistics for Bowling Green Bay

CCA axes one (eigenvalue 0.286) and two (eigenvalue 0.057) explain 38.6% of the total variance in the data, with a total of 46.9% being explained by all axes (Table 3.2).

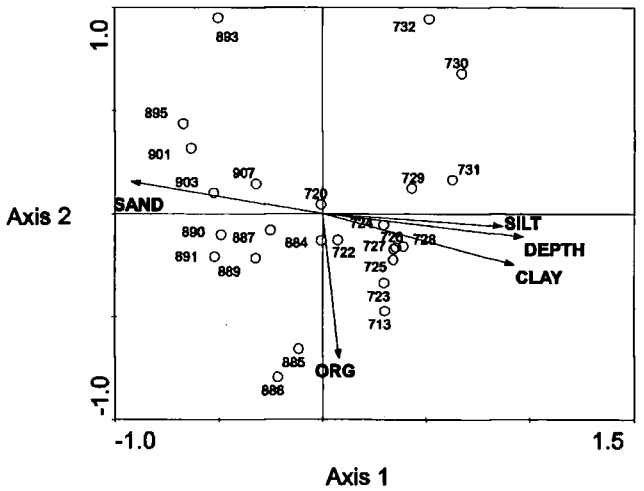

Fig. 3.11 Bowling Green Bay CCA site - environment biplot.

A strong environmental gradient within the data is identifiable, consisting of depth, sand, silt and clay fractions (Fig. 3.11). Deeper samples can be seen plotted on the left of the ordination plot, in addition to those with high sand fractions; samples to the right of the plot show comparably shallow depths and higher silt and clay fractions. Organic content plots away from the dominant gradient, correlating well with CCA axis 2.

As a result, the distribution of sites (Fig. 3.11) is a function of the constituent environmental variable scores on all axes. These are represented qualitatively by measuring the perpendicular position of the site along the environmental variable of interest. For example, it can be seen that sample 895 has one of the largest sand fractions, lowest silt and clay fractions (Appendix 7). Similarly it can be seen that sample 895 is the deepest. These principles are applied to inferences made along any gradient drawn on a biplots. Values, in this case sites, that are far from the origin, are better represented in the biplots than the abundances of values near the origin (Jongman *et al.*, 1995) and this should be noted when interpreting biplots, specifically species data. For Bowling Green Bay, samples 720, 722 and

884 all plot near the origin and therefore care should be taken with their interpretation.

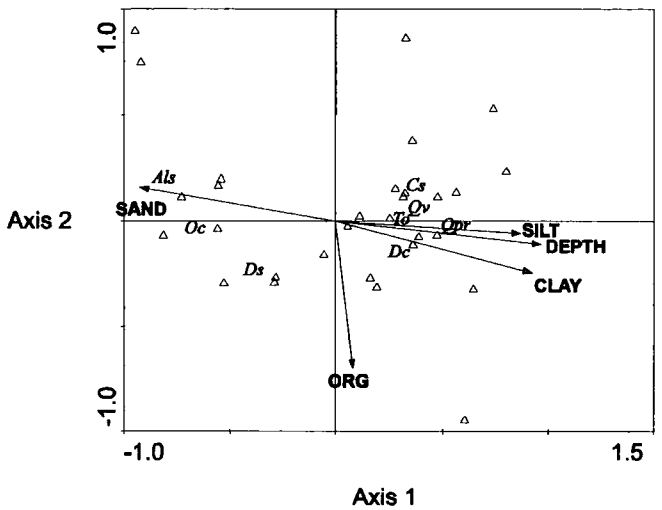

Fig. 3.12 Bowling Green Bay CCA species - environment biplot. *Dc – D. complanata, To – T. oblonga, Cs – C. sydneyensis, Ds – D. striata, Als – A. lessonii, Oc - O. complanata, Qpr – Q. pseudoreticulata and Qv – Q. vernusta.*

Adopting the methodology of interpretation, it can be noted that species plotting at deeper elevations with high sand, relatively low silt and clay fractions include *A. lessonii, D. striata* and *O. complanata* (Fig. 3.12). The remaining dominant species plot in the shallower depths and show little preference to the largely irrelevant organic content variable.

3.5.5 Foraminiferal Distributions of Cleveland Bay

Cleveland Bay encompasses 2 transects (Fig. 3.4) and the results for these are presented separately.

3.5.6 Foraminiferal Distributions of Cleveland Bay - Transect 1

I have identified 22 species from 11 sampling stations within Cleveland Bay Transect 1. Six species are identified as being dominant in relative abundance (Fig. 3.13) (Appendix 5), and these include *Q. venusta, C. sydneyensis, Ammonia tepida, Cribrononion oceanicus, D. complanata* and *T. oblonga*. The near-shore

environment is dominated by *C. sydneyensis* and *A. tepida,* with *D. complanata* showing a sustained presence throughout the remaining stations within the transect. Distributions of other species demonstrate an approximately equal relative abundance in the mid-shore and off-shore sections of the transect. The total counts vary within the near shore stations before reaching consistent level of around 1,700 individuals per $5cm^3$ of sediment.

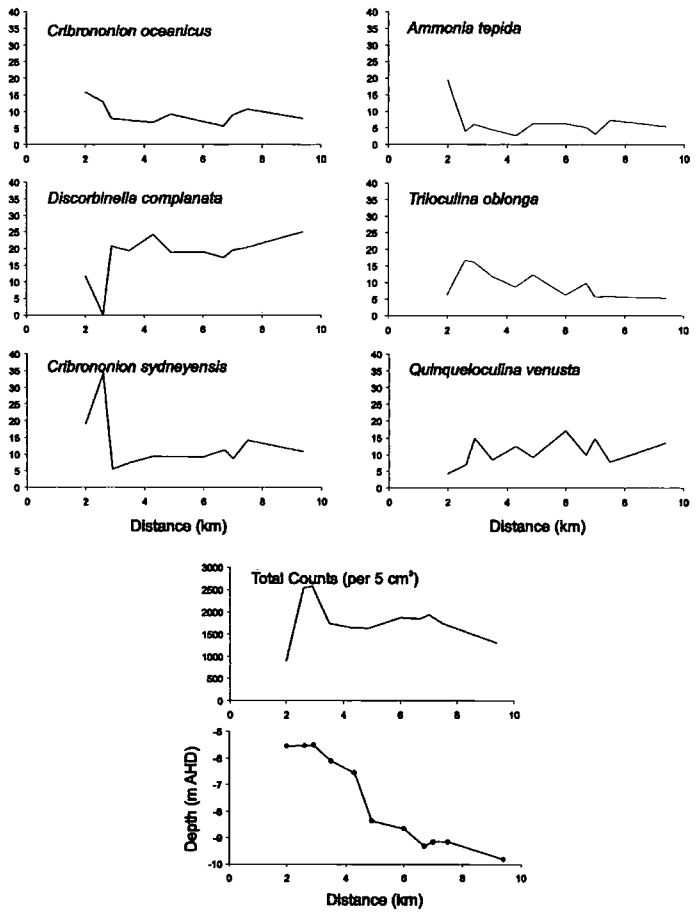

Fig. 3.13 Species distribution with respect to distance offshore for Transect 1

3.5.7 Cluster Analysis, Detrended Correspondence Analysis and Zonal Elevation of Cleveland Bay - Transect 1

Transect 1 demonstrates 2 clusters (Fig. 3.14) supported by DCA analysis (Fig. 3.15). Zone 1 comprises 9 sites and is dominated by *D. complanata* and *Q. venusta*. Zone 2 encompasses 2 sites with *Cribrononion sydneyensis*, *C.*

oceanicus and *A. tepida* dominating. Zone 1 displays a depth range of -5.5 to -9.8m AHD shows a range of -5.5 to -5.6m AHD (Fig. 3.16a).

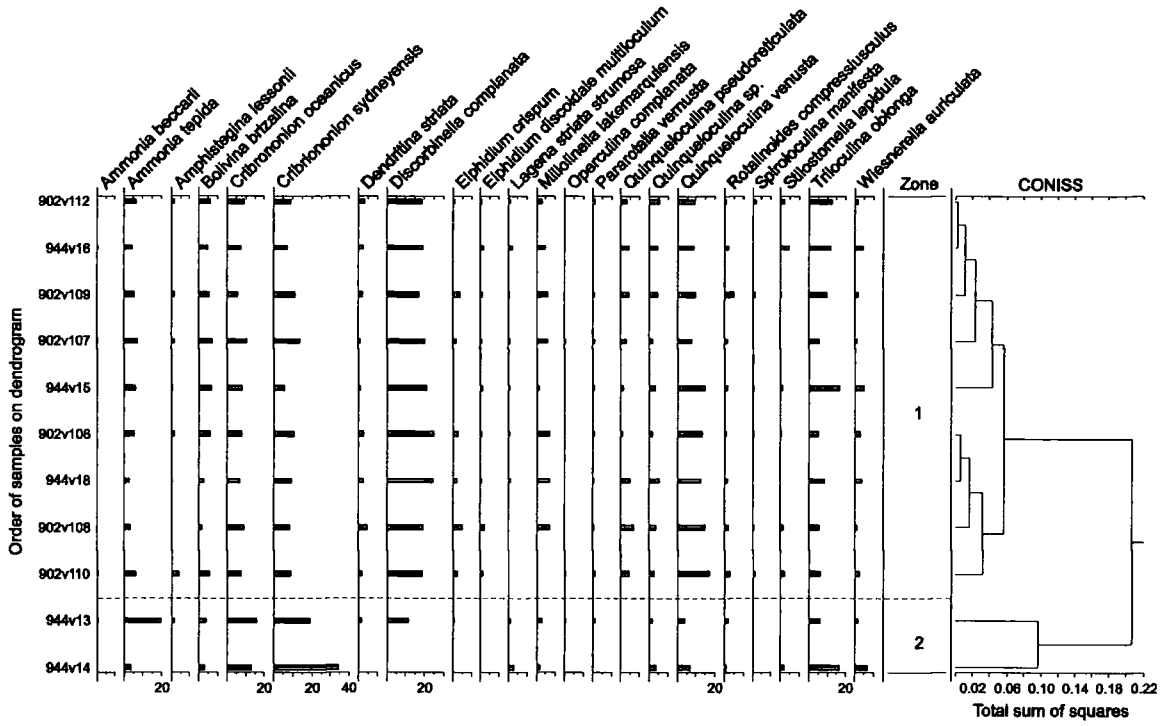

Fig. 3.14 Cleveland Bay foraminiferal distributions for Transect 1

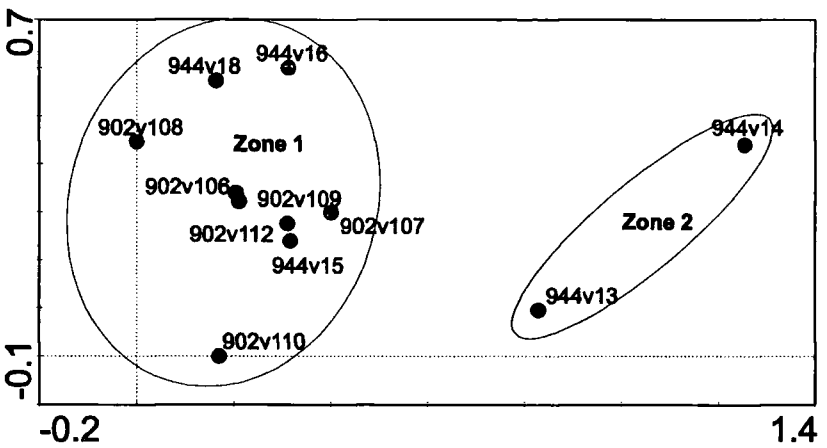

Fig. 3.15 DCA analysis of Cleveland Bay Transect 1 foraminiferal assemblages

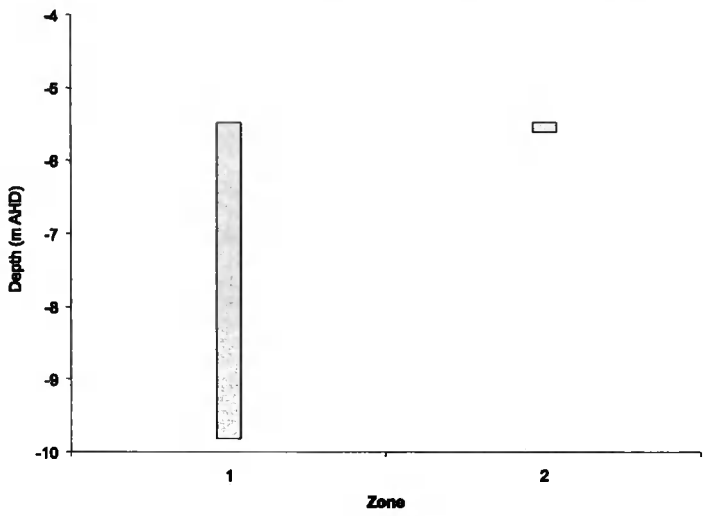

Fig. 3.16a Elevational range of the two foraminiferal zones highlighted for Transect 1

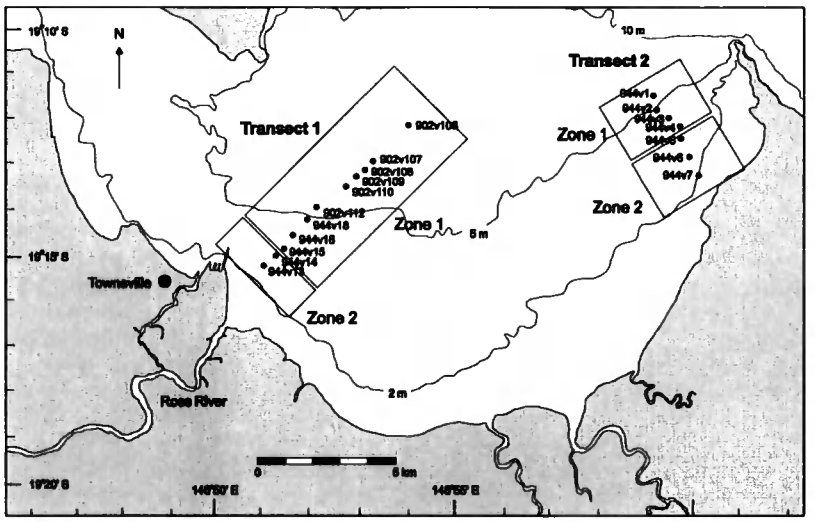

Fig. 3.16b Cleveland Bay illustrating the geographical distribution of Zones 1 and 2 as identified in Fig. 3.16a and Fig. 3.23

3.5.8 Environmental Variables for Cleveland Bay - Transect 1

At all stages throughout Transect 1 the sand fraction is dominant and ranges from a minimum value of 44.3% to a maximum of 96.0% (Fig. 3.17). The silt fraction is considerably lower, though has high values in the near shore end (45.2%) compared to offshore stations (Appendix 8). The clay and organic content remain low and consistent throughout. Depth shows no statistically significant

correlation with any of the other variables, though strong intercorrelations are exhibited between sand, silt, clay and organics (Table 3.3).

	Sand	Silt	Clay	Organics	Depth
Sand	1				
Silt	*-0.9696*	1			
Clay	*-0.6628*	0.4595	1		
Organics	*-0.7936*	*0.7070*	*0.7158*	1	
Depth	-0.4047	0.5554	-0.2311	0.1330	1

Table 3.3 Intercorrelations between environmental variables for Transect 1. Italics denotes >90% significance of correlation.

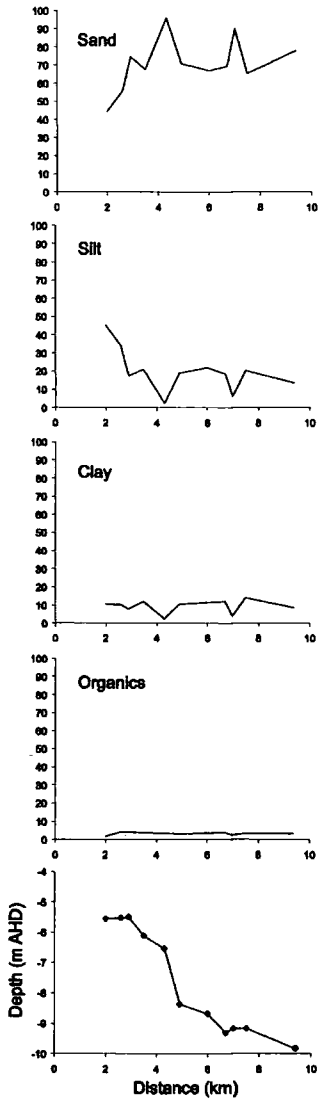

Fig. 3.17 Environmental variables plotted with respect to distance for Transect 1

3.5.9 Relationship between Foraminifera and the subtidal environments of Cleveland Bay - Transect 1 (CCA)

CCA axes one (eigenvalue 0.094) and two (eigenvalue 0.038) explain 47.0% of the total variance in the data, with a total of 55.7% being explained by all axes (Table 3.4) (Fig. 3.18).

Axes	1	2	3	4	Total inertia
Eigenvalues	0.094	0.038	0.016	0.008	0.280
Species-environment correlations	0.914	0.842	0.869	0.787	
Cumulative percentage variance					
of species data	33.5	47.0	52.6	55.6	
of species-environment relation	60.3	84.5	94.6	100.0	
Sum of all eigenvalues					0.280
Sum of all canonical eigenvalues					0.156

Table 3.4 CCA summary statistics for Cleveland Bay Transect 1

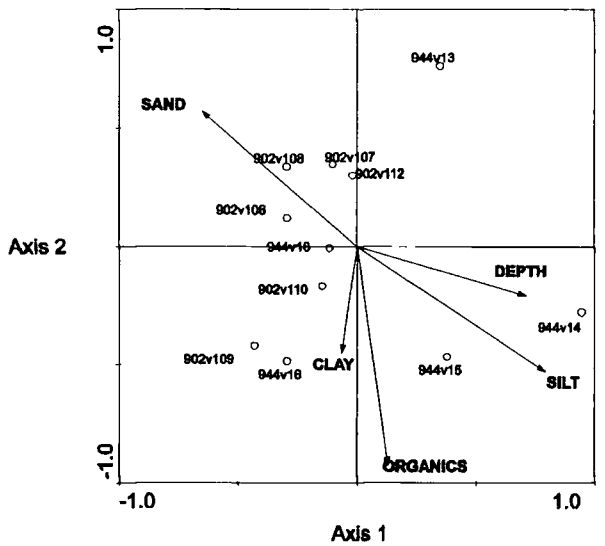

Fig. 3.18 Cleveland Bay Transect 1 CCA site - environment biplot

The environmental gradient displayed shows a general lack of agreement with any sites (Fig. 3.18), the exception being that sand shows to be the dominant variable with many sites plotting along this variable.

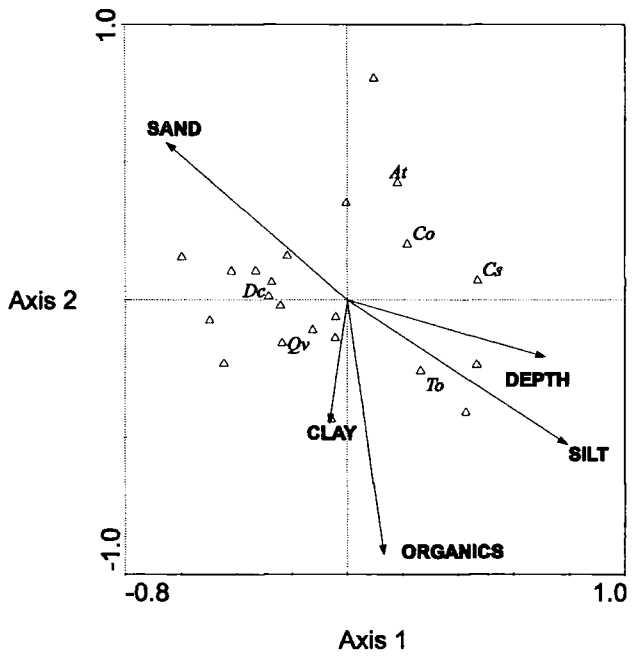

Fig. 3.19 Cleveland Bay Transect 1 CCA species - environment biplot. *Qv – Q. venusta, Cs – C. sydneyensis, At – A. tepida, Co – C. oceanicus, Dc – D. complanata and To – T. oblonga.*

The dominant foraminiferal distributions on the species-environment biplot (Fig. 3.19) show a wide scatter around the origin of CCA axes 1 and 2. Following the stated methodology, distributions clustered near the origin should be treated with care, especially in the context of the limited use of the environmental gradients shown earlier. Like the site samples, however, foraminiferal species plot more towards the sand fraction, reinforcing the dominance of this variable.

3.5.10 Foraminiferal Distributions of Cleveland Bay - Transect 2

I have identified 22 species from 7 sampling stations within Cleveland Bay Transect 2. Five species are identified as dominant (Fig. 3.20) (Appendix 5) and these include *Q. pseudoreticulata, Q. venusta, C. sydneyensis, Pararotalia vernusta* and *A. lessonii. Pararotalia vernusta* dominates the near shore environment, with relative abundance falling dramatically moving towards the centre of the transect as *Q. pseudoreticulata* and *Q. venusta* increase their presence. The offshore section of the transect attains comparable values of each of *Q. pseudoreticulata, Q. venusta, C. sydneyensis* and *A. lessonii.* The total

counts generally decrease with distance from the shore, peaking at 707 individuals and falling to 325 per 5cm^3 of sediment.

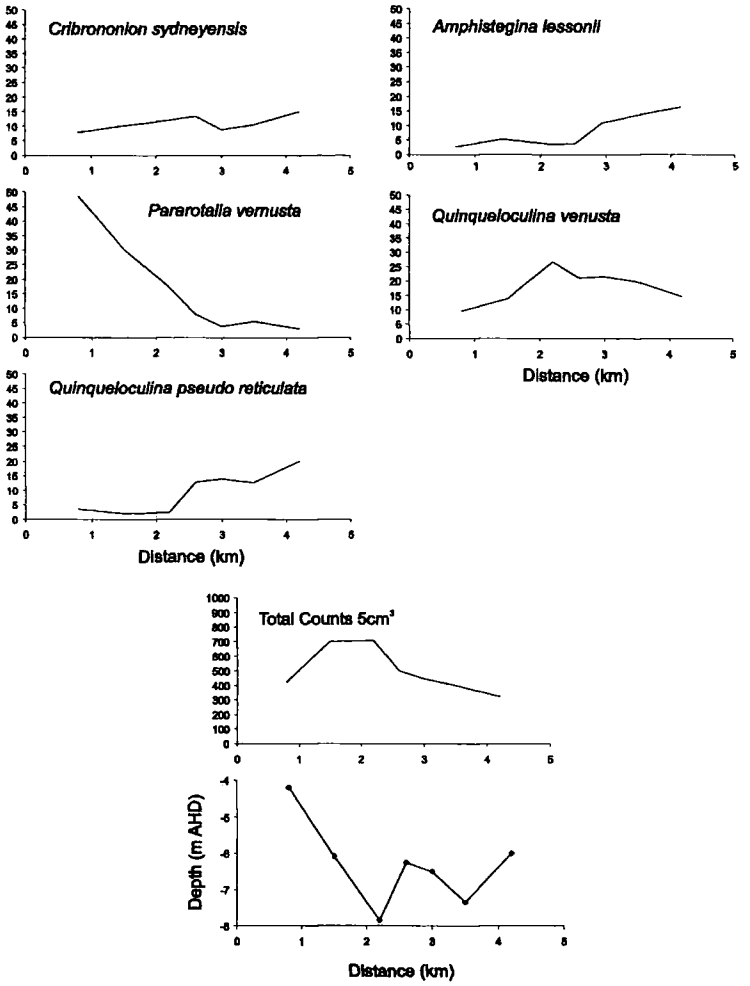

Fig. 3.20 Species distribution with respect to distance offshore for Transect 2

3.5.11 Cluster Analysis, Detrended Correspondence Analysis and Zonal Elevation of Cleveland Bay - Transect 2

Transect 2 also demonstrates 2 clusters (Fig. 3.21) supported by DCA analysis (Fig. 3.22). Zone 1 comprises 4 sites and is dominated by *Q. venusta, A. lessonii* and *Q. pseudoreticulata*. Zone 2 encompasses 3 sites with *P. vernusta* and *Q. venusta* having significant relative abundances. Zone 1 displays a depth range of -6.0 to -7.4m AHD, separately defined from zone 2, showing a range of -

4.2 to -7.9m AHD (Fig. 3.23). The elevational range of the clustered zones is shown on Fig. 3.16b.

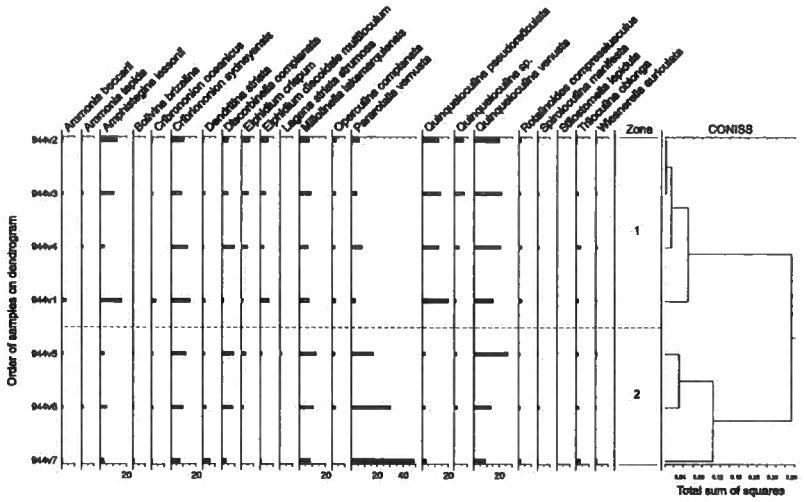

Fig. 3.21 Cleveland Bay foraminiferal distributions for Transect 2

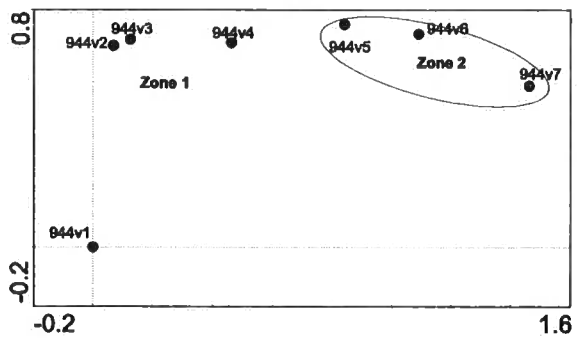

Fig. 3.22 DCA analysis of Cleveland Bay Transect 2 foraminiferal assemblages

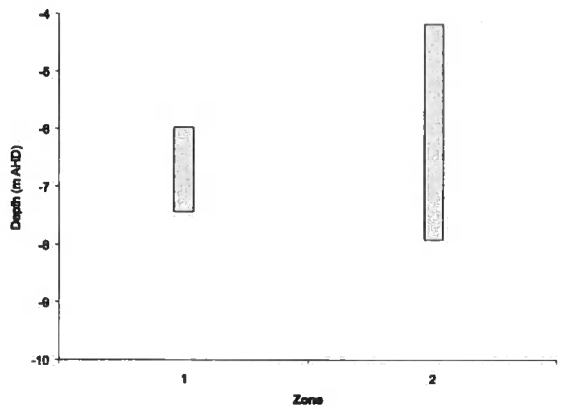

Fig. 3.23 Elevational range of the two foraminiferal zones highlighted for Transect 2

3.5.12 Environmental Variables for Cleveland Bay - Transect 2

Throughout, the sand fraction is dominant and ranges from a minimum value of 84.0% to a maximum of 97.6% (Fig. 3.24) (Appendix 8). The silt, clay and organic content remain low and consistent throughout. Depth shows no statistically significant correlation with any of the variables though strong intercorrelations are exhibited between sand, silt, clay and organics.

	Sand	Silt	Clay	Organics	Depth
Sand	1				
Silt	*-0.9861*	1			
Clay	*-0.9624*	*0.9040*	1		
Organics	*-0.6893*	*0.6913*	0.6420	1	
Depth	-0.5535	0.6239	0.4084	0.1313	1

Table 3.5 Intercorrelations between environmental variables for Transect 2. Italics denotes >90% significance of correlation.

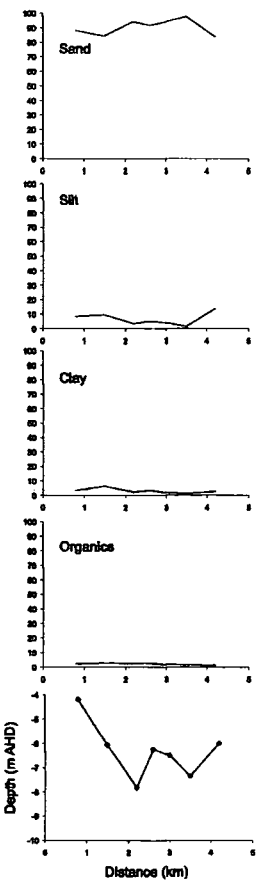

Fig. 3.24 Environmental variables plotted with respect to distance for Transect 2

3.5.13 Relationship between Foraminifera and the subtidal environments of Cleveland Bay - Transect 2 (CCA)

CCA axes one (eigenvalue 0.237) and two (eigenvalue 0.071) explain 76.6% of the total variance in the data, with a total of 87.6% being explained by all axes (Table 3.6) (Fig. 3.25).

Axes	1	2	3	4	Total inertia
Eigenvalues	0.237	0.071	0.023	0.014	0.402
Species-environment correlations	0.966	0.996	1.000	0.999	
Cumulative percentage variance					
of species data	59.0	76.6	82.4	85.9	
of species-environment relation	67.4	87.5	94.1	98.1	
Sum of all eigenvalues					0.402
Sum of all canonical eigenvalues					0.352

Table 3.6 CCA summary statistics for Cleveland Bay Transect 2

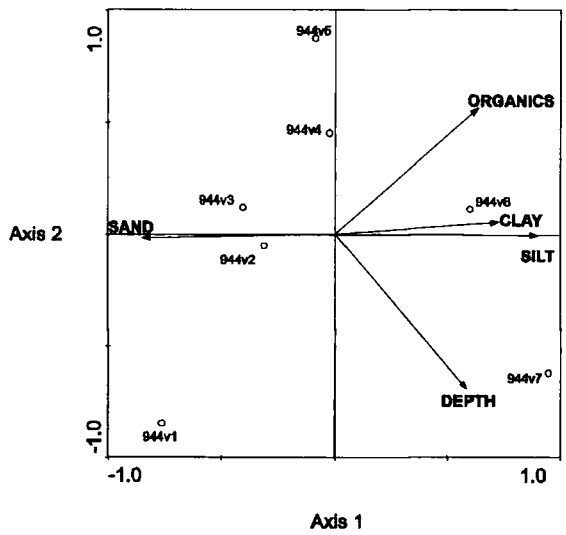

Fig. 3.25 Cleveland Bay Transect 2 CCA site - environment biplot

The environmental gradient depicted shows a clear correlation with CCA axis 1, and reflects intercorrelations shown (Fig. 3.25). Sand again dominates with organic content and depth showing approximately equal correlations with both CCA axes.

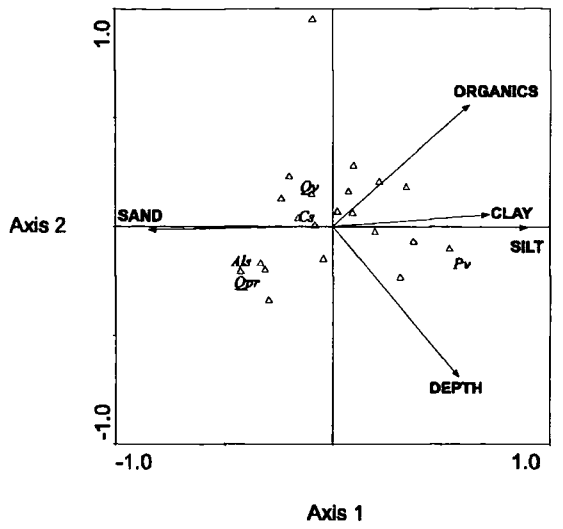

Fig. 3.26 Cleveland Bay Transect 2 CCA species - environment biplot. *Qpr - Q. pseudoreticulata, Qv – Q. venusta, Cs - C. sydneyensis, Pv – P. vernusta, Als – A. lessonii.*

This transect demonstrates a similar clustering of species around the origin, with the notable exception of *P. vernusta*, plotting towards the silt and clay fractions some distance from the ambiguous origin (Fig. 3.26). Following stated methodology, origin clustered distributions should be treated with care, especially in this context noting the limited use of the environmental gradients.

3.6 Discussion

Studies using foraminifera to derive environmental information around Australia are limited in their extent. These studies include work by Cann *et al.* (2000) using Holocene foraminifera as indicators of relative estuarine-lagoonal and oceanic influences in estuarine sediments of the Murray River; Horton *et al.* (2003) using contemporary inter-tidal foraminiferal distributions of a mangrove environment, GBR coastline; Wang and Chappell (2001) using foraminifera as Holocene environmental indicators in the South Alligator River, and Woodroffe (2002) using inter-tidal foraminifera as a palaeoenvironmental reconstruction technique for the GBR coastline. However, these studies use inter-tidal benthic foraminiferal distributions, a technique employed across the world (Scott and Medioli, 1978, 1980; Gehrels, 1994; de Rijk, 1995; Horton, 1999; Horton *et al.*, 1999a). However, subtidal studies are scarce. With specific reference to two

fundamental aspects of this project, the work of Yokoyama *et al.* (2000) and M^{c}Intyre (1996) are paramount. Yokoyama *et al.* (2000) developed a classification assigning a marine zone, derived through foraminifera, to sedimentary facies from the Bonaparte Gulf, Western Australia. However this classification has only 4 zones (open marine, shallow marine, marginal marine and brackish) giving a somewhat limited constraint with respect to depth. Furthermore, foraminiferal data are not presented to support this study. M^{c}Intyre (1996) demonstrates a similar system of classification for samples collected from Cleveland Bay, defining 6 environments (tidal flat, beach, inner shelf, eastern inner shelf, mid-shelf and Chenier ridge), again derived from foraminifera. Though as a necessary prerequisite for a quantitative palaeoenvironmental reconstruction (QPR) technique, elevational constraint is paramount and therefore both of these studies lack defined niches.

3.6.1 Foraminiferal sub-tidal distribution in Bowling Green Bay

There is a constrained range of foraminiferal species found in the subtidal sediments of Bowling Green Bay, with the assemblage being dominated by *A. lessonii*, *D. striata* and *O. complanata*. The ecological effect of depth can be split into direct and indirect factors. Direct factors include pressure changes and light intensity with evidence in the literature for each factor having a controlling effect (Boltovskoy and Wright, 1976; Sen Gupta, 1999).

Multivariate analysis (CCA) shows that *A. lessonii* and *O. complanata* dominate deeper environments (Fig. 3.27).

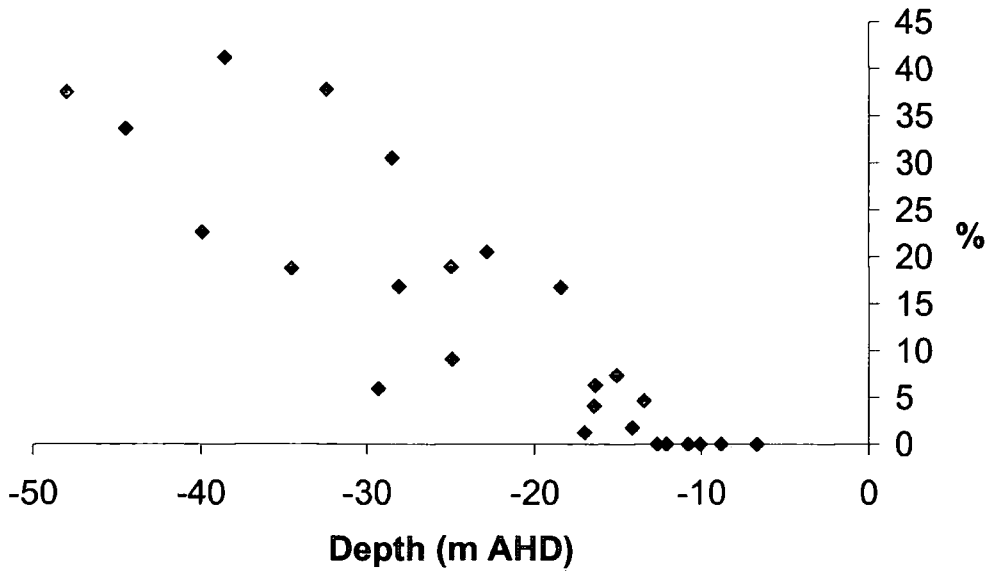

Fig. 3.27 *A. lessonii* distribution with respect to depth for Bowling Green Bay

M^{c}Intyre (1996) notes that *Amphistegina* sp. is common (10-20%) increasing to abundant (>20%) in the eastern inner shelf of Cleveland Bay and mid shelf regions of the GBR lagoon. This complements the distributions presented here where *A. lessonii* increases in abundance from 0% at -6.7m AHD (inner bay) to 38% at -48.0m AHD (outer shelf). Hottinger (1977) notes that *A. lessonii* has a depth range to approximately 90m below sea level, most abundant at 35-40m, where this study identifies a peak of 41.2% of the assemblage in Bowling Green Bay. Langer and Lipps (2003) identify a cluster of lagoonal sediments in their study of Madang Reef, Papua New Guinea, dominated by *Amphistegina* sp. This cluster occurs on the lagoon floor at depths of between 19 and 41m, a very similar environment to the GBR lagoon. The genus *Amphistegina* occupies a substrate that is coarse carbonate dominated (Murray, 1991). Orpin (1999) notes the GBR to be the largest modern example of a mixed terrigenous-carbonate system on earth. In addition the species has marine salinity, temperatures in excess of 20°c, and a depth of 0-130 m on coral reefs or in lagoons (M^{c}Intyre, 1996; Langer and Lipps, 2003).

D. complanata under multivariate analysis (CCA) shows dominance in shallower environments, supported by empirical evidence (Fig. 3.28).

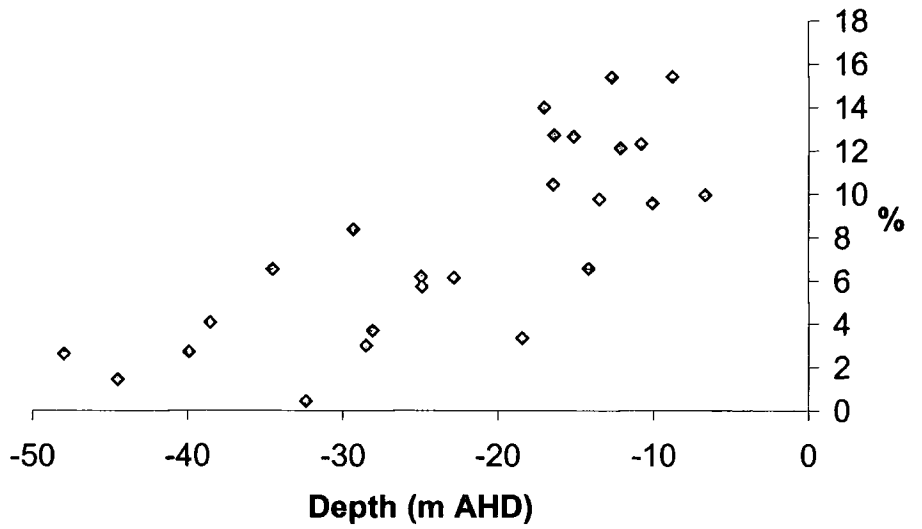

Fig. 3.28 *D. complanata* distribution with respect to depth for Bowling Green Bay

However, this species is absent from other subtidal benthic studies in the region (M^{c}Intyre, 1996) in addition to intertidal studies (Woodroffe 2002; Horton *et al.*, 2003) and in the wider Australian context (Yokoyama *et al.*, 2000). The species of the genus *Discorbinella* are epifaunal preferring firm coarse sand substrates in a normal marine salinity environment in areas with warm inner shelves extending from 0-50m (Murray 1991). However the tests used in this study were unbroken with no signs of abrasion or etching, thereby reducing the possibility of post depositional movement. *Q. pseudoreticulata* and *Q. venusta* exhibit a negative correlation with depth. Gould and Stewart (1955) show that *Quinqueloculina* species are epifaunal and inhabit plants or sediments in marine - hypersaline (32-65$^{o}/_{oo}$) lagoons and mid shelf environments (0-30m). M^{c}Intyre (1996) illustrates that these species account for up to 20% of the assemblage for five out of six environments, and because species are confined to Cleveland Bay with a maximum depth of 15m, this may support the inference that this species prefers shallow water environments.

D. striata demonstrates a unimodal relationship to depth (Fig. 3.29) with an increase in abundance to a peak at approx. -25m AHD tailing off to a low percentage distribution at -48.0m AHD.

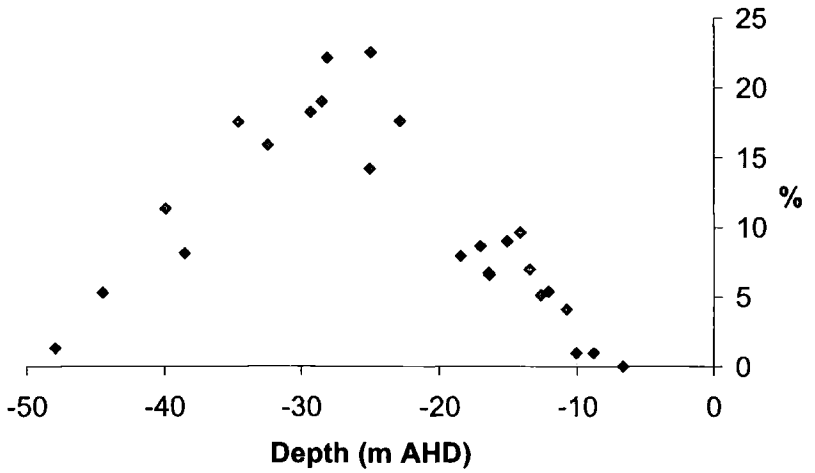

Fig. 3.29 *D. striata* distribution with respect to depth for Bowling Green Bay

This species is not identified in the study of M^{c}Intyre (1996) for Cleveland Bay, though they are found in small numbers within Bowling Green Bay in this study. This may be indicative of the patchy distribution of this species, as with all foraminifera.

Bowling Green Bay exhibits 2 clusters of foraminiferal distribution (Fig. 3.9) and is supported by DCA analysis (Fig. 3.7). These zones demonstrate elevational niches (Fig. 3.8a), as a result of species-specific relationships with depth (Fig. 3.8b). However, further analysis was necessary to bring together environmental variables and species distributions to further understand controlling influences, testing the hypothesis that foraminiferal distributions are related to subtidal depth. The correlations presented in association with multivariate analysis show that depth and sand fraction appear to be the dominant environmental factors in this embayment; the deeper the elevation, the greater sand fraction. Boltovskoy and Wright (1976) note that the ecological effects of depth are difficult to assess because of variance in other ecological factors with depth. Nevertheless, various morphological and distributional attributes of the foraminifera indicate there is a depth effect. These include temperature, light intensity, pressure, oxygen and calcium carbonate concentration. This development suggests that studies by M^{c}Intyre (1996) and Yokoyama *et al.* (2000) can be built upon to further to test the

hypothesis that foraminiferal distributions are controlled by subtidal depth, and that a quantitative technique to show this relationship can be developed.

3.6.2 Foraminifera sub-tidal distribution from Cleveland Bay

Seven species dominate in absolute numbers along Transect 1, including *D. complanata*, *C. sydneyensis* and *C. oceanicus*. The environmental correlations show that organic content and sand fraction appear to be the dominant environmental factors in this embayment, noting that the correlation between organics and sand is a negative one. Dominant species in Transect 2 include some from Transect 1 with the addition of *P. vernusta* and *Q. pseudoreticulata.* Sand again dominates this environment, though correlations between sand and organic content are not as strong as in Transect 1, with depth being more influential here than in Transect 1.

Murray and Wright (1974) note that the genus *Pararotalia*, one of the dominant taxa along Transect 1 and 2, is epifaunal and prefers coarse grained, warm marine, inner shelf habitats. This study shows that this species prefers shallow, sandier than average environments, supporting Murray and Wright's (1974) conclusion. The genus is noted in studies from the local area, such as M^{c}Intyre (1996), who depicts common (10-20% relative abundance) to abundant (>20% relative abundance) levels in tidal flat and beach environments respectively for Cleveland Bay. M^{c}Intyre (1996) illustrates that in the eastern inner shelf (the same spatial location as Transect 2 in this study) sediment is coarse carbonate sand, derived from reefs adjacent to Cape Cleveland. This is considerably different to the inner shelf environment (Transect 1), defined also as a muddy sand (M^{c}Intyre, 1996). However the sediment composition here is controlled less by frequent currents and waves, more by episodic high energy events (Orpin, 1999; Orpin and Woolfe, 1999). Other environmental characteristics appear to be exerting a more controlling influence in an embayment where the distribution of foraminifera appears to have a poor relationship with depth. *P. vernusta* shows a preference for this eastern inner shelf environment (Transect 2), and is not found in the inner shelf sites (Transect 1) in significant numbers. Further, intertidal studies

(Sandfly and Saunders Creek, Cleveland Bay - Woodroffe, 2002; Cocoa Creek, Cleveland Bay - Horton *et al.*, 2003) observe that the species is common (≤20%). Other species, such as *A. lessonii* and *Q. pseudoreticulata*, common to both Bowling Green and Cleveland Bay, are largely confined to this eastern inner shelf (Transect 2) in Cleveland Bay, potentially indicating a preference for more exposed environments as found in the inner and outer shelf sections of Bowling Green Bay.

Transects 1 and 2 both exhibit 2 clusters of foraminiferal distribution that are supported by DCA analysis. Multivariate analysis (CCA) shows a large scatter of species with respect to all environmental variables for Transect 1, identifying no individually dominant variable controlling foraminiferal distribution. The same analysis on Transect 2 shows a stronger environmental gradient, with *A. lessonii* preferring sandier environments to *P. vernusta*. This data for both transects demonstrate that foraminiferal relationships to subtidal depth are largely arbitrary within the confines of Cleveland Bay.

3.7 Conclusions

I have collected 43 samples from Bowling Green and Cleveland Bay containing 31 species. Bowling Green Bay samples are dominated by *T. oblonga, C. sydneyensis, Q. venusta, D. complanata, D. striata* and *A. lessonii*. Cleveland Bay is dominated by *C. sydneyensis, C. oceanicus, D. complanata* and *Q. venusta* with the addition of *P. vernusta*, which is not dominant in Bowling Green Bay.

Multivariate analysis for Bowling Green Bay shows a strong environmental gradient dominated by depth and sand fraction. Several species, such as *A. lessonii, D. striata* and *D. complanata* demonstrate individual relationships to depth, with the two clusters being demonstrated to have elevational constraints. Analysis of Cleveland Bay samples shows that depth is a poor constraint on foraminiferal distributions. Clusters show elevational overlap along both transects.

Analysis of environmental variables shows sand to be dominant throughout all substrates tested for Bowling Green and Cleveland Bay. Depth and sand

fraction display a strong correlation within Bowling Green Bay, but not in Cleveland Bay. Silt, clay and organic fractions shown limited influence within all samples studied, exclusive of intercorrelations.

Subtidal distributions of selected species and total assemblages in Bowling Green Bay can therefore be suggested to be relatable to depth. This answers the hypothesis that foraminiferal assemblages can be linked to subtidal depth in selected locations, hence highlighting the potential use of subtidal benthic foraminiferal distributions as a tool for reconstructing palaeoenvironments. However there are many environmental variables not measured within this study, such as salinity, temperature, light intensity and chemical composition. This provides a limitation to the scope of the study and would benefit from further environmental variables being analysed.

Chapter 4

The Development and Application of a Subtidal Transfer Function, Great Barrier Reef, Australia

4.1 Introduction

The Great Barrier Reef (GBR) lagoon and shelf encompass a range of contemporary marine biological indicators closely related to relative sea-level (RSL), including coral reefs and mangroves. Concerns over future sea-level changes are of great importance to coastal managers and scientists concerned with climate change (Horton *et al.,* 2003). However, the wealth of scientific knowledge indicates that RSL responses are characteristically complex and spatially heterogeneous (Peltier *et al.,* 2002). Therefore it is essential to critically re-assess the concepts of global SL change in both regional and local contexts, integrating expert scientific knowledge with future climate-based predictions of change.

One of a number of approaches used to reconstruct past RSL changes has been microfossil assemblages, such as foraminifera, which are found widely in post-glacial coastal deposits. Over the past 50 years, microfossil-based sea-level indicators have been widely used to generate RSL reconstructions for the U.K., Europe and elsewhere (e.g. Godwin, 1940; Gehrels, 1994; Edwards, 2001; Shennan and Horton, 2002). However, these techniques have been semi-quantitative in their nature (Shennan *et al.,* 1983) assessing the use of transgressive and regressive stratigraphic contacts. Scholars have attempted, using the transfer function technique, to change these earlier techniques into a

quantitative tool for RSL reconstruction, though is restricted to tidal elevations between mean sea level (MSL) and highest astronomical tide (HAT).

Transfer functions provide comparatively precise reconstruction tools of former sea levels using a statistically based relationship between contemporary foraminiferal assemblages, their measured association to sea level and their fossil counterparts (Horton *et al.,* 1999a; Edwards and Horton, 2000; Gehrels, 2000; Gehrels *et al.,* 2001; Horton *et al.,* 2000). A growing number of microfossil-based studies in coastal environments throughout Australia (Wang and Chappell, 2001; Cann *et al.,* 2000) and specifically the GBR lagoon (Woodroffe, 2002; Horton *et al.,* 2003) increase our understanding of contemporary distributions and their applicability to RSL reconstructions. However, the focus in these studies is on intertidal distributions, with only a limited number of semi-quantitative studies (e.g. McIntyre, 1996; Yokoyama *et al.,* 2001) on sub-tidal distributions. The sub-tidal environment is crucial, given the small percentage of the marginal marine environment incorporated in intertidal areas, as reflected by Larcombe *et al.* (1995) who have >60% of their sea-level index points as subtidal in origin. The limited insight an intertidal study can provide highlights how sub-tidal microfossil-based studies can be vital in advancing our understanding of a coastal environment.

Therefore the aims of this chapter are:

- To develop the first foraminifera-based transfer function based on sub-tidal foraminiferal distributions
- To test the applicability of the transfer function to produce a new generation of accurate and precise RSL reconstructions from subtidal sediment.
- To compare these findings with the wider literature for the GBR, Australia and far-field sites.

4.2 Study Area

The same study area is used as in Chapter 3 (Fig. 3.1 and 3.2). Thirteen vibracores were taken for analysis and are located within Cleveland Bay, extending

through the inner shelf, mid shelf and to the outer shelf (Fig. 4.1). For further site information see section 3.2.

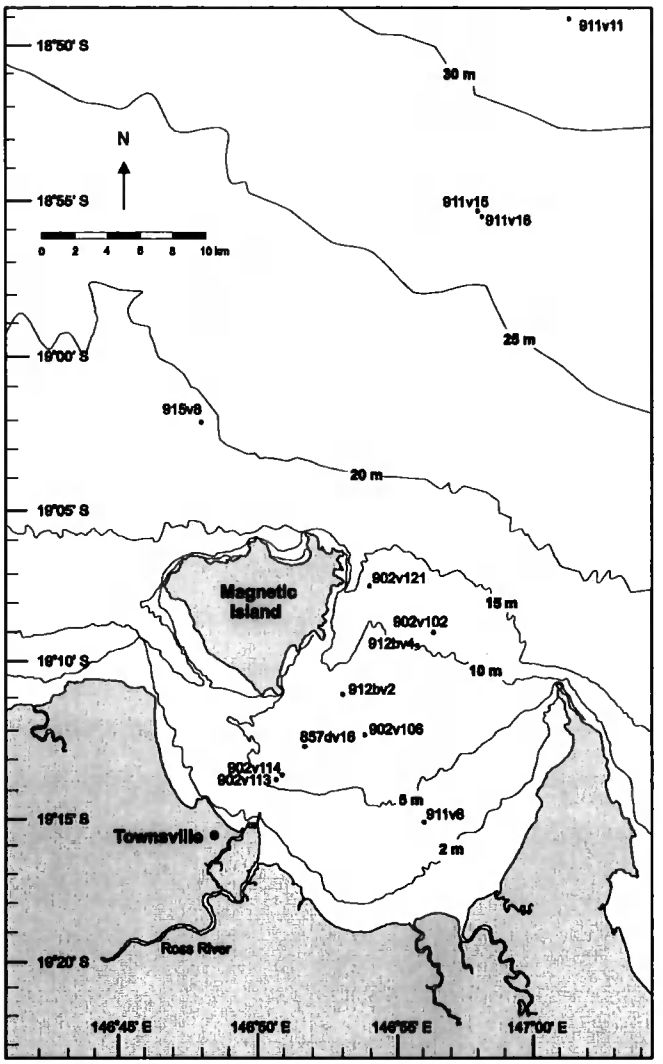

Fig. 4.1 Core locations for fossil samples in Cleveland Bay and the mid shelf

4.3 Methodology

In order to reconstruct former sea-levels it is necessary to collect reliable field data from a known geographical region that can be dated (e.g. radiocarbon), assigned an elevation accurate to an ordnance datum and subsequent reference tidal levels to produce a sea level index point. Each sample is validated biostratigraphically, as part of a core, as a RSL index point with an indicative

meaning or reference water level (RWL). The RWL (Fig. 4.2) refers to the altitude relative to the fossil tidal regime represented by the dated sample and is assigned an error term, the indicative range (van de Plassche, 1986; Horton *et al.*, 2000).

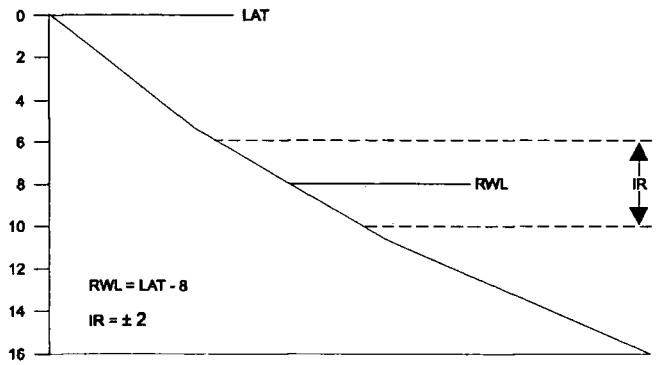

Fig. 4.2 Schematic diagram of the indicative meaning illustrating the Indicative Range (IR) and Reference Water Level (RWL). LAT = Lowest Astronomical Tide.

4.3.1 Sampling Strategy

Australia is relatively seismically stable and is situated at the centre of the Australian-Indian plate. Holocene sea-level records from the Australian continent are dominated by eustatic processes and modified by hydro-isostasy. By studying sea-level changes in Australia we further our understanding of a range of mechanisms impacting on RSL. The samples from vibracores (Fig. 4.1) were chosen under prior knowledge of the RSL history for the region (Carter *et al.*, 1993; Larcombe *et al.*, 1995), noting that the sea-level transgression across the shelf may leave deposits offshore. In conjunction, a suite of dated vibracores was available through work by Larcombe *et al.* (1995). This allowed predetermined Holocene time periods of specific interest to be sampled, establishing the timing and magnitude of the MHHS in an attempt to understand more about the timing of meltwater cessation and sourcing.

4.3.2 Laboratory Preparation and Dating Techniques

Foraminiferal preparation followed standard methods of Scott and Medioli (1980) as shown in Appendix 1. Loss-on-ignition and particle size data were taken following methods outlined in Appendix 3 and 4 respectively. Elevations are

calculated from a depth sounding to the subtidal surface, with additions being made for the keel draft to correct the reading relative to sea level. The adjusted depth reading is converted into a depth relative to AHD by placing the sampling vessel into a tidal context, through use of the date and time of sample collection and tide gauge records. A conservative depth error is incorporated into the RSL reconstruction to take into account additional factors, such as waves. Radiocarbon ages (bulk and AMS) are converted to calibrated years B.P. (Table 4.2), from radiocarbon dates shown in Larcombe *et al.,* (1995) using CALIB 4.3 (Stuiver and Reimer, 1993), the most up-to-date package available. The dates are calculated using the probability distribution method (B), reported as calendar years before present (1950 AD) with an age range that contains 95.4% of the area under the probability distribution curve (± 2σ). During this process, samples were corrected for the marine reservoir effect (450 yrs - Australia) which had previously been uncorrected.

4.3.3 Transfer Function Development

I have combined the three foraminiferal training sets presented in Chapter 3 to generate a regional dataset. This will introduce noise into the dataset as a result of factors outlined in Section 3.6. However, it is deemed beneficial to combine datasets because it will increase the range of contemporary coastal environments available to the transfer function (Horton, 1997; Horton and Edwards, *in press*). Horton and Edwards (*in press*) note that transfer functions developed from regional training sets are better suited to the analysis of fossil material than those derived from local data since they incorporate a greater range and variety of modern analogues. Local training sets, whilst giving a slight increase in precision, suffer from severely restricted predictive power due to the abundance of 'no modern analogue' situations. Horton and Edwards (*in press*) conclude that interpretations based on transfer functions derived from local training sets should be treated with caution. Individual transfer functions have been generated for Bowling Green and Cleveland Bay (Appendix 9 and 10 respectively) and they show no significant improvement on the regional. The combined dataset consists of three differing environments, dominated by sand fraction with differing elevational settings (see

sections 3.5.1.2 and 3.5.2.2). To minimise the taxonomic, methodological and taphonomic differences, the modern training set is of consistent taxonomy and quality.

Transfer functions provide relatively precise reconstruction tools of former sea levels using a statistically based relationship between contemporary foraminiferal assemblages, their measured association to sea level and their fossil counterparts. To estimate former sea-levels, we have to model the responses of the same taxa in relation to the environmental variable of interest. This requires a contemporary training set derived from taxa preserved in surface sediments. Therefore the contemporary relationship between foraminiferal assemblages and sea levels is modelled statistically and the resulting function is then to transform the fossil assemblages into quantitative estimates of former sea levels (Birks, 1995). However, in order to achieve this reconstruction, it is first necessary to consider the underlying species - environment response (Birks, 1995), either linear or unimodal based (Fig. 4.3).

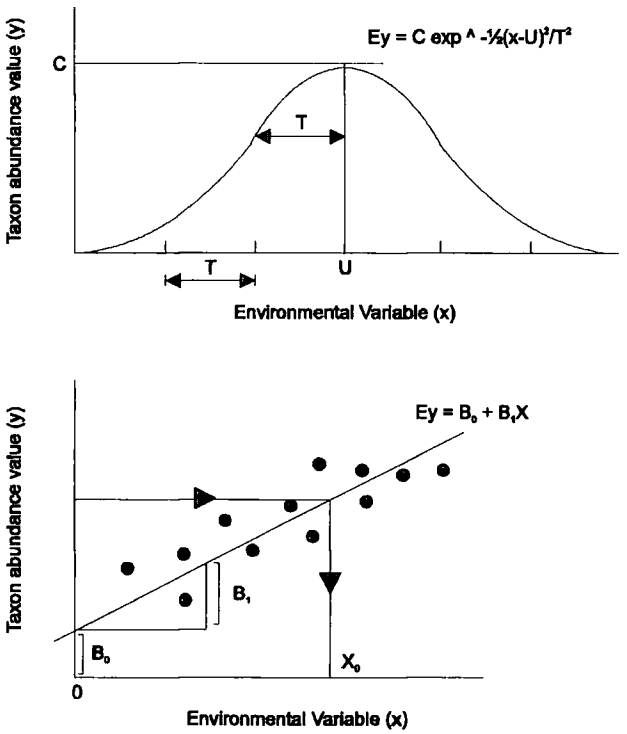

Fig. 4.3 Taxon response models (after ter Braak, 1988; Birks, 1995)

Detrended Canonical Correspondence Analysis (DCCA) is used to decipher the length of the environmental gradient and thus which model of response is to be considered as most appropriate. If the length of the environmental gradient is less than 2 standard deviation (SD) units, then the taxa are deemed to be behaving monotonically along the gradient and linear-based regression and calibration methods are appropriate. If the environmental gradient exceeds 2 SD units in length, the taxa are considered to be showing their optima within the measured gradient, and thus unimodal-based (Gaussian) methods are applicable (Birks, 1995). The DCCA technique was applied to the training set and a value of 2.329 SD units was generated. It is appropriate, therefore, to use unimodal-based (Gaussian) methods of analysis and the Weighted-Averaging Partial Least Squares (WA-PLS) transfer function technique.

In reality, species-environment relationships are unimodal as each taxon grows and reproduces best at a particular optimum value of an environmental variable, and cannot survive where the value of the environmental variable is either too high or too low (ter Braak, 1987). Strictly speaking, ecological response curves are not quite so straight forward as portrayed by the Gaussian-type unimodal models (Birks, 1995). However, just as linear models are deemed appropriate for modelling only approximately linear responses, unimodal models are useful in developing statistical techniques for data showing mostly unimodal responses (ter Brak and Prentice, 1988).

WA-PLS is a regression technique, developed by ter Braak and Juggins (1993), and is an inverse procedure (ter Braak 1995). In the past, inverse and classical methods of Weighted Averaging (WA) have been applied extensively as a means to develop transfer functions (Gehrels, 1994; Horton 1999). However this technique (WA) assumes that only one environmental variable is important and thus neglects the influences of other environmental variables. As a result, WA-PLS out performs WA with the ability to dramatically reduce the root mean squared error of prediction (RMSEP) (Birks, 1995) and is used widely (Edwards and Horton, 2000; Horton *et al.,* 2003). Birks (1995) also notes that WA-PLS outperforms WA when concerned with edge effects, where in certain instances the optima of taxa

are overestimated at the lower end of the scale, and underestimated at the high end (Hill and Gauch, 1980).

It is essential to appraise the validity of the result by considering the associated reconstruction errors. A cross-validation technique was used with simple jack-knifing or 'leave-one-out' methodology (ter Braak and Juggins, 1993) to assign a value to the environmental variable of interest when the matching analogue has been omitted, hence 'leave-one-out'. The prediction errors are then accumulated to form the Root Mean Squared Error of Prediction (RMSEP) (Birks, 1995). This provides a more accurate error in assessing the performance of the transfer function. Bootstrapped-estimated sample-specific errors were also calculated for fossil samples as an alternative to the general application of the RMSEP, latterly calculated for the entire dataset. The performance of each transfer function was assessed in terms of the RMSEP, the maximum bias and the squared correlation (r^2), a measure of the strength of the relationship between observed versus predicted values. The statistics were calculated as 'apparent' measures in which the whole training set was used to generate the transfer function and assess the predictive ability. The data were also jack-knifed to assess the predictive performance of the transfer function, with one outlying sample being removed from the training set, significantly improving the model.

4.4 Results

The training set contains 43 samples with 31 species from three study sites, Bowling Green Bay and Cleveland Bay (Transects 1 and 2).

Component	Apparent RMSE (m)	Prediction RMSEP (m)	Apparent r^2	Prediction r^2	Apparent maximum bias (m)	Prediction maximum bias (m)
1	3.62	4.21	0.90	0.86	5.13	6.41
2	2.54	3.45	0.95	0.91	4.39	6.42
3	*2.02*	*3.33*	*0.97*	*0.91*	*3.94*	*7.38*
4	1.70	3.31	0.98	0.91	2.91	7.43
5	1.37	3.71	0.99	0.89	2.83	9.67

Table 4.1 Table of apparent and prediction (Jack-knifed) errors of estimation associated with the foraminiferal based sub-tidal transfer function.

The transfer function produces results for 5 components (Table 4.1). The selection of the component to be used for a reconstruction relies on the process of parsimony (Horton *et al.,* 2003), the lowest component that gives an acceptable model. I have chosen component 3 because of its significant improvement in performance when considering the jack-knifed errors of prediction for components 1 and 2; prediction errors are lower and squared correlations are higher. Therefore using component 3, the transfer function is strong where r^2_{jack}=0.91 and the RMSEP=3.33 m, showing a cluster of points in the shallower depths (<10m AHD), a sparse zone (10-25m AHD) before an increase towards the deepest elevations (Fig. 4.4). The residuals show a consistent band of deviation for all depths (±3m) with the exception of one point, approximately 7m offset.

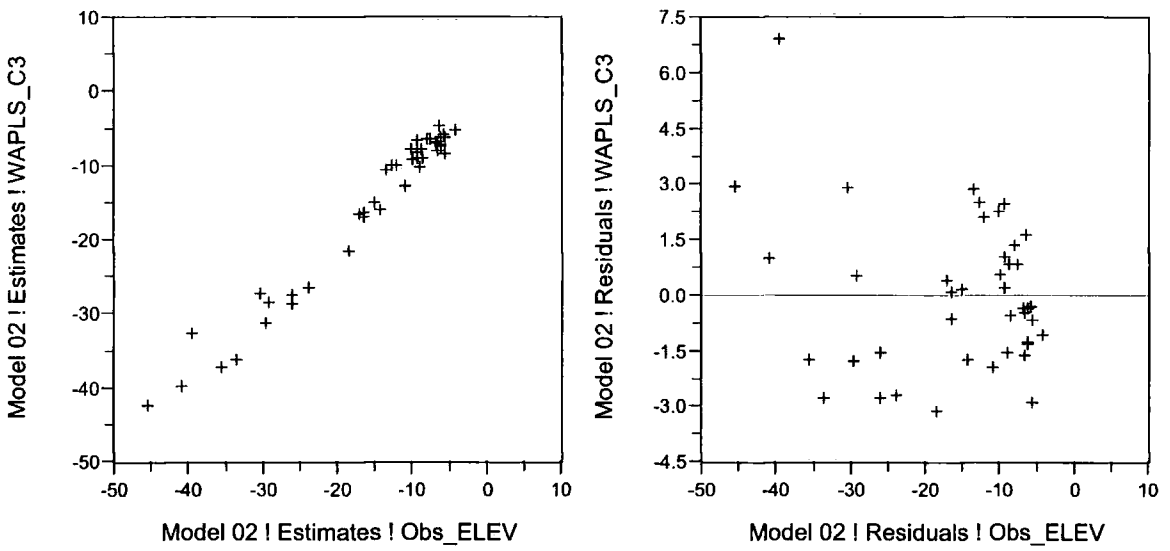

Fig. 4.4 Scatter plot illustrating the relationship between observed and predicted depth for the foraminiferal transfer function (WA-PLS - Component 3) and associated residuals.

Foraminiferal based transfer functions also produce a weighted average optimum and tolerance for each species (Fig. 4.5).

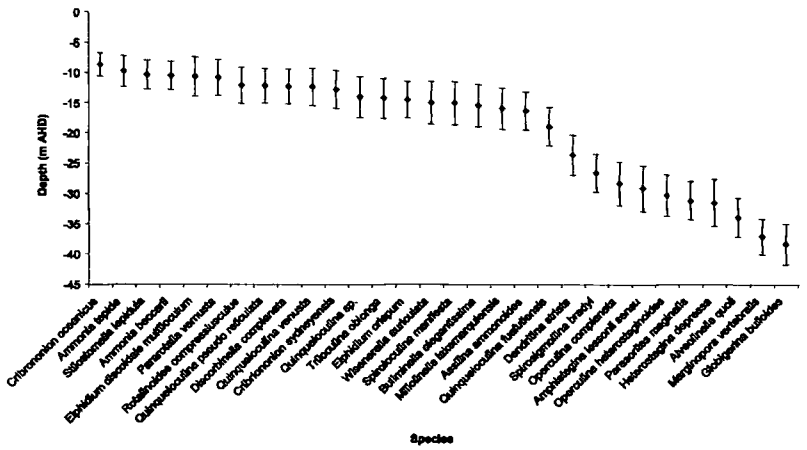

Fig. 4.5 Species optima (centre point) and tolerance shown as error bars for the entire training set

Weighted averages show ≤20 species having similar optima and tolerances to subtidal depth, ranging between -11 and -16m AHD, and include the dominant species *Pararotalia vernusta*, *Quinqueloculina pseudoreticulata*, *Discorbinella complanata*, *Quinqueloculina venusta*, *Cribrononion sydneyensis* and *Triloculina oblonga*. Species towards the shallower optimum depths display narrower tolerances, such as *Cribrononion oceanicus* and *Ammonia tepida* (Fig. 4.5), perhaps indicative of upward limit of marine influence. However, towards the deeper optima elevations, dominant species such as *Dendritina striata*, *Operculina complanata* and *Amphistegina lessonii* all display larger tolerances to subtidal depth. In general all species display a tolerance for subtidal depth, though importantly they show individual niches within the elevational range, albeit with limited overlap for the key species that have been identified, potentially highlighting that a transfer function used to reconstruct subtidal depth is likely to be effective.

4.5 Application of the Subtidal Foraminiferal-based Transfer Function

I have shown that the transfer function developed has a strong potential for reconstructing former sea levels through generation of a reference tidal level for each fossil sample. However, this reference tidal level needs to be placed within the spectrum of the current tidal regime (Fig. 3.5). Thus RSL is calculated from the following equation:

$$RSL_{(i)} = E_{(i)} - RWL_{(i)}$$

where $RSL_{(i)}$ is the RSL for sample *i*, $E_{(i)}$ is the depth (m AHD) for sample *i* and $RWL_{(i)}$ is the reference water level (m AHD) for sample *i*.

The consideration of errors within the reconstruction is also vital. Altitudinal errors of each index point shown were calculated using the following formula, following established methods (IGCP, 1986):

$$x_i = \sqrt{(a^2_i + b^2_i + c^2_i + d^2_i + e^2_i)}$$

where x_i is the total altitudinal error (m) of the sea-level indicator; a_i is the elevational error estimate (Zagorskis, *pers. comm.* 2003); b_i is the depth sounder discrepancy; c_i is the tidal change; d_i is the error of sample location within the core; e_i is the indicative range of the sea-level indicator generated by the transfer function, expressed as a bootstrap estimated of sample specific error. Two vessels were used to collect contemporary samples, and fossil samples were collected by Larcombe *et al.*, (1995). All altitudinal errors (d) for communal core samples were duplicated form Larcombe *et al.*, (1995), and range from 0.3-0.5m (Table 4.2).

Sample	Laboratory Code	Age (^{14}C yrs)	± Error (yrs)	Sample Depth (m AHD)	RWL (M AHD)	± Error (m)	RSL (m AHD)	± Error (m)	Age (cal. yr BP)	± Error (yr)
857dv16 (72)	GAK - 7224	6310	170	-11.18	-13.56	1.32	2.38	1.36	7194	351
902v102 (55)	2453	2270	144	-14.93	-11.85	0.90	-3.08	0.95	2376	344
902v106 (265)	3550	8110	210	-12.45	-5.34	2.24	-7.11	2.30	9075	545
902v113 (142)	3553	7840	170	-9.42	-0.69	2.42	-8.73	2.47	8665	330
902v114 (169)	3552	7660	200	-10.09	2.61	6.62	-12.70	6.64	8541	400
902v121 (85)	2449	2860	213	-16.23	-13.76	2.99	-2.47	3.01	3110	506
911v11 (62)	2210	8380	125	-37.60	-30.23	3.02	-7.37	3.06	9316	339
911v15 (46)	2211	2100	164	-27.90	-23.67	2.85	-4.23	2.89	2191	421
911v16 (48)	2215	4200	78	-28.80	-28.06	1.98	-0.74	2.05	4787	211
911v8 (213)	2443	6153	95	-6.41	-8.60	1.94	2.19	1.97	7043	213
912bv2 (153)	2455	6740	250	-11.93	-8.67	2.08	-3.26	2.10	7638	475
912bv4 (172)	2444	7741	97	-13.40	-11.14	1.36	-2.26	1.40	8635	235
915v8 (35)	2313	2670	193	-19.92	-13.00	0.84	-6.92	0.89	2838	469

Table 4.2 Thirteen reinterpreted and new sea level index points (SLIPs) for the central GBR lagoon. The laboratory code refers to those stated in Larcombe *et al.* (1995) and Larcombe and Carter (1998).

Analysis of the key elements of Table 4.2 shows that the bootstrapping errors are large when compared to indicative ranges of other inter-tidal studies in the same region (Horton *et al.*, 2003), ranging between ±0.84 to ±6.62m. However the application of this technique sub-tidally has not been carried out till now and so such errors must stand. The dating errors are large, ranging from ± 185 to ± 949 yrs. Foraminiferal characteristics of the fossil samples (Fig. 4.6) show a similar group of dominant species as for the contemporary environment, with the addition of *A. beccarii*, *Bolivina brizalina*, *Spirosigmoilina bradyi* and *Wiesnerella auriculata* as important species.

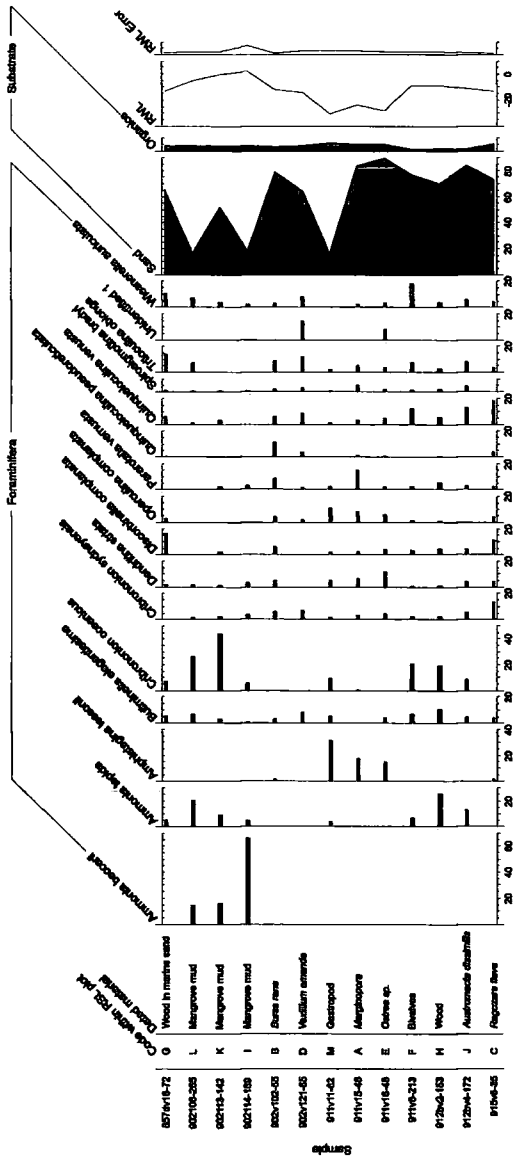

Fig. 4.6 Foraminiferal, sand and organic characteristics of 13 fossil samples in Table 4.2

Significant biological points to note are the dominance of *A. beccarii* in sample 902v114 (169), *A. lessonii* in sample 911v11 (62) and *C. oceanicus* in sample 902v113 (142). The sand fraction continues its dominance throughout, with the notable exceptions of samples 902v106 (265), 902v114 (169) and 911v11 (62) not attaining the minimum level of 40% found in contemporary samples. The organic content of the samples again is consistent throughout, not exceeding 6.3%.

4.6 Analysis of the Subtidal Foraminiferal-based Transfer Function

Analysis of the foraminifera and substrate characteristics in fossil samples show subtle and more obvious differences to the contemporary samples. A new dominant species is present in three samples (902v106 (265), 902v113 (142) and 902v114 (169), namely *A. beccarii*, showing values in excess of 20% up to 70%. These samples containing *A. beccarii* are sampled from a mangrove, indicative of an intertidal environment, and in two cases have a low sand fraction. Woodroffe (2002) notes that the contemporary mangrove creeks of Cleveland Bay, specifically Sandfly Creek, contain an abundance (0-40%) of *A. beccarii* with the substrates in some cases dominated by silts and clays. This supports the concept that these fossil samples may have shallow subtidal or intertidal origin. However, the range of contemporary environments studied here does not extend into the intertidal zone and hence a lack of modern analogue to this fossil assemblage. Furthermore, the RWL generated reflects the intertidal and shallow subtidal nature of *A. beccarii*, placing them at shallow depths. Thus this issue is of limited concern. Another potential problem is taphonomy being post-depositional changes are the result of diagenetic processes. These include selective preservation of foraminifera, transportation of tests away from (loss) and into the assemblage (mixing), bioturbation, infaunal foraminifera and predation on foraminifera.

The vast majority of species, however, have contemporary analogues for the fossil assemblages. In addition, species such as *C. oceanicus* show far greater abundances in fossil assemblages (>40%) when compared to contemporary distributions. *A. lessonii* demonstrates dominance in three selected samples each with a low elevation RWL. Sample 911v11 (62) shows both a high *A. lessonii*

abundance and a low sand content, a situation that is not found in the contemporary training set. With these noted exceptions, the fossil data show comparable foraminiferal abundances and substrate characteristics to the contemporary training set.

The transfer function generated for contemporary data builds upon the hypothesis in Chapter 3, illustrating that foraminiferal assemblages can be related to subtidal depth. The transfer function displays a strong relationship between observed and predicted depths (r^2=0.97) with a RMSEP (3.3m). Intertidal transfer functions for the region display much smaller errors (RMSE) than presented here, with Horton *et al.* (2003) demonstrating an error range of ±0.07m in Cocoa Creek. Foraminiferal assemblages within this intertidal zone show rapid changes over a tightly constrained elevation range. Hence, the tightly constrained elevational range coupled with regularly spaced sampling stations will produce smaller errors within an intertidal environment. Within this study, the sampling regime displays a concentration of samples around the shallower depths, though beyond the -10m AHD depth samples show a greater elevational spread. Therefore relatively large elevation ranges between samples, when compared to intertidal studies, can only result in larger errors.

4.7 Reinterpretation of existing GBR sea-level data using the subtidal foraminiferal based transfer function

One of the aims of this study is to take subtidal foraminiferal data and use the transfer function technique to help to create a more accurate picture of the RSL for the central GBR. Furthermore, this can be achieved by reinterpreting samples used in this locality (Larcombe *et al.,* 1995), with 9 of the 13 index points having previously been analysed (Larcombe *et al.,* 1995) and assigned a RSL. This reinterpretation process has generated a substantial movement in the reconstructed RSL for the dated samples (Fig. 4.7).

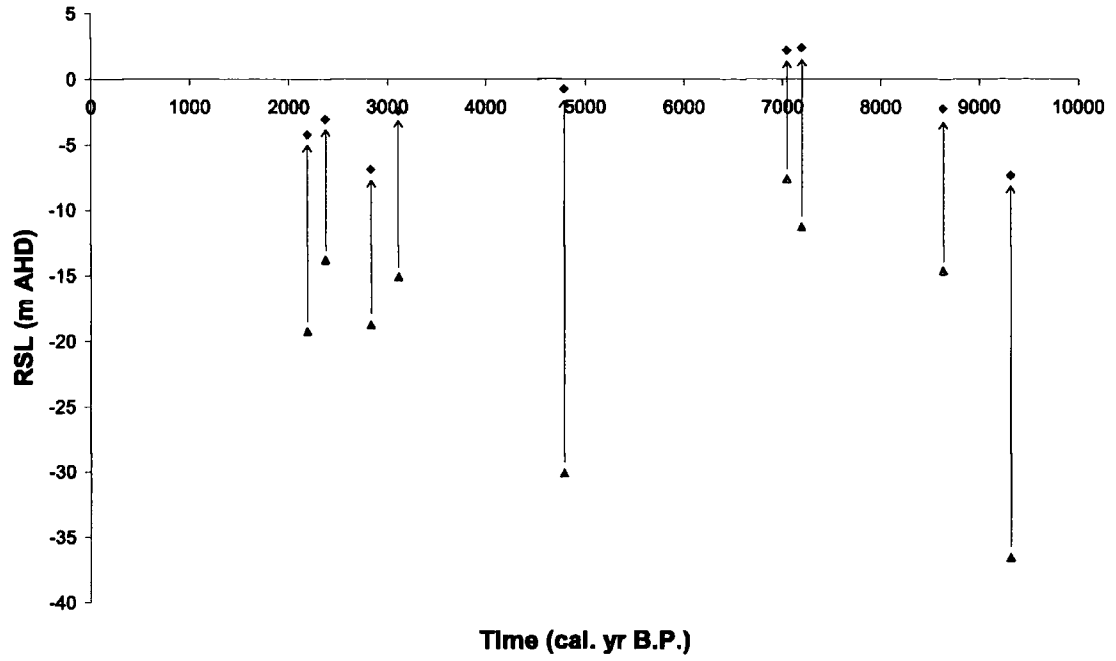

Fig. 4.7 Comparison of the SLIPs generated in this study (diamonds) as reinterpretations of those in Larcombe *et al.* (1995) (triangles).

All reinterpreted samples have been raised in elevation, ranging from a 9.81m to a 29.35m increase. This technique shows an increase in the precision of subtidal sea-level indicators when compared with Larcombe *et al.* (1995), because all the subtidal indicators presented are not corrected for their indicative meaning. In this study, a sample is assigned a RWL, using the new transfer function, and corrected for its depth as shown in the sea-level equation (Section 4.5). This may allow both intertidal and subtidal indicators to constrain the sea-level envelope and hence derive a more accurate sea-level curve. The precision of the technique when compared to Yokoyama *et al.* (2000) is also favourable, because formation height definitions of brackish (2m), marginal marine (-4m), shallow marine (-10m) and open marine (-20m) are vague. The transfer function technique presented here has the potential to generate more tightly constrained reconstruction errors (<1m) than those defined in Lambeck *et al.* (2002) for the data presented in Yokoyama *et al.* (2000). This is the first subtidal transfer function to be applied to quantitative RSL reconstructions and thus shows potential, both as a tool for reinterpretation of the existing regional dataset (Larcombe *et al.*, 1995) and also for application to sediments where matching intertidal analogues are scarce.

4.8 New Sea Level Index Points from the central GBR Lagoon

Strictly speaking, SLIPs from differing spatial locations should not be plotted on the same sea-level graph without consideration of the spatial effects of tectonics, isostatic movements and local factors (*pers. comm.,* Milne 2003). However, in this scenario, it is appropriate to plot all 13 SLIPs on the same sea level graph, as the noted spatial effects are negligible (*pers. comm.,* Milne 2003) (Fig. 4.8).

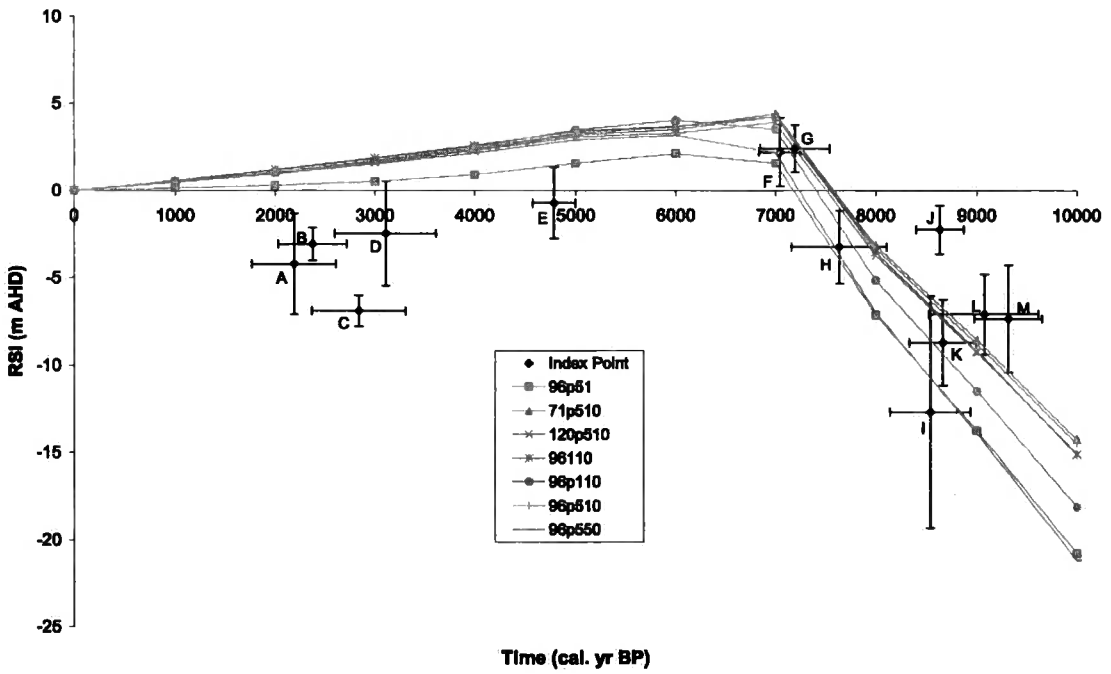

Fig. 4.8 13 SLIPs reconstructed for the Central GBR lagoon and 7 modelled SL responses for the same location (*pers. comm.,* Milne 2003).

The plot shows a limited scatter between the data points and the modelled predictions (Fig. 4.8). Evidence from Yokoyama *et al.* (2001) shows a similar trend of sea-level prediction for the GBR (23°30'S 152°15'E) as shown by Milne (*pers. comm.*, 2003). This, coupled with evidence presented in Chapter 2 of sea-level records, suggests that the predicted trends shown by both modellers are relatively accurate. The models themselves are seven differing approaches, reflecting differing sea-level scenarios, all based on the ICE-3G model (Tushingham and Peltier, 1991) but revised to produce a good fit to the Barbados record (Fairbanks, 1989). The earth models used are all spherically symmetric (no lateral changes in

properties) but include realistic density and elastic structure with depth (from seismic constraints). In summary, therefore, it seems reasonable to make the assumption that the modelled predictions are accurate in character, when compared with observed data from the region, and thus validate the SLIPS generated in this study.

4.8.1 The Transgression

Analysing the data in general shows that there are 3 areas of interest (Fig. 4.8). The first depicts a transgression in general agreement with the modelled predictions, illustrating an early Holocene rapid sea-level rise of potentially 17m up to a MHHS of approximately +2m, between 9,000 and 7,000 yrs BP (within the constraints of error). Further interest surrounds the nature of each index point, as information is known about the foraminiferal and environmental information, though the material radiocarbon dated may also help us to understand each individual scenario (Fig. 4.6). The transgression SLIPs contain dated material including bulk mangrove muds, wood and carbonate shells. Analysing these index points from an ecological perspective shows that there is strength in the technique as some samples have been independently assigned a RSL comparable to modelled predictions. However, samples L, M and particularly J produce slightly higher results than the modelled scenarios. This may be due to contamination of older carbon or errors associated with the reconstructed RWL or measurement depth. Point I displays the largest elevational range of all SLIPs and with further analysis of foraminiferal assemblages, a potential explanation can be identified. The abundance of *A. beccarii* in this assemblage is the largest in this study (~70%). Given the lack of modern analogue, an error of ±6.6m for the RWL signifies a limited number of species (~30%) for the transfer function to base a reconstruction on and hence a large sample-specific error range. Furthermore, this sample shows a RWL of +2.6m AHD, spurious as samples were not collected above -4.2m AHD, thus supporting the spurious nature of this SLIP.

Comparison to the transgression SLIPs to the wider literature shows that Larcombe *et al.* (1995) note a rapid regression within the rapid transgression at ca.

8-8.6k ^{14}C years BP (Fig. 2.16). My SLIPs, after calibration, plot in the area of interest with respect to the rapid oscillations though they do not seem to identify a clear trend as a result of the lack of SLIPs studied in this specific time-interval. Hence, resolution of the 'blip' question surrounding a sharp switch in RSL movements around 8-8.6k ^{14}C kyr BP raised by Larcombe *et al.* (1995) is unlikely, as the vertical resolution of this technique for elevational errors is insufficiently precise coupled with a lack of SLIPs studied for this time-period.

Rapid transgression and RSL rise may have preserved *in situ* fossil assemblages. Dunbar and Dickens (2003) note that during the RSL rise model of the GBR shelf, conditions of moderate river flux behind incipient reefs, and the sedimentation patterns during transgression phases, have aggraded behind these reefs (as Karst hills) at a sea-level lowstand. Thus the rapid transgression and RSL rise could swiftly place fossil sub-tidal sediments in depths where wave interactions, storm surges and tidal influences would have limited influence. As a result, sediments may be preserved in an accurate assemblage of foraminifera to match the depth characteristics of the palaeo-conditions at that time. The geographical location of the core sites is also interesting as seven of the eight sites are located within present day Cleveland Bay. Dominant wave patterns and currents move from the southeast to the northwest along the lagoon (McIntyre, 1996; Orpin, 1999) and therefore protection from storms, swell waves and tidal influences from that prevailing direction may have been given in the past by Cape Cleveland (Fig. 3.2). This protection may have prevented reworking of the sediments and subsequent sample preservation.

4.8.2 The mid-Holocene Highstand

The second aspect of interest from the RSL plot are those SLIPs located in just prior to and during the MHHS itself, specifically points F, G and H. They illustrate a MHHS of between 2.2-2.4m AHD at between 7-7.2k cal. yrs BP, showing an excellent fit to the modelled predictions. Data points around the MHHS are crucial to geophysical modellers as they help to constrain both the timing and amplitude of the highstand, hence the timing of global meltwater shutdown and

information on the sources of global meltwater. Direct comparison to the local literature show that Larcombe *et al.* (1995) identify the MHHS at ca. 5.5k ^{14}C years BP with an amplitude of +1m AHD. This illustrates that the data presented here peaks slightly higher and sooner than that of Larcombe *et al.* (1995), though for more conclusive evidence further samples should be taken around this time period to give a better representation. Australian literature shows a range of amplitudes and timings of the MHHS varying between +0.8m AHD (±0.25m) at 3810 cal. yrs BP for Port Hacking, central New South Wales (NSW) to +3.0m AHD (±0.5m) 2960 cal. yrs BP for Wasphead in southern NSW (Baker *et al.*, 2001a). This shows that the MHHS found in this study occurs earlier and within the range of MHHSs shown for other regions of Australia, thus highlighting the spatial differences in eustatic sea-level changes in addition to individual reconstruction errors at each site. Further errors that are applicable to all reconstructions using biological indicators are discussed in Section 4.9.

4.8.3 The Regression

The third aspect of interest are the SLIPs depicting a RSL regression of approximately 4m from around 5k - 2k cal. yrs BP. Two of the index points (D and E) show the potential to plot in agreement with the modelled predictions when considering the errors, though the general trend is one of an underestimation of sea levels. The SLIPs (A-E) may indeed be valid index points, with a growing wealth of evidence for a double highstand (Baker *et al.*, 2001b; Bezerra *et al.*, 2003) being identified globally. In addition, the modelled predictions may be overestimating the height of RSL, as work by Lambeck (2002) shows that this can be a factor, especially along the Queensland coast. However, this is unlikely as there is an absence of documented evidence of RSL being significantly below present between the MHHS and present values within Australia (Larcombe *et al.*, 1995; Cann *et al.*, 2000; Baker *et al.*, 2001a; Belperio *et al.*, 2002; Lambeck 2002).

The materials dated to create these points are all carbonates and are unlikely to all be transport of newer material. An error in the transfer function prediction of a RWL is a distinct possibility, with the assemblages plotting

significantly below model predictions. There is a lack of *A. beccarii*, an intertidal and shallow subtidal species, in all samples. Two samples contain relatively high abundances of *A. lessonii*, a deeper water species, in addition to two others having a significant proportion of the 'unidentified' species. These factors may have resulted in an 'inappropriately' low RWL being assigned through the transfer function, and hence, with the elevational correction, a suppressed former sea level. The differing results from the samples may have been aided by potential mixing of the shallow subtidal sediments during the MHHS and regression, given the knowledge of changeable sea-level histories for this and similar locations during the time-period.

Post-depositional sediment compaction may be an additional explanation for the dipping trend below present values for reconstructed index points in this study. This process is defined as 'the group of interlinked processes whereby the sediment within a growing stratigraphic column diminishes in volume, on account of burial and self-weight, leading to a rearrangement of the mineral skeleton, and in the case of vegetable matter, a loss of mass as the result of biological and chemical decay' (Allen, 2000). The problem of sediment compaction was recognised in studies by Bloom (1964), Kaye and Barghoorn (1964) and Tooley (1982; 1985), and has applicable error margins of up to 90% of the original substrate height. However, this must be placed into context for this region, as organic rich soils and peat potentially can reduce by 90%, though granular materials, such as sands, clays and silts more often found on the GBR shelf, can potentially loose less than 10% of their height (Paul and Barras, 1998). Carter *et al.* (1993) model a period of large-scale terrigenous input to the GBR shelf throughout the Holocene, and hence show suitable substrates to be present (Larcombe and Carter, 1998). Water loading must also be considered a factor, given the location of these vibracores, often in excess of 15m of water (Fig. 4.1). Spatial variation of sediment compaction is also of relevance because throughout Cleveland Bay, Larcombe and Carter (1998) note differences in the thickness of Holocene deposits, related to palaeo-river channels infilled with sediments. In combination with the work of Carter *et al.* (1993) (Fig. 2.15), this depicts a network of sinuous palaeo-river channels (since the LGM) on the Central GBR shelf that

could undergo compaction to a greater extent than other shelf samples in thinner sediments.

4.9 Limitations with the sea-level reconstruction

All palaeoenvironmental reconstruction techniques have errors and the transfer function is no exception, including errors with transfer function RWL prediction and depth. More fundamental than this, however, is the question of sub-sampling from a core and grab sample database.

However, greater magnitude sources of error applicable to all samples are discussed here, focussing on RWLs and dating. Studies within the region (Woodroffe, 2002; Horton *et al.,* 2003) and globally (Horton *et al.,* 1999a; Edwards and Horton, 2000; Gehrels, 2000; Gehrels *et al.,* 2001; Horton *et al.,* 2000) note that a lack of contemporary analogues for a transfer function inhibits the reconstruction of fossil samples. However, within this study only 4 species fall into this category. The concept of post-depositional change is also a factor in the transfer function RWLs. However it is noted by scientists that the dead assemblage is an accurate proxy for the living one (Murray, 1991; Scott *et al.,* 2001) though given the subtidal sedimentary regime outlined by Orpin and Woolfe (1999) for GBR embayments, the potential for sediment mixing and sorting is high. Either of these sources of error can result in a change of the assemblage characteristics and thus generate indifferent RWLs. Finally, the patchy distribution of foraminifera is a general source of error for RWL generation. Studies from around the world, including the Bay of Biscay (Fontanier *et al.,* 2003), Western Australia (Li *et al.,* 1999) and the Antarctic Peninsula (Gray *et al.,* 2003) all note patchy distributions of subtidal benthic foraminifera. Localised intertidal studies (Woodroffe, 2002; Horton *et al.,* 2003) also note a patchy distribution, which can cause further no-analogue problems. To minimise this I have adopted a regional approach.

From a dating perspective, the incorporation of reworked older carbon material is the major dating concern. This does not exclude the potential

incorporation of younger carbon as modern cross-shelf sediment-transport processes are poorly known (Orpin *et al.*, 1999; Heap *et al.*, 2001). Orpin and Woolfe (1999) identify high-energy transition zones and low energy environments within embayments along the GBR coast, and therefore I suggest that inclusion of older carbon is quite feasible in the largest contemporary example of a mixed terrigenous-carbonate system on earth (as defined by Orpin and Woolfe, 1999). Consideration is also taken for other sources of error, including temporal variations in ^{14}C production, isotopic fractionation and marine carbon circulation, though they are considered to be of a greater scale than can be assessed for this study. Furthermore, the radiocarbon dates used in this study were finalised during 1985-91, and thus error ranges are greater than if more modern dating techniques, such as AMS, were employed.

4.10 Future Applications

Future applications of this technique may build on existing subtidal studies, such as Yokoyama *et al.* (2000), where semi-quantitative reconstructions exist. Potential reinterpretation of these reconstructions could be based on this transfer function, though more appropriately a new transfer function should be created, given the differing carbonate nature of the subtidal environments. Finally, considering transfer function studies completed within the region (Horton *et al.*, 2003) and the results of this study, the potential exists to combine these approaches and create a 'shallow-marine' transfer function, encompassing both the inter-tidal and subtidal environments. This amalgamation may help widen the window of our understanding of contemporary benthic foraminiferal distributions and assemblages, and hence enable us to attain a greater number of analogues as inputs for future quantitative palaeoenvironmental reconstructions.

4.11 Conclusions

Building on conclusions drawn from Chapter 3, subtidal benthic foraminifera have been shown to have a quantifiable relationship to depth. As a result, the first subtidal foraminiferal based transfer function has been created. The transfer

function shows a strong relationship between observed and predicted depths and encompasses a range of subtidal environments and depths.

The transfer function has been applied to 13 fossil samples, generating RWLs for each. These RWLs have been incorporated into the RSL equation and converted into former sea levels. Reinterpretation of index points presented by Larcombe *et al.* (1995) by correcting for the RWL shows a general increase in elevation, raising all points by between 9.81 - 29.35m. These reinterpreted index points have been validated by geophysical model predictions.

The RSL curve shows a good agreement with the trends of the geophysical models, and the wider literature for Australia as a whole. The transgression from the early Holocene through to the MHHS is well documented and is supported by the SLIPs generated here. The regression from a MHHS to present values is less well documented and several arguments are presented for this and other potential outliers. Each explanation may only form part of the answer, and, indeed, the answer may be a combination of these factors. In addition, the study would have benefited from more dated samples to place on this curve, in order to resolve both the 'blip', identified by Larcombe *et al.* (1995), and the full extent of the MHHS.

The limitations of the technique are identified and these must always be considered when drawing interpretations from results. However, there are several potential applications both as a new technique in its own right, and as an amalgamation with intertidal transfer functions to create a 'shallow-marine' composite. Improvements in the reconstructed error range for SLIPs promises to afford plentiful opportunities to apply this new technique to rapid sea-level transgressions across the GBR and other continental shelves. This has the potential to increase our understanding of Holocene sea-level change and hence the eustatic sea-level signal, providing valuable inputs for geophysical modellers, amongst others, in their attempts to understand the redistribution of ice and meltwater since the last glacial maximum.

Chapter 5

Conclusion

5.1 Conclusions

Three contemporary subtidal environments were selected from two embayments (Bowling Green Bay and Cleveland Bay) along the Central Great Barrier Reef lagoon, Australia. These embayments exhibit differing subtidal environmental characteristics, both between the embayments and within an embayment (Cleveland Bay).

Contemporary samples were collected from both embayments for microfossil and environmental analysis. Three environmental variables were collected at each station (depth, loss-on-ignition and grain-size) for ecological and logistical considerations. Foraminiferal analysis reveals 31 species to be significant in the region, dominated by *Amphistegina lessonii* and *Dendritina striata* in Bowling Green Bay. Cleveland Bay is dominated by differing species, *Discorbinella complanata* and *Cribrononion sydneyensis* for Transect 1, *Pararotalia vernusta* and *Quinqueloculina venusta* for Transect 2.

Cluster analysis shows clear zones of foraminiferal assemblages for all three environments, supported by Detrended Correspondence Analysis. Bowling Green Bay shows two zones with discrete elevational ranges, whereas Cleveland Bay exhibits elevational zones with overlap for both environments.

Multivariate analysis shows that the sand fraction is the most important variable measured for all environments. Bowling Green Bay shows a strong environmental gradient in both depth and sand fraction. Key species inhabit distinct environments, such as *A. lessonii* inhabiting deeper sandy localities, *D.*

complanata residing in shallow elevational finer grained substrates and *D. striata* demonstrating a unimodal tolerance to mid-range depths. Cleveland Bay samples show depth as a poor constraint on foraminiferal distributions whilst maintaining sand as the dominant regional variable.

Three local datasets have been combined to generate a regional training set of foraminiferal assemblages to develop the first subtidal foraminiferal transfer function. The results show there is a strong relationship between the observed and model predicted (WA-PLS) depths (r^2=0.97), indicative of species-specific tolerances to specific-elevational levels.

The transfer function has been applied to 13 fossil samples, generating reference water levels and relative sea-levels for each. These sea-level index points have been validated by geophysical models and plotted on a curve. Reinterpretation of index points presented by Larcombe *et al.* (1995) shows a general increase in elevation, raising all points by between 9.81 - 29.35m. The new RSL curve shows a comparable trend with the geophysical models, and the wider literature for Australia as a whole, depicting a rapid transgression to a well constrained mid-Holocene highstand, followed by a regression down to present values.

The limitations of this study fall into two categories, elevational and dating. Elevational errors can be traced throughout the reconstruction, to include pre-transfer function calibration of sample depths using tidal data, mechanical errors such as depth-finders on sampling vessels and general human error. Post transfer function depth limitations include selective preservation in the fossil record and absent matching analogues. The contribution of the latter is the largest elevational limitation to this reconstruction.

5.2 Research recommendations

Whilst it is vital to consider errors with a palaeoenvironmental reconstruction technique, it is also important to identify the benefits of the technique. The potential of this technique is promising as a tool for quantitative RSL reconstructions from subtidal shelf sediments. Furthermore, re-interpretation of existing SLIPs for the region and the more general application to other areas (e.g. Yokoyama *et al.*, 2001 – NW Australia) also shows potential. Attempts must be made to reduce the comparatively large error bars associated with the elevational reconstruction and thus it must be an important aim to collect as much contemporary foraminiferal data as feasible. Specific expeditions should be undertaken to sample more regular depth intervals from the coastline, through the inner, mid and outer shelves, past the reef break and out onto the shelf break into deeper elevations. The increased spectrum of sampling will hopefully reduce some of the reconstructed RWL elevations by encompassing more foraminiferal assemblages as analogues for the transfer function. Furthermore, in such an environment of late-Pleistocene and early Holocene transgression, vibracores should be taken along the GBR shelf to try and capture subtidal sediments deposited during a rapid transgression.

Acquisition of fossil samples during time-periods of pre-determined interest is always difficult, and to a certain extent it is a process of trial and error. However, results show that samples collected from Cleveland Bay vibracores are well dated and preserved, through the transgression up to the MHHS. Further sampling here may prove fruitful in attempts to constrain the MHHS and thus the implications for modellers are strong.

References

- Allen, J. R. L. (2000). Morphodynamics of Holocene salt marshes: a review sketch from the Atlantic and Southern North Sea coasts of Europe. *Quaternary Science Reviews*, **19**, 1155-1231.

- Baker T.F. (1993). Absolute sea level measurements, climate change and vertical crustal movements, *Global and Planetary Change*, **8**, 149-159.

- Baker, R. G. V. and Haworth, R. J. (2000). Smooth or oscillating late Holocene sea-level curve? Evidence from the palaeo-zoology of fixed biological indicators in east Australia and beyond. *Marine Geology*, **163** (1-4), 367-386.

- Baker, R. G. V., Haworth, R. J. and Flood, P. G. (2001a). Inter-tidal fixed indicators of former Holocene sea levels in Australia: a summary of sites and a review of methods and models. *Quaternary International*, **83-85**, 257-273.

- Baker, R. G. V., Haworth, R. J. and Flood, P. G. (2001b). Warmer or cooler late Holocene marine palaeoenvironments?: interpreting southeast Australian and Brazilian sea-level changes using fixed biological indicators and their $\delta^{18}O$ composition. *Palaeogeography, Palaeoclimatology, Palaeoecology*, **168**, 249-272.

- Ball, D. F. (1964). Loss on ignition as an estimate of organic matter and organic carbon in non calcareous soils. *Journal of Soil Science*, **15**, 84-92.

- Bard, E., Hamelin, B., Arnold, M., Montaggioni, L., Cabioch, G., Faure, G. and Rougerie, F. (1996). *Nature*, **382**, 241-244.

- Baxter, A. J. and Meadows, M. E. (1999). Evidence for Holocene sea level change at Verlorenlei, Western Cape, South Africa. *Quaternary International,* **56**, 65–79.

- Beaman, R., Larcombe, P. and Carter, R. M. (1994). New evidence for the Holocene sea-level high from the inner shelf, Central Great Barrier Reef, Australia. *Journal of Sedimentary Research*, **64**, 881-885.

- Belperio A. P. (1983). Terrigenous sedimentation in the central Great Barrier Reef lagoon: a model from the Burdekin region. *Bur. Min. Resour. J. Aust. Geol. Geophys.,* **8**, 179–190.

- Belperio, A. P., Harvey, N. and Bourman, R. P. (2002). Spatial and temporal variability in the Holocene sea-level record of the South Australian coastline. *Sedimentary* Geology, **150**, 153-169.

- Bezerra, F. H. R., Barreto, A. M. F. and Suguio, K. (2003). Holocene sea-level history on the Rio Grande do Norte State coast, Brazil. *Marine Geology*, **196** (1-2), 73-89.

- Birks, H. J. B. (1995). Quantitative palaeoenvironmental reconstructions. In: Maddy, D. and Brew, J. S. (eds). *Statistical modelling of quaternary science data.* Technical guide no 5, Quaternary research association. Cambridge, 161-254.

- Bittencourt, A. C. S. P., Martin, L., Vilas-Boas, G. S. and Flexor, J. M. (1979). Quaternary marine formations of the state of Bahia (Brazil). 1978 International Symposium on Coastal Evolution in the Quaternary Proceedings, São Paulo, 232–253.

- Bloom, A. L. (1964). Peat accumulation and compaction in a Connecticut salt marsh, *Journal of Sedimentary Petrology*, **34**, 599-603.

- Boltovskoy, E. and Wright, R. (1976). Recent Foraminifera. Dr. W. Junk b.v. - Publishers - The Hague.

- Bronniman, P. and Whittaker, J. E. (1993) Taxonomic revision of some recent agglutinated foraminifera from the Malay Archipelago in the Millett Collection, Natural History Museum, London. *Bull. Nat. Hist. Mus. London.* **59**, 107–124.

- Buzas, M. A. and Culver, S. J. (2001). On the relationship between species distribution-abundance-occurrence and species duration, *Historical Biology*, **15**,151-159.

- Cann, J. H., Bourman, R. P. and Barnett, E. J. (2000). Holocene foraminifera as indicators of relative estuarine-lagoonal and oceanic influences in estuarine sediments of the Murray River, South Australia. *Quaternary Research*, **53**, 378-391.

- Carter, R. M. and Johnson, D. P. (1986). Sea level controls on the post-glacial development of the Great Barrier Reef, Queensland. *Marine Geology*, **71**, 137-164.

- Carter, R. M., Carter, L. and Johnson, D. P. (1986). Submergent shorelines in the SW Pacific: evidence for an episodic post-glacial transgression. *Sedimentology*, **33**, 629-649.

- Carter, R. M., Johnson, D. P. and Hooper, K.G. (1993). Episodic post-glacial sea-level rise and the sedimentary evolution of a tropical embayment (Cleveland Bay, Great Barrier Reef shelf, Australia). *Australian Journal of Earth Science,* **40**, 229–255.

- Chappell, J. and Polach, H. (1991). Post-glacial sea level rise from a coral record at Huon Peninsula, Papua New Guinea. *Nature*, **349**, 147-149.

- Chase, T. N., Knaff, J. A., Pielke, R. A. and Kalnay E. (2003). Changes in global monsoon circulations since 1950, *Natural Hazards*, **29**, 229-254.

- Clark, J. A., Farrell, W. E. and Peltier, W. R. (1978). Global changes in post glacial sea level : a numerical calculation. *Quaternary Research*, **9**, 265-287.

- Culver, S. J. (1990). Benthic foraminifera of Puerto Rican mangrove-lagoon systems: potential for palaeoenvironmental interpretations, *Palaios*, **5**, 34-51.

- Culver, S. J. and Snedden, J. W. (1996). Foraminifera and their implications for the formation of New Jersey shelf sand ridges. *Palaios*, **11**, 161-175.

- de Rijk, S., (1995). Salinity control on the distribution of salt marsh Foraminifera (Great Marshes, Massachusetts). *Journal of Foraminiferal Research*, **25**, 156-166.

- Dunbar, G. B. and Dickens, G. R. (2003 *in press*). Massive siliciclastic discharge to slopes of the Great Barrier Reef Platform during sea-level transgression: constraints from sediment cores between 15°S and 16°S latitude and possible explanations, *Sedimentary Geology, In Press.*

- Edwards, R. J. (2001). Mid- to late Holocene relative sea-level changes in Poole Harbour, southern England. *Journal of Quaternary Science,* **16**, 201–220.

- Edwards, R. J. and Horton, B. P. (2000). High Resolution Records of Relative Sea Level Change from U.K. Salt-marsh Foraminifera. *Marine Geology*, **169**, 41-56.

- Edwards, R. L., Beck, J. W., Burr, G. S., Donahue, D. J., Chappell, J. M. A, Bloom, A. L., Druffel, E. R. M. and Taylor, F. W. (1993). A large drop in atmospheric $^{14}C/^{12}C$ and reduced melting in the Younger Dryas, documented with ^{230Th} ages of corals. *Science*, **260**, 962-967.

- Fairbanks, R. G. (1989). A 17,000-year glacio-eustatic sea level record: influence of glacial melting rates on the Younger Dryas event and deep-ocean circulation. *Nature*, **342**, 637-642.

- Fairbridge, R. W. (1961). Eustatic changes in sea level. In: *Physics and Chemistry of the Earth.* **4**. (Ed.: L. H. Athrens) Pergamon Press, London, 98-185.

- Fatela, F., and Taborda, R. (2002). Confidence limits of species proportions in microfossil assemblages, *Marine Micropaleontology*, **45**, 169-174.

- Fleming, K., Johnston, P., Zwartz, D., Yokoyama, Y., Lambeck, K. and Chappell, J. (1998). Refining the eustatic sea-level curve since the Last Glacial Maximum using far- and intermediate- field sites. *Earth and Planetary Science Letters* **163**, 327–42.

- Fontanier, C., Jorissen, F., J., Chaillou, G., David, C., Anschutz, P. and Lafon, V. (2003). Seasonal and inter-annual variability of benthic foraminiferal faunas at 550 m depth in the Bay of Biscay, *Deep Sea Research Part I: Oceanographic Research Papers,* **50** (4), 457-494.

- Funnell B. M. and Swallow J. E. (1997). Intra-sample, inter-sample and down-core microvariation in sea-surface temperature estimates obtained from planktonic foraminifera in the NE Atlantic, *Journal of Micropalaeontology,* **16**, 163-174.

- Gehrels, W. R., (1994). Determining relative sea-level change from saltmarsh foraminifera and plant zones on the coast of Maine, USA. *Journal of Coastal Research*, **10**, 990-1009.

- Gehrels, W. R. (2000). Using foraminiferal transfer functions to produce high-resolution sea-level records from salt-marsh deposits, Maine, USA. *Holocene,* **10**, 367–376.

- Gehrels, W. R., Roe, H. M. and Charman, D. J. (2001). Foraminifera, testate amoebae and diatoms as sea-level indicators in UK saltmarshes: a quantitative multiproxy approach. *Journal of Quaternary Science*, **163**, 201–220.

- Gischler, E. (2003). Holocene lagoonal development in the isolated carbonate platforms off Belize. *Sedimentary Geology,* **159** (1-2), 113-132.

- Godwin, H. (1940). Studies in the post-glacial history of British vegetation. III: Fenland pollen diagrams. IV: Post-glacial changes of relative land and sea level in the English Fenland. *Philosophical Transactions of the Royal Society of London* B, **230**, 239-303.

- Gould, H. R. and Stewart, R. H. (1955). Continental terrace sediments in North-eastern Gulf of Mexico. In Hough, J. L. (ed) *Finding Ancient Shorelines* of Economic Palaeontologists and Mineralogists Special Publication, **3**, 111-138.

- Gray, S. C., Sturz, A., Bruns, M. D., Marzan, R. L., Dougherty, D., Law, H. B., Brackett, J. E. and Marcou, M. (2003). Composition and distribution of sediments and benthic foraminifera in a submerged caldera after 30 years of volcanic quiescence, *Deep Sea Research Part II: Topical Studies in Oceanography,* **50** (10-11), 1727-1751.

- Hah Jun Woo, Culver S. J. and Oertel G. F. (1997). Benthic foraminiferal communities of a barrier-lagoon system, Virginia, U.S.A, *Journal of Coastal Research,* **13**, 1192-1200.

- Haslett, S. K. (2001). The Palaeoenvironmental implications of the distribution of intertidal foraminifera in a tropical Australian estuary: a reconnaissance study. *Aust. Geogr. Stud.* **39**, 67–74.

- Hayward, B. W., Grenfell, H. R., Reid, C. M. and Hayward, K. A. (1999). Recent New Zealand shallow-water benthic foraminifera; taxonomy, ecological distribution, biogeography, and use in palaeoenvironmental assessment. Institute of Geological and Nuclear Science Ltd., Lower Hutt, New Zealand.

- Heap, A. D., Dickens, G. R. and Stewart, L. K. (2001). Late Holocene sediment in Nara Inlet, central Great Barrier Reef platform, Australia: sediment accumulation on the middle shelf of a tropical mixed clastic/carbonate system, Marine Geology, **176**, 39-54.

- Hill, M. O. and Gauch, H. G. (1980). Detrended correspondence analysis; an improved ordination technique, *Vegetatio*, **42**, 47-58.

- Horton, B. P. (1997). Quantification of the indicative meaning of a range of Holocene sea-level index points from the western North Sea, *Ph.D. Thesis*, Department of Geography, University of Durham, United Kingdom.

- Horton, B. P. (1999). The contemporary distribution of intertidal foraminifera of Cowpen Marsh, Tees Estuary, UK: implications for studies of Holocene sea-level changes. *Palaeogeography, Palaeoclimatology, Palaeoecology Special Issue*, **149**, 127-149.

- Horton, B. P. and Edwards, R., J. (*in press*). The application of local and regional transfer functions to reconstruct former sea levels, North Norfolk, England.

- Horton, B. P., Edwards, R. J. and Lloyd, J. M. (1999a). Reconstruction of former sea level using a foraminiferal-based transfer function. *Journal of Foraminiferal Research*, **29**, 117-129.

- Horton, B. P., Edwards, R. J. and Lloyd, J. M. (1999b). UK intertidal foraminiferal distributions: implications for sea-level studies. *Marine Micropaleontology*, **36**, 205-223.

- Horton, B. P., Edwards, R. J. and Lloyd, J. M. (2000). Implications of a microfossil transfer function in Holocene sea level studies. In: Shennan, I and Andrews, J. (eds) Holocene land-ocean interaction and environmental change around the North Sea. Geological Society, London. Special Publications **166**, 275-298.

- Horton, B. P., Larcombe, P., Woodroffe, S. A., Whittaker, J. E., Wright, M. R. and Wynn, C. (2003). Contemporary foraminiferal distributions of a mangrove environment, Great Barrier Reef coastline, Australia: implications for sea-level reconstructions. *Marine Geology,* **198** (3-4), 225-243.

- Hottinger, L. (1977). Distribution of larger Peneroplidae, *Borelis* and *Nummulitidae* in the Gulf of Elat, Red Sea. *Utrecht Micropalaeontological Bulletin*, **15**, 35-109.

- Islam, M. S. and Tooley, M. J. (1999). Coastal and sea level changes during the Holocene in Bangladesh, *Quaternary International*, **55**, 61-75.

- Jongman, R. H. G., ter Braak, C. J. F. and van Tongeren, O. F. R. (1995). Data analysis in community and landscape ecology. Cambridge University Press.

- Kaye, C. A. and Barghoorn, E. S. (1964). Late Quaternary sea-level change and crustal rise at Boston, Massachusetts, with notes on the autocompaction of peat, *Bulleting of the Geological Society of America*, **75**, 63-80.

- Laborel, J. (1986). Vermetid gastrapods as sea level indicators. In : van de Plassche, O. (Ed.), Sea-level Research. Geo Books, Norwich.

- Lambeck, K. (1999). Shoreline displacements in southern-central Sweden and the evolution of the Baltic Sea. *Journal of the Geological Society of London* **156**, 465–68.

- Lambeck, K. (2002). Sea level change from mid-Holocene to recent time : An Australian example with global implications. Ice sheets, Sea level and the Dynamic Earth. American Geophysical Union.

- Langer, M. R. and Lipps, J. H. (2003). Foraminiferal distribution and diversity, Madang Reef and Lagoon, Papua New Guinea. *Coral Reefs*, **22**, 143-154.

- Larcombe, P., Carter, R. M., Dye, J., Gagan, M. K. and Johnson, D. P. (1995). New evidence for episodic post-glacial sea level rise, central Great Barrier Reef, Australia. *Marine Geology*, **127**, 1-44.

- Larcombe, P. and Carter, R. M. (1998). Sequence architecture during the Holocene transgression : an example from the Great Barrier Reef shelf, Australia. *Sedimentary Geology*, **117**, 97-121.

- Li, Q., James, N. P., Bone, Y. and McGowran, B. (1999). Palaeoceanographic significance of recent foraminiferal biofacies on the southern shelf of Western Australia: a preliminary study, *Palaeogeography, Palaeoclimatology, Palaeoecology*, **147** (1-2), 101-120.

- Lighty, R. G., Macintyre, I. G. and Stuckenrath, R. (1982). *Acropora palmata* framework: a reliable indicator of sea level in the western Atlantic for the past 10,000 years. *Coral Reefs,* **1**, 125–130.

- Lipps, J. H. (1993). Fossil prokaryotes and protests, Boston: *Blackwell Scientific Publications*, 342 p.

- Loeblich, A. R. and Tappan, H. (1994). Foraminifera of the Sahul Shelf and Timor Sea. Cushman Found. *Foraminifer. Res. Spec. Publ.* **31**, 661 pp.

- Long A. (2001). Mid-Holocene sea-level change and coastal evolution. *Progress in Physical Geography*, **25**(3), 399-408.

- Long, A. J., Roberts, D. H. and Wright, M. R., (1999). Isolation basin Stratigraphy and Holocene relative sea-level change on Arevprinsen Eijland, Disko Bugt, West Greenland. *Journal of Quaternary Science.* **14**, 323–345.

- Long, A. J. and Roberts, D. H., (2002). A revised chronology for the 'Fjord Stage' moraine in Disko Bugt, West Greenland. *Journal of Quaternary Science,* **17**, 561–579.

- Long, A. J. and Roberts, D. H. (2003). Late Weichselian deglacial history of Disko Bugt, West Greenland, and the dynamics of the Jakobshavns Isbrae ice stream. *Boreas*, **32**, 208–226.

- Long, A. J., Roberts, D. H. and Rasch, M. (2003). New observations on the relative sea level and deglacial history of Greenland from Innaarsuit, Disko Bugt. *Quaternary Research*, **60** (2), 162-171.

- Loubere P. (2003). Remote vs. local control of changes in eastern equatorial Pacific bioproductivity from the Last Glacial Maximum to the present, *Global and Planetary Change*, **35**, 113-126.

- M^{c}Gregor, H., V. and Gagan, M., K. (2003). Diagenesis and geochemistry of Porites corals from Papua New Guinea: Implications for paleoclimate reconstruction, *Geochimica et Cosmochimica Acta*, **67**, 2147-2156.

- M^{c}Intyre, C. (1996). The Holocene Sedimentology and Stratigraphy of the Inner Shelf of the Great Barrier Reef; Deposits of Buried Shorelines. *M.Sc. Thesis*, Department of Earth Sciences, James Cook University of North Queensland, Townsville, Queensland.

- Meehl, G. A., Strand, W. G., Washington, W. M., Arblaster, J. M. and Bettge, T. W. (2000). Anthropogenic forcing and decadal climate variability in sensitivity experiments of twentieth- and twenty-first-century climate, *Journal of Climate*, **13**, 3728-3744.

- Miller, D. E., Yates, R. J., Parkington, J. E. and Vogel, J. C. (1993). Radiocarbon-dated evidence relating to a mid-Holocene relative high sea-level on the southern Cape Coast, South Africa. *South Africa Journal Science,* **89**, 35–44.

- Murray, J. W. (1991). Ecology and Palaeoecology of Benthic Foraminifera. Longman Scientific and Technical, Harlow, 397 pp.

- Murray, J. W. (2000). When does environmental variability become environmental change? In: Environmental Micropaleontology, Vol. **15** of *Topics in Geobiology*, edited by Ronald E. Martin. Kluwer Academic/ Plenum Publishers, New York, 2000.

- Murray J. W. (2001). The niche of benthic foraminifera, critical thresholds and proxies, *Marine Micropaleontology*, **41**, 1-7.

- Murray, J. W. and Wright, C. A. (1974). Palaeogene Foraminiferida and Palaeoecology, Hampshire and Paris basins and the English Channel. *Special Papers in Palaeontology*, **14**, 1-171.

- Nakada, M. and Lambeck, K. (1990). Late Pleistocene and Holocene sea-level change along the Australian coast. *Palaeogeography, Palaeoclimatology, Palaeoecology*, **89**, 143-176.

- Nakada, M., Kimura, R., Okuno, J., Moriwaki, K., Miura, H. and Maemoku, H. (2000). Late Pleistocene and Holocene melting history of the Antarctic ice sheet derived from sea-level variations. *Marine Geology* **167**, 85–103.

- Nunn, P. D. (2001). Significance of emerged Holocene corals around Ovalau and Moturiki islands, Fiji, southwest Pacific. *Marine Geology*, **163** (1-4), 345-351.

- Oerlemans J. (2003). A quasi-analytical ice-sheet model for climate studies, *Non-linear Processes in Geophysics*, **10**, 441-452.

- Oliver, J. (1978). The climatic environment of the Townsville area. In : Hopley, D. (ed.), Geographical Studies of the Townsville Area, Monograph Series, Department of Geography, James Cook University of North Queensland, *Occasional Paper,* **2**, 3-17.

- Orpin, A. R. (1999). Sediment transport, portioning and unmixing relationships in the mixed terrigenous-carbonate system of the Great Barrier Reef, Burdekin shelf sector, Australia. *Ph.D. Thesis*, Department of Earth Sciences, James Cook University of North Queensland, Townsville, Queensland, Australia.

- Orpin, A. R. and Woolfe, K. J. (1999). Unmixing relationships as a method of deriving a semi-quantitative terrigenous sediment budget, central Great Barrier Reef lagoon, Australia, *Sedimentary Geology*, **129**, 25-35.

- Orpin, A. R., Haig, D. W. and Woolfe K. J. (1999). Sedimentary and foraminiferal facies in Exmouth Gulf, in arid tropical north-western Australia, *Australian Journal of Earth Sciences*, **46**, 607-621.

- Patterson R. T. and Fishbein E. (1989). Re-examination of the statistical methods used to determine the number of point counts needed for micropaleontological quantitative research. *J. Paleontology.* **63**, 245–248.

- Paul, M. A. and Barras, B. F. (1998). A geotechnical correction for post-depositional sediment compression: examples from the Forth Valley, Scotland, *Journal of Quaternary Science*, **13** (2) 171-176.

- Peltier, W. R., (1998a). Global glacial isostatic adjustment and coastal tectonics. In: Stewart, I., Vita-Finzi, C. (Eds.), Coastal Tectonics. Geol. Soc. London Spec. Publ. **146**, 1–29.

- Peltier, W. R., (1998b). Post glacial variations in the level of the sea; implications for climate dynamics and solid-earth geophysics. Review of Geophysics, **36**, 603-689.

- Peltier W. R., Shennan I., Drummond R. and Horton, B. P. (2002). On the postglacial isostatic adjustment of the British Isles and the shallow viscoelastic structure of the Earth, *Geophysical Journal International*, **148**, 443-475.

- Phelger, F. B. (1970). Foraminiferal populations and marine marsh processes. *Limnology and Oceanography,* **15**, 522-534.

- Phelger, F. B. and Walton, W. R. (1950). Ecology of marsh and bay foraminifera, Barnstable, Massachusetts, *American Journal of Science,* **248**, 274-294.

- Pirazzoli, P. A. (1996). Sea level changes : The last 20,000 years. Wiley and Sons. Chichester.

- Plater, A. J., Ridgway, J., Rayner, B., Shennan, I., Horton, B. P., Haworth, E. Y., Wright, M. R., Rutherford, M. M. and Wintle, A. G. (2000). *Sediment*

provenance and flux in the Tees Estuary: the record from the Late Devensian to the present. In: Shennan, I and Andrews, J. (eds) Holocene land-ocean interaction and environmental change around the North Sea. Geological Society, London. Special Publications **166**, 275-298.

- Queensland Department of Transport. (1999). The Official Tide Tables and Boating Safety Guide 1999. Mineral House, Brisbane, Qld, 236 pp.

- Scott, D. B. and Medioli, F. S. (1978). Vertical zonation of marsh foraminifera as accurate indicators of former sea levels. *Nature*, **272**, 528-531.

- Scott, D. B. and Medioli, F. S. (1980). Living vs. total foraminifera populations: their relative usefulness in palaeoecology. *Journal of Paleontology*, **54**, 814-831.

- Scott, D. B. and Hermelin, J. O. R. (1993). A device for precision splitting of micropaleontological samples in liquid suspension, *Journal of Paleontology*, **67**, 151-154.

- Scott, D. B., Brown, K. Collins, E. S. and Medioli, F. S. (1995). A new sea-level curve from Nova Scotia: evidence for a rapid acceleration of sea-level rise in the late mid-Holocene. *Canadian Journal of Earth Sciences*, **32**, 12pp.

- Scott, D. B., Medioli, F. S. and Schafer, C. T. (2001). Monitoring in coastal environments using Foraminifera and Thecamoebian indicators. Cambridge: Cambridge University Press.

- Sen Gupta, B. K. (1999). Modern Foraminifera. *Kluwer Academic Publishers, Dordrecht*, 7-36.

- Shackleton, N. J., Berger, A. and Peltier, W. R. (1990). An alternative astronomical calibration of the lower Pleistocene timescale based on ODP site 677. *Transactions of the Royal Society of Edinburgh : Earth Sciences*, **81**, 251-261.

- Shennan, I. (1989). Holocene crustal movements and sea-level changes in Great Britain. *Journal of Quaternary Science,* **4**, 77-89.

- Shennan, I. and Horton, B. P. (2002). Holocene land- and sea-level changes in Great Britain. *Journal of Quaternary Science*, **17** (5-6), 511-526.

- Shennan, I., Tooley, M. J., Davis, M. J. and Haggart, B. A. (1983). Analysis and interpretation of Holocene sea-level data, *Nature*, **302**, 404-406.

- Shennan, I., Lambeck, K., Horton, B. P., Innes, J. B., Lloyd, J.M., McArthur, J. J. and Rutherford, M. M. (2000a). *Holocene Isostacy and relative sea-level changes on the east coast of England.* In: Shennan, I and Andrews, J. (eds) Holocene land-ocean interaction and environmental change around the North Sea. Geological Society, London. Special Publications **166**, 275-298.

- Shennan, I., Lambeck, K., Horton, B. P., Innes, J., Lloyd, J., McArthur, J., Purcell, T. and Rutherford, M. (2000b). Late Devensian and Holocene records of relative sea-level changes in northwest Scotland and their implications for glacio-hydro-isostatic modelling. *Quaternary Science Reviews*, **19**, 1103-1135.

- Smithers, S. G. and Woodroffe, C. D. (2001). Coral microatolls and 20th century sea level in the eastern Indian Ocean. *Earth and Planetary Science Letters,* **191**, 173-184.

- Stuiver, M. and Reimer, P. J. (1993). Extended ^{14}C data base and revised CALIB 3.0 ^{14}C age calibration program, *Radiocarbon,* **35** (1), 215-230.
- Suguio, K., Martin, L., Bittencourt, A. C. S. P., Dominguez, J. M. L., Flexor, J. M. and Azevedo, A. E. G. (1985). Flutuações do nível relativo do mar durante o Quaternário Superior ao longo do litoral Brasileiro e suas implicações na sedimentação costeira. *Rev. Bras. Geoci.* **15**, 273–286.
- Tarasov, L. and Peltier, W. R. (2003). Greenland glacial history, borehole constraints, and Eemian extent, *Journal of Geophysical Research B: Solid Earth*, **108**, 4-1 - 4-20.
- ter Braak, C. J. F. (1986). Canonical correspondence analysis: a new eigenvector technique for multivariate gradient analysis, *Ecology*, **67**, 1167-1179.
- ter Braak, C. J. F. (1987). Ordination, *in* Jongman, R. H. G., ter Braak, C. J. F., and van Tongeren O. F. R. (Eds.), Data analysis in community and landscape ecology. *AC Wageningen*, 91-173.
- ter Braak, C. J. F. (1987). Ordination. In: *Data analysis in community and landscape ecology.* (Eds.: Jongman. R. H. G., ter Braak, C. J. F. and van Tongeren) AC Wageningen, 91-173.
- ter Braak, C. J. F. (1995). Ordination. In: *Data analysis in community and landscape ecology.* (Eds.: Jongman. R. H. G., ter Braak, C. J. F. and van Tongeren) Cambridge University Press, 91-169.
- ter Braak, C. J. F. and Prentice, I. C. (1988), A theory of gradient analysis, *Advances in Ecological research*, **18**, 271-317.
- ter Braak, C. J. F. and Juggins, S. (1993). Weighted averaging partial least squares regression (WA-PLS): an improved method for reconstructing

environmental variables form species assemblages, *Hydrobiologia*, **269/270**, 485-502.

- Tooley, M. J. (1982). Introduction, *Proceedings of the Geologists' Association,* **93** (1), 3-6.

- Tooley, M. J. (1985). Sea levels, *Progress in Physical Geography*, **9** (1) 113-120.

- Tooley, M. J. (1992). Recent sea-level changes, In: *Saltmarshes* (Ed. Allen, J. R. L.) Cambridge University Press, pp.19-40.

- Tooley, M. J. (1993). Long term changes in eustatic sea level, In: *Climate and sea level change* (Ed. Warrick, R. A.), Cambridge University Press, pp.81-107.

- Tushingham A. M. and Peltier W. R. (1991). Ice-3G: a new global model of late Pleistocene deglaciation based upon geophysical predictions of post-glacial relative sea level change, *Journal of Geophysical Research*, **96**, 4497-4523.

- Van de Plassche, O., (Ed). (1986). *Sea-level research: a manual for the collection and evaluation of data.* Geobooks, Norwich. 617pp.

- Van de Plassche O., Van der Borg K. and De Jong A. F. M. (2002). Relative sea-level rise across the Eastern Border fault (Branford, Connecticut): Evidence against seismotectonic movements, *Marine Geology*, **184**, 61-68.

- Walton, W. R. (1952). Techniques for recognition of living foraminifera: Contributions from Cushman foundation for Foraminiferal Research, **3**, 56-60.

- Wang, P. and Chappell, J. (2001). Foraminifera as Holocene environmental indicators in the South Alligator River, Northern Australia. *Quaternary International*, **83-85**, 47-62.
- Woodroffe, C. D., Kennedy, D. M., Hopley, D., Rasmussen, C. E. and Smithers, S. G. (2000). Holocene reef growth in the Torres Strait. *Marine Geology*, **170**, 331-346.
- Woodroffe, S. A. (2002). The development and application of Quantitative Palaeoenvironmental Reconstruction Techniques in Sea Level Studies: The Great Barrier Reef Coastline, Australia. *M.Sc. Thesis*, Department of Geography, University of Durham, United Kingdom.
- Wynn-Jones, R. (1994). The Challenger Foraminifera. Oxford Science Publications, Oxford.
- Yassini, I. and Jones, B. G. (1995). Foraminiferida and Ostracoda from Estuarine and Shelf Environments on the South-eastern Coast of Australia. University of Wollongong Press, Wollongong, NSW, pp. 484.
- Yokoyama, Y., Lambeck, K., De Deckker, P., Johnston, P. and Fifield, L. K. (2000). Timing of the Last Glacial Maximum from observed sea-level minima. *Nature,* **406**, 713–716.
- Yokoyama, Y., Purcell, A., Lambeck, K. and Johnston, P. (2001). Shore-line reconstruction around Australia during the Last Glacial Maximum and Late Glacial Stage, *Quaternary International*, **83-85**, 9-18.

Appendix

A.1 Microfossil Preparation

Samples of $5cm^3$ are passed through a nest of 500µm and 63µm sieves using light water pressure from a fine spray. The coarse fraction is then inspected before being retained for further analysis. Fine organics that pass through the 500µm are separated from the foraminifera by a process of decantation and wet splitting. The act of wet splitting removes these fine organics by allowing the sediment to settle out into a cylindrical vessel split into 8 equal parts (Scott and Hermelin, 1993; Horton, 1997). All sediment is then stored in a plastic vial until counting.

A.2 Scanning Electron Microscope (SEM) Photography

The species shown correspond to those shown on Plate 1 and 2. Where appropriate, apertural and neutral views are shown. Notation of scale bars is not feasible.

Plate 1	*Ammonia tepida* (Cushman 1926)	A
	Amphistegina lessonii (Parker, Jones and Brady 1865)	B
	Bolivina brizalina (Brady 1884)	C
	Cribrononion oceanicus (Cushman 1926)	D
	Cribrononion sydneyensis (Brady 1884)	E
	Dendritina striata (Brady 1884)	F
	Discorbinella complanata (d'Orbigny, 1839)	G
	Operculina complanata (Defrance 1822)	H

Plate 2	*Pararotalia vernusta* (Brady 1884)	I
	Quinqueloculina pseudoreticulata (Parr 1941)	J
	Quinqueloculina venusta (Karrer 1868)	K
	Triloculina oblonga (d'Orbigny, 1839)	L
	Wiesnerella auriculata (Egger, 1895)	M
	Spiroloculina manifesta (Cushman and Todd, 1944)	N
	Rotalinoides compressiusculus (Brady 1884)	O
	Ammonia beccarii (Brünnich, 1772)	P

A.3 **Loss-On-Ignition** (after Ball, 1964)

The organic carbon content of a sample is an important variable in palaeoenvironmental reconstruction. Loss-On-Ignition (LOI) is the most widely applied method of determining the organic carbon content at lower cost and with comparatively quick results, when compared with more accurate titration methods or colorimetry techniques.

1. Accurately weigh 5g of sediment and place in a weighed crucible.
2. Leave to oven dry over night (110°C) and then re-weigh crucible containing sample.
3. Place crucible and sample in a muffle furnace preheated to 550°C for 5 hours
4. Remove from furnace, cool in dessicator and re-weigh.
5. Perform the following equation to calculate the percentage of organic carbon the sample originally contained.

$$\text{Loss on ignition (\%)} = \left(\frac{A-B}{B}\right)\times 100$$

A = mass of oven dried sample

B = the ignited mass of ash

A.4 Particle Size Analysis

Particle size is determined using an electrical sensor called a Coulter laser Granulometer, using a minimum of two runs of 90 seconds each per sample. The output is a spreadsheet containing data simplified into the percentage of material by volume in the clay, silt and sand fractions. Particles greater than 2000μm are not accepted into the analysis. The methodology for sample preparation follows.

1. Place approximately 3g of sediment in a plastic vial.
2. Add 20mls of distilled water and 5mls of 100% hydrogen peroxide (H_2O_2) to the sample.
3. The sample will effervesce. If this is extreme, allow the sample to settle for a time before covering each tube with foil and placing in a boiling water bath for 2 hours.
4. If organic material is still remaining, repeat this stage again until all is oxidised.
5. Centrifuge the samples at 4000rpm for 4 minutes and carefully decant half of the supernatant liquid off. Top up with distilled water , centrifuge, and decant off the supernatant water.
6. Add 20mls of distilled water to the tube, then 2ml of sodium hexametaphosphate (NaPO3) solution, to act as a deflocculant. The sample is now ready for analysis.

A.5 Regional dataset of raw foraminifera counts

Sample	1	2	3	4	5	6	7	8	9	10	11	12
Alveolinella quoii	0	0	0	0	0	0	0	0	0	0	0	0
Ammonia beccarii	2	1	4	3	7	10	1	8	0	0	0	2
Ammonia tepida	3	4	9	2	3	9	3	9	0	13	5	7
Amphistegina lessonii	12	40	3	11	18	4	10	0	0	0	0	0
Assilina ammonoides	9	0	0	0	0	0	0	0	0	0	0	0
Bolivina brizalina	6	3	14	9	3	5	2	4	15	9	5	6
Cribrononion oceanicus	13	3	0	7	3	0	6	0	9	0	7	0
Cribrononion sydneyensis	11	16	18	24	25	15	32	36	43	31	43	10
Dendritina striata	15	19	21	18	22	22	15	12	12	11	2	2
Discorbinella complanata	29	8	34	28	31	15	21	36	27	33	20	30
Elphidium crispum	9	9	11	6	6	11	5	15	3	4	1	3
Elphidium discoidale multiloculum	1	0	1	0	0	4	0	1	0	3	0	0
Globigerina bulloides	0	0	0	1	0	0	0	0	0	1	0	0
Heterostegina depressa	0	10	0	1	0	4	2	1	0	0	0	0
Marginopora vertebralis	0	1	0	0	0	0	0	0	0	0	0	0
Miliolinella lakemarquiensis	31	26	17	12	11	31	2	15	14	17	10	22
Nonion sp.	0	0	2	2	0	0	1	2	1	1	1	1
Operculina complanata	3	29	5	13	9	5	8	2	4	1	2	0
Operculina heterosteginoides	0	0	4	0	0	8	0	0	0	0	0	0
Pararotalia vernusta	15	26	9	15	21	3	7	0	2	2	2	2
Parasorites marginalis	0	2	1	6	4	0	0	0	0	0	0	0
Quinqueloculina funafutiensis	18	0	10	14	16	8	12	6	8	13	20	1
Quinqueloculina pseudoreticulata	10	10	10	25	17	10	34	8	20	7	3	12
Quinqueloculina sp.	0	3	9	4	6	6	5	9	10	19	12	17
Quinqueloculina venusta	12	16	9	30	29	14	27	21	34	23	35	19
Rotalinoides compressiusculus	2	0	4	3	4	5	5	5	8	10	9	4
Spiroloculina manifesta	1	0	0	2	1	1	1	6	1	1	0	14
Spirosigmoilina bradyi	4	6	6	14	3	0	1	0	0	3	0	0
Stilostomella lepidula	0	0	4	2	0	3	1	4	3	4	5	8
Triloculina oblonga	6	7	24	12	3	18	14	18	7	45	14	42
Wiesnerella auriculata	4	0	3	4	3	5	0	5	2	1	6	0
TOTAL	**216**	**239**	**232**	**268**	**245**	**216**	**215**	**223**	**223**	**252**	**202**	**202**

A.5 cont...

Sample	13	14	15	16	17	18	19	20	21	22	23	24	25
Alveolinella quoii	0	0	9	0	0	0	5	2	0	7	0	6	9
Ammonia beccarii	23	0	0	0	0	2	0	0	0	0	0	0	0
Ammonia tepida	7	0	4	0	0	0	0	0	0	2	1	1	1
Amphistegina lessonii	0	50	22	52	41	12	88	46	50	86	70	91	63
Assilina ammonoides	0	0	0	0	0	0	0	0	0	0	0	0	0
Bolivina brizalina	2	4	5	4	9	6	1	4	5	10	8	1	1
Cribrononion oceanicus	0	1	0	1	1	0	0	0	0	0	0	0	0
Cribrononion sydneyensis	27	21	7	15	14	9	12	14	21	8	10	5	8
Dendritina striata	0	43	55	39	54	37	37	43	25	3	11	18	39
Discorbinella complanata	21	15	14	17	9	17	1	16	6	6	3	9	6
Elphidium crispum	3	7	10	5	6	5	4	3	0	2	0	2	2
Elphidium discoidale multiloculum	11	0	2	0	0	0	0	1	3	3	0	0	0
Globigerina bulloides	2	0	1	1	3	0	0	9	14	5	12	0	0
Heterostegina depressa	0	1	2	2	0	0	1	5	3	14	0	0	2
Marginopora vertebralis	0	0	0	0	0	0	3	0	5	0	2	0	1
Miliolinella lakemarquiensis	36	12	11	25	18	31	12	8	14	5	14	18	6
Nonion sp.	0	0	0	0	0	0	0	0	1	1	0	0	0
Operculina complanata	2	16	13	34	17	8	41	19	13	13	50	21	19
Operculina heterosteginoides	0	0	9	0	0	12	0	13	2	7	0	0	0
Pararotalia vernusta	2	10	8	6	12	3	2	2	2	1	0	2	4
Parasorites marginalis	0	5	4	6	7	0	4	5	14	2	2	4	3
Quinqueloculina funafutiensis	0	15	0	9	5	0	0	2	1	6	3	3	5
Quinqueloculina pseudoreticulata	6	8	7	11	5	0	5	2	1	3	3	3	7
Quinqueloculina sp.	2	4	3	1	4	13	4	2	4	12	1	3	2
Quinqueloculina venusta	21	15	8	15	23	0	6	6	13	7	10	16	16
Rotalinoides compressiusculus	5	1	2	2	3	3	1	0	1	0	4	1	0
Spiroloculina manifesta	17	0	3	3	1	2	0	11	1	2	2	1	1
Spirosigmoilina bradyi	0	6	8	13	6	0	2	7	5	3	0	10	6
Stilostomella lepidula	3	0	1	0	0	0	0	2	0	0	0	0	0
Triloculina oblonga	19	6	27	9	3	45	2	14	11	14	2	3	1
Wiesnerella auriculata	0	4	8	5	3	0	2	7	3	5	0	3	2
TOTAL	**209**	**244**	**243**	**275**	**244**	**205**	**233**	**243**	**218**	**227**	**208**	**221**	**204**

A.5 Cont...

Sample	26	27	28	29	30	31	32	33	34
Alveolinella quoii	0	0	0	0	0	0	1	0	0
Ammonia beccarii	0	1	0	0	1	0	1	0	0
Ammonia tepida	11	13	7	11	13	12	40	6	13
Amphistegina lessonii	3	4	1	4	9	3	4	0	2
Assilina ammonoides	0	0	0	0	0	0	0	0	0
Bolivina brizalina	13	15	4	12	11	11	8	9	14
Cribrononion oceanicus	16	20	20	12	15	17	33	22	17
Cribrononion sydneyensis	20	27	19	24	19	17	40	73	12
Dendritina striata	5	2	10	5	4	6	3	0	2
Discorbinella complanata	50	42	44	37	40	35	24	0	45
Elphidium crispum	5	4	12	9	5	2	1	0	0
Elphidium discoidale multiloculum	1	1	4	2	2	1	0	0	2
Globigerina bulloides	1	1	0	1	1	0	0	0	0
Heterostegina depressa	0	0	0	0	0	0	0	0	0
Marginopora vertebralis	0	0	0	0	0	0	0	0	0
Miliolinella lakemarquiensis	13	12	16	13	1	6	6	4	3
Nonion sp.	1	2	0	1	0	2	2	6	1
Operculina complanata	0	1	0	0	1	0	1	0	0
Operculina heterosteginoides	0	1	0	0	0	0	0	0	0
Pararotalia vernusta	1	2	1	1	3	2	3	0	2
Parasorites marginalis	0	0	0	0	0	0	0	0	0
Quinqueloculina funafutiensis	14	13	16	17	23	18	10	10	26
Quinqueloculina pseudoreticulata	3	6	16	9	9	6	0	0	3
Quinqueloculina sp.	3	5	9	9	6	10	3	10	7
Quinqueloculina venusta	25	16	33	21	36	17	9	14	32
Rotalinoides compressiusculus	2	4	5	11	6	2	5	2	4
Spiroloculina manifesta	2	0	2	3	3	4	1	0	2
Spirosigmoilina bradyi	0	2	3	3	1	2	2	1	2
Stilostomella lepidula	1	0	4	1	5	4	0	4	2
Triloculina oblonga	10	12	13	21	13	23	13	30	35
Wiesnerella auriculata	5	1	2	3	4	3	3	13	11
TOTAL	**205**	**207**	**241**	**230**	**231**	**203**	**213**	**204**	**237**

A.5 Cont...

Sample	35	36	37	38	39	40	41	42	43
Alveolinella quoii	0	0	0	0	0	0	0	0	0
Ammonia beccarii	2	0	7	1	2	0	2	3	1
Ammonia tepida	9	5	0	2	3	2	0	5	0
Amphistegina lessonii	0	1	32	29	23	7	7	12	5
Assilina ammonoides	0	0	0	0	0	0	0	0	0
Bolivina brizalina	10	5	1	0	0	1	2	2	3
Cribrononion oceanicus	15	13	0	0	1	4	0	6	1
Cribrononion sydneyensis	15	18	30	23	19	27	26	25	16
Dendritina striata	6	5	4	2	4	2	3	6	12
Discorbinella complanata	39	47	2	10	9	19	19	20	7
Elphidium crispum	0	5	2	14	11	10	7	4	0
Elphidium discoidale multiloculum	3	1	13	14	8	5	2	0	1
Globigerina bulloides	0	1	0	0	0	0	0	0	0
Heterostegina depressa	0	0	0	0	0	0	0	0	0
Marginopora vertebralis	0	0	0	0	0	0	0	0	0
Miliolinella lakemarquiensis	10	14	16	16	19	13	28	26	17
Nonion sp.	5	2	0	0	0	0	0	0	0
Operculina complanata	0	0	5	7	6	4	4	6	1
Operculina heterosteginoides	0	0	1	0	0	0	0	0	0
Pararotalia vernusta	0	1	6	12	8	16	37	75	99
Parasorites marginalis	0	0	0	0	0	0	0	0	0
Quinqueloculina funafutiensis	14	11	0	0	0	0	0	0	0
Quinqueloculina pseudoreticulata	9	9	40	28	30	26	5	5	7
Quinqueloculina sp.	9	11	2	14	16	6	3	5	0
Quinqueloculina venusta	17	24	29	44	47	43	57	34	19
Rotalinoides compressiusculus	5	3	5	4	3	5	1	3	4
Spiroloculina manifesta	0	0	0	1	1	3	2	2	2
Spirosigmoilina bradyi	2	2	1	0	3	1	2	2	0
Stilostomella lepidula	9	0	0	0	0	0	0	0	0
Triloculina oblonga	24	17	3	1	3	7	3	5	7
Wiesnerella auriculata	9	8	1	1	1	2	2	1	2
TOTAL	**212**	**203**	**200**	**223**	**217**	**203**	**212**	**247**	**204**

A.5 Regional dataset sample converter

AIMS 713	1
AIMS 720	2
AIMS 722	3
AIMS 723	4
AIMS 724	5
AIMS 725	6
AIMS 726	7
AIMS 727	8
AIMS 728	9
AIMS 729	10
AIMS 730	11
AIMS 731	12
AIMS 732	13
AIMS 884	14
AIMS 885	15
AIMS 886	16
AIMS 887	17
AIMS 889	18
AIMS 890	19
AIMS 891	20
AIMS 893	21
AIMS 895	22
AIMS 901	23
AIMS 903	24
AIMS 907	25
902v106	26
902v107	27
902v108	28
902v109	29
902v110	30
902v112	31
944v13	32
944v14	33
944v15	34
944v16	35
944v18	36
944v1	37
944v2	38
944v3	39
944v4	40
944v5	41
944v6	42
944v7	43

A.6 Fossil dataset of raw foraminifera counts

Sample	1	2	3	4	5	6	7	8	9	10	11	12
Alveolinella quoii	0	0	0	1	0	5	16	6	0	0	0	0
Ammonia beccarii	0	30	33	0	0	0	0	0	0	0	0	0
Ammonia tepida	12	41	19	0	0	5	0	0	15	56	29	0
Amphistegina lessonii	1	0	1	4	1	42	37	33	1	0	0	4
Assilina ammonoides	0	3	4	0	0	10	0	0	0	0	12	0
Bolivina brizalina	12	14	7	8	17	7	0	9	15	24	10	9
Cribrononion oceanicus	17	54	90	0	0	13	1	0	47	43	20	0
Cribrononion sydneyensis	0	4	5	14	14	2	6	11	5	5	12	34
Dendritina striata	4	4	2	12	0	7	14	26	1	3	9	11
Discorbinella araucana	0	0	0	0	0	0	0	1	0	0	0	0
Discorbinella complanata	37	0	5	15	0	2	5	9	7	11	10	29
Elphidium crispum	1	0	2	11	2	4	4	1	0	0	0	1
Elphidium discoidale multiloculum	2	0	2	8	1	0	2	0	0	0	4	4
Globigerina bulloides	0	1	0	0	0	2	2	0	0	4	0	0
Heterostegina depressa	0	0	0	0	1	1	4	3	0	0	0	4
Lagena striata strumosa	0	1	1	0	2	2	0	0	1	2	0	2
Marginopora vertebralis	0	0	0	0	0	2	0	0	0	0	0	0
Miliolinella labiosa	0	0	0	0	0	0	0	0	0	0	0	0
Miliolinella lakemarquiensis	10	3	2	8	7	0	9	2	2	7	4	22
Operculina complanata	7	0	0	10	4	15	18	13	3	2	0	11
Operculina heterosteginoides	0	0	0	1	0	0	1	0	0	0	0	2
Pararotalia vernusta	0	0	5	19	4	3	32	5	6	12	8	6
Parasorites marginalis	1	2	1	1	0	0	0	5	0	0	1	1
Pseudohauerina occidentalis involuta	0	0	0	0	0	0	2	0	0	0	0	0
Quinqueloculina funafutiensis	18	9	1	14	0	0	0	5	15	11	16	16
Quinqueloculina pseudoreticulata	2	0	1	26	7	0	4	1	0	2	0	9
Quinqueloculina sp.	12	0	0	17	12	3	2	7	3	0	7	10
Quinqueloculina venusta	15	2	7	14	18	2	7	11	29	12	29	46
Rotalinoides compressiusculus	1	0	8	4	3	0	3	1	8	1	8	3
Spirolina cylindracea	0	0	0	0	0	0	0	1	0	0	0	0
Spiroloculina manifesta	3	0	0	2	0	0	1	2	3	1	2	0
Spirosigmoilina bradyi	4	2	2	6	6	1	12	5	4	6	10	0
Stilostomella lepidula	1	0	0	4	13	0	1	0	1	0	1	2
Triloculina oblonga	32	15	0	21	25	3	11	9	18	7	19	9
Unidentified 1	0	0	0	0	13	0	0	0	0	0	0	0
Unidentified 2	0	0	0	0	7	0	0	0	0	0	0	0
Unidentified 3	0	0	0	0	0	0	0	1	2	0	0	0
Unidentified 4	0	0	0	0	0	0	0	0	0	0	0	0
Unidentified 5	0	0	0	0	0	0	3	0	0	0	0	0
Unidentified 6	0	0	0	0	0	0	10	13	0	0	0	0
Unidentified 7	0	0	0	0	0	0	1	0	0	0	0	0
Unidentified 8	0	0	0	1	0	0	0	0	0	0	0	0
Unidentified 9	0	0	0	0	0	0	0	0	0	0	0	1
Unidentified 10	0	0	0	0	31	0	0	17	0	0	0	0
Unidentified 11	6	0	0	0	0	0	0	0	1	2	0	0
Unidentified 12	0	0	0	0	0	0	0	0	0	0	1	0
Unidentified 13	0	0	0	0	0	0	0	10	0	0	0	0
Valvulineria rugosa	1	0	0	0	0	0	0	6	0	0	0	0
Wiesnerella auriculata	24	16	8	7	18	0	5	7	41	9	14	12
TOTAL	**223**	**201**	**206**	**228**	**206**	**131**	**213**	**220**	**228**	**220**	**226**	**248**

A.6 Fossil dataset sample converter

857dv16 (72)	1
902106 (265)	2
902113 (142)	3
902v102 (55)	4
902v121 (85)	5
911v11 (62)	6
911v15 (46)	7
911v16 (48)	8
911v8 (213)	9
912bv2 (153)	10
912bv4 (172)	11
915v8 (35)	12

A.7 Bowling Green Bay - Environmental variables

Sample	Depth (m AHD)	Organic Content (%)	Sand (%)	Silt (%)	Clay (%)
732	-6.7	3.1	76.8	16.4	6.8
731	-8.8	3.7	69.8	17.0	13.2
730	-10.1	4.0	65.8	21.6	12.6
729	-10.8	3.5	76.4	13.5	10.1
728	-12.1	4.1	75.3	13.7	11.0
727	-12.7	3.7	77.9	11.8	10.3
726	-13.5	4.0	76.2	12.6	11.3
725	-14.2	3.8	76.6	12.3	11.1
724	-15.1	3.4	78.8	11.4	9.8
713	-16.4	5.2	72.3	15.4	12.3
723	-16.4	3.9	75.9	12.9	11.1
722	-17.0	3.5	85.5	8.2	6.3
720	-18.5	2.9	89.2	6.3	4.5
884	-22.8	4.9	79.8	13.0	7.2
885	-24.9	6.3	78.3	13.6	8.1
886	-25.0	7.2	79.9	13.1	7.1
887	-28.1	4.8	85.9	9.6	4.6
907	-28.5	2.7	94.1	4.1	1.8
889	-29.3	4.7	87.6	8.7	3.7
890	-32.4	3.6	95.6	3.1	1.4
891	-34.6	4.2	92.8	5.5	1.7
903	-38.5	3.2	93.0	5.1	1.9
893	-39.9	3.2	93.3	5.0	1.7
901	-44.5	3.1	93.4	5.0	1.7
895	-48.0	2.2	94.4	4.2	1.4

A.8 Cleveland Bay - Environmental variables

Sample	Depth (m AHD)	Organic Content (%)	Sand (%)	Silt (%)	Clay (%)
KG944v13	-5.6	1.9	44.3	45.2	10.4
KG944v14	-5.5	4.2	55.6	34.2	10.1
KG944v15	-5.5	4.2	74.7	17.4	7.8
KG944v16	-6.1	3.8	67.5	20.6	11.9
KG944v18	-6.5	3.5	96.0	2.0	1.9
KG902v112	-8.4	3.1	70.8	18.8	10.4
KG902v110	-8.7	3.8	66.8	21.8	11.4
KG902v109	-9.3	4.1	69.5	18.7	11.8
KG902v108	-9.2	2.4	90.1	6.1	3.8
KG902v107	-9.2	3.3	65.5	20.4	14.1
KG902v106	-9.8	3.2	77.7	13.5	8.8
KG944v1	-6.0	1.4	83.6	13.7	2.7
KG944v2	-7.4	1.5	97.6	1.4	1.0
KG944v3	-6.5	1.8	93.9	4.2	1.8
KG944v4	-6.3	2.9	91.6	5.3	3.1
KG944v5	-7.9	2.4	94.0	3.7	2.3
KG944v6	-6.1	2.6	84.0	9.5	6.5
KG944v7	-4.2	2.3	88.0	8.5	3.6

A.9 Bowling Green Bay transfer function

	Component 1	Component 2	Component 3	Component 4	Component 5
RMSE	4.4091	2.8688	2.2257	1.9454	1.513
r^2	0.86392	0.94239	0.96532	0.97351	0.98398
Ave_Bias	-0.015311	0.0075947	0.0040694	0.0034964	-0.0011113
Max_Bias	7.6357	3.5799	3.2231	2.6657	2.1644
Jack_R2	0.7908	0.79817	0.79756	0.77261	0.70678
Jack_Ave_Bias	0.24566	-0.16769	-0.28807	-0.16616	-0.45308
Jack_Max_Bias	10.804	10.095	10.429	10.54	11.751
RMSEP	5.4886	5.3793	5.411	5.7175	6.5023

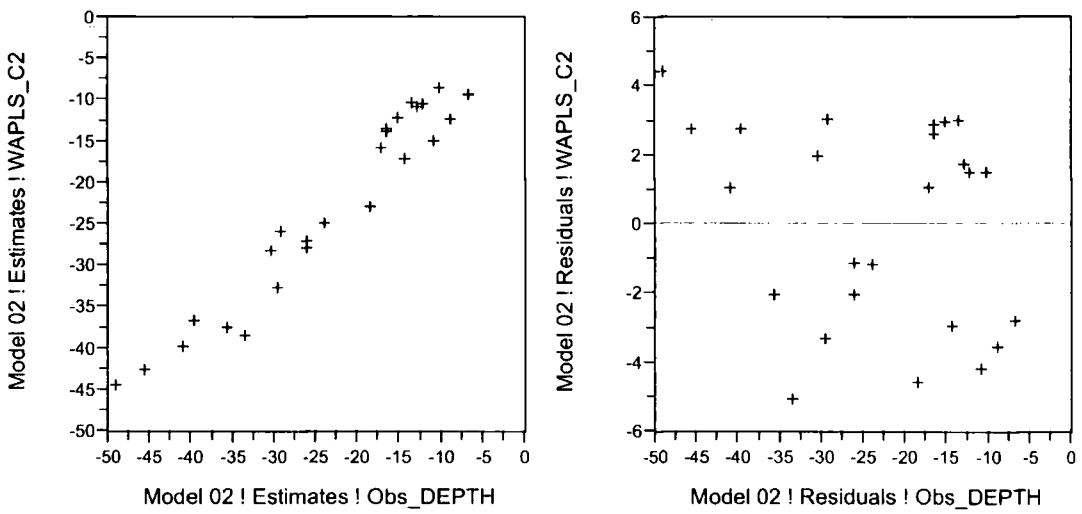

A.10 Cleveland Bay transfer function

	Component 1	Component 2	Component 3	Component 4	Component 5
RMSE	1.2302	1.0062	0.80844	0.65632	0.30315
r^2	0.4108	0.60582	0.74555	0.8323	0.96422
Ave_Bias	0.0044332	7.88E-04	0.0016542	0.0013135	-1.65E-04
Max_Bias	1.7369	1.3712	0.93694	0.91276	0.21423

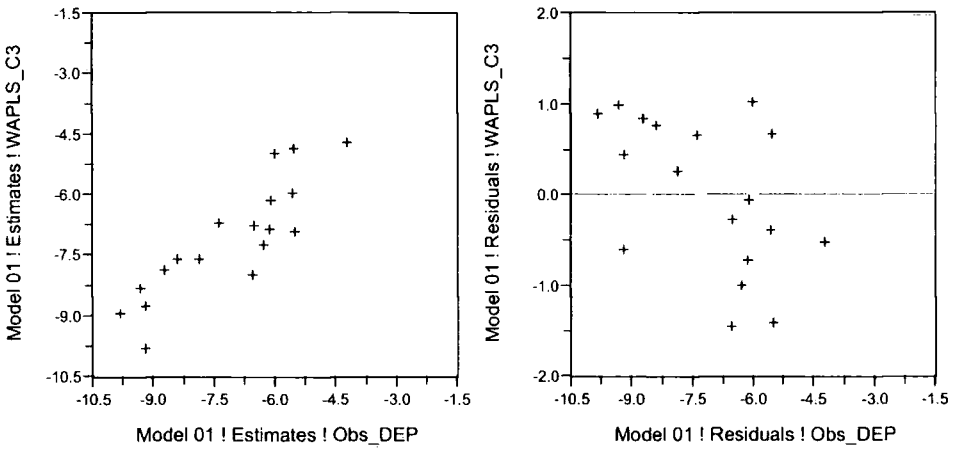

A.11 Glossary of Terminology

AHD	Australian Height Datum
BGB	Bowling Green Bay
BP	Before Present (1950)
CB	Cleveland Bay
CCA	Canonical Correspondence Analysis
DCA	Detrended Correspondence Analysis
FBIs	Fixed Biological Indicators
GBR	Great Barrier Reef
LGM	Last Glacial Maximum – 18 k.a. BP (±3k.a.), the most recent climatic minimum.
MHHS	Mid-Holocene High Stand – RSL Holocene highstand in far field locations.
MSL	Mean Sea Level – Average sea-level over a fixed period of time.
NSW	New South Wales
RMSEP	Root Mean Squared Error of Prediction – Transfer function error term
RSL	Relative Sea Level - The position and height of sea relative to the land.
WA	Weighted Averaging – Transfer function
WA-PLS	Weighted-Averaging Partial Least Squares – Transfer function (regression)

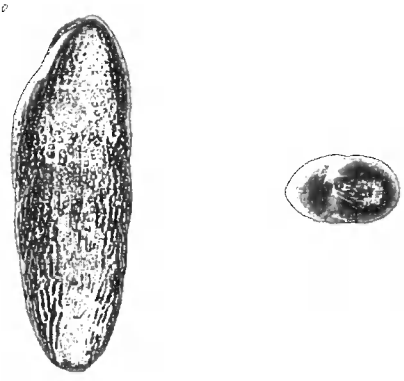

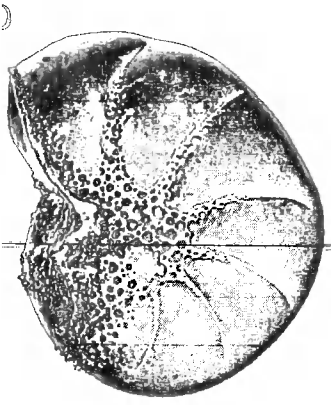

E

F

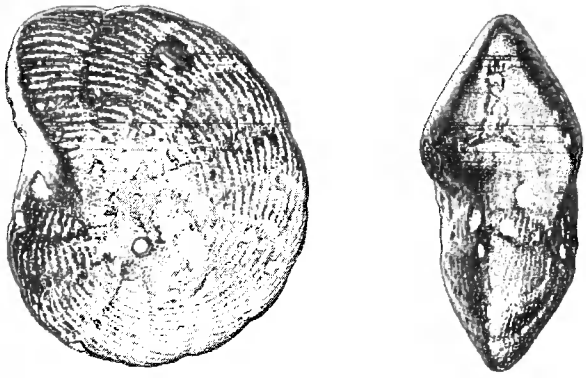

G

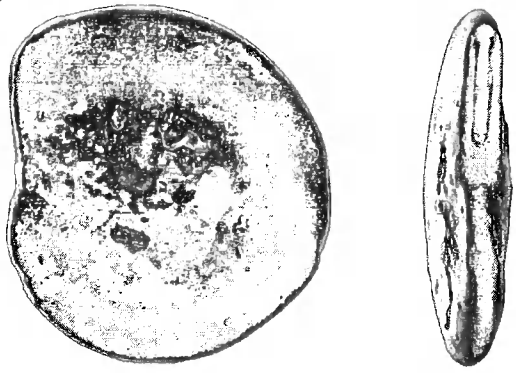

H

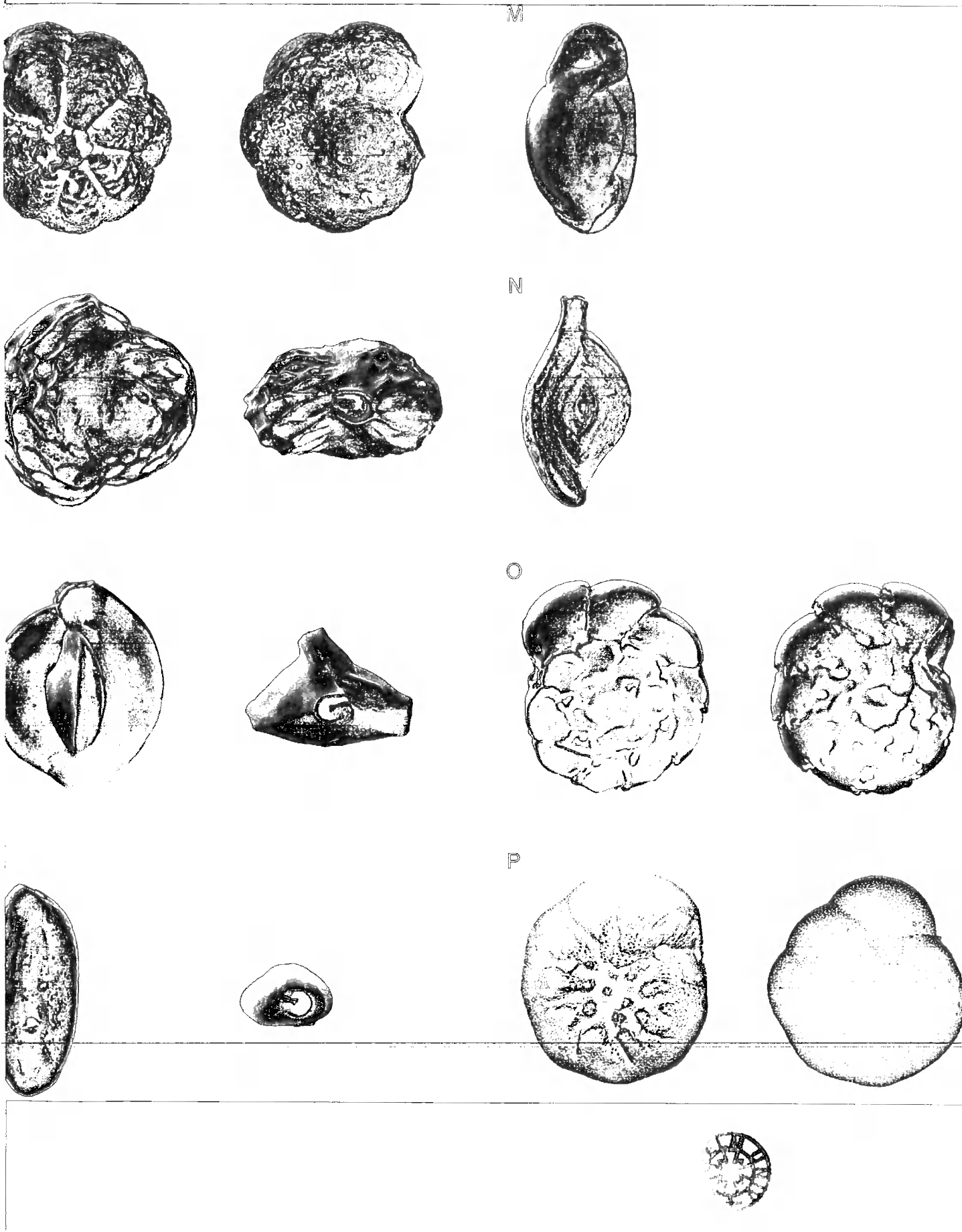
M
N
O
P